AD-773 184

NANOSECOND PULSE ANTENNA NARHORN

Robert D. Wengenroth, et al

General Electric Company

Prepared for:

Rome Air Development Center
Air Force Systems Command

October 1973

UNCLASSIFIED

SECURITY CLASSIFICATION OF THIS PAGE (When Data Entered)

REPORT DOCUMENTATION PAGE		READ INSTRUCTIONS BEFORE COMPLETING FORM
1. REPORT NUMBER RADC-TR-73-308	2. GOVT ACCESSION NO.	3. RECIPIENT'S CATALOG NUMBER AD 773 184
4. TITLE (and Subtitle) Nanosecond Pulse Antenna "Narhorn"		5. TYPE OF REPORT & PERIOD COVERED Final - 15 Dec 69 - 1 Jul 73
		6. PERFORMING ORG. REPORT NUMBER EH-61777
7. AUTHOR(s) Robert D. Wengenroth, Alan E. Blume Maurice C. Swanson, Wayne S. Kenyon Byron A. Tietjen		8. CONTRACT OR GRANT NUMBER(s) F30602-70-C-0073
9. PERFORMING ORGANIZATION NAME AND ADDRESS General Electric Company Heavy Military Electronic Systems Syracuse, NY 13201		10. PROGRAM ELEMENT, PROJECT, TASK AREA & WORK UNIT NUMBERS Job Order No. 45060444
11. CONTROLLING OFFICE NAME AND ADDRESS Rome Air Development Center (OCTP) Air Force Systems Command Griffiss Air Force Base, New York 13441		12. REPORT DATE October 1973
		13. NUMBER OF PAGES ~~154~~ 143
14. MONITORING AGENCY NAME & ADDRESS(if different from Controlling Office) Same		15. SECURITY CLASS. (of this report) Unclassified
		15a. DECLASSIFICATION/DOWNGRADING SCHEDULE N/A

16. DISTRIBUTION STATEMENT (of this Report)

Approved for Public Release. Distribution Unlimited.

17. DISTRIBUTION STATEMENT (of the abstract entered in Block 20, if different from Report)

Same

18. SUPPLEMENTARY NOTES

RADC Project Engineer: Frank E. Welker (OCTP)

19. KEY WORDS (Continue on reverse side if necessary and identify by block number)

Antenna
Folded conical horn
Nanosecond radar
S-band

20. ABSTRACT (Continue on reverse side if necessary and identify by block number)

This technical report discusses the design and fabrication of an antenna for the Nanosecond Radar Laboratory of the Rome Air Development Center. The folded type antenna was designed and built under Contract F30602-70-C-0073. The RF performance has been determined by computation and model measurement. Gain is over 39 dB with beamwidths about 1.5 degrees in the E-plane and 1.9 degrees in the H-plane. The first E-plane sidelobes with the government

(Continued)

DD FORM 1 JAN 73 1473 EDITION OF 1 NOV 65 IS OBSOLETE

UNCLASSIFIED

SECURITY CLASSIFICATION OF THIS PAGE (When Data Entered)

20.

furnished horn input transition may be about -12 dB. With a low mode-conversion transition, the first E-plane sidelobes would be -16 dB or better, and the first H-plane sidelobes -20 dB or better. The shielded nature of the antenna provides distant sidelobes mostly below the isotropic gain level. The mechanical construction is of aluminum sheet on an aluminum support structure. The elevation drive is geared and the azimuth drive is accomplished through wheels in an unusual tripod structure. The antenna presents an aerodynamically unbalanced load. The control system follows binary command signals or manual motion controls.

NANOSECOND PULSE ANTENNA
"NARHORN"

Robert D. Wengenroth
Maurice C. Swanson
Byron A. Tietjen
Alan E. Blume
Wayne S. Kenyon

Heavy Military Electronic Systems
General Electric Company

FOREWORD

This final report was prepared by the General Electric Company, Heavy Military Electronic Systems, Syracuse, New York, under Contract F30602-70-C-0073, Job Order No. 45060444, with Rome Air Development Center. The work at HMES, under Requisition EH-61777, was performed in the Period of 15 December 1969 through 1 July 197_, by members of the staff of Advance Microwave Development, Radar Mechanical and Environmental Engineering, and Sonar Control Systems. Major contributors to this report include M. C. Swanson, B. A. Tietjen, S. W. Kanyon, and R. D. Wengenroth. A. E. Blume, at the General Electric Research and Development Center in Schenectady served as a consultant.

Mr. Frank W. Welker (OCTP) is the RADC Project Engineer.

This report has been reviewed by the Office of Information, RADC, and approved for release to the National Technical Information Service.

This report has been reviewed and is approved.

APPROVED: Frank E Welker
FRANK E. WELKER
Project Engineer/OCTP

APPROVED: William T. Pope
WILLIAM T. POPE
Assistant Chief
Surveillance and Control Division

FOR THE COMMANDER: Carlo P. Crocetti
CARLO P. CROCETTI
Chief, Plans Office

ABSTRACT

This technical report discusses the design and fabrication of an antenna for the Nanosecond Radar Laboratory of the Rome Air Development Command. The folded cone type antenna was designed and built under Contract F30602-70-C-0073.

The RF performance has been determined by computation and model measurement. Gain is over 39 dB with beamwidths about 1.5 degrees in the E-plane and 1.9 degrees in the H-plane. The first E-plane sidelobes with the government furnished horn input transition may be about -12 dB. With a low mode-conversion transition, the first E-plane sidelobes would be -16 dB or better, and the first H-plane sidelobes -20 dB or better. The shielded nature of the antenna provides distant sidelobes mostly below the isotropic gain level.

The mechanical construction is of aluminum sheet on an aluminum support structure. The elevation drive is geared and the azimuth drive is accomplished through wheels in an unusual tripod structure. The antenna presents an aerodynamically unbalanced load. The control system follows binary command signals or manual motion controls.

EVALUATION

The objective of this effort was to design and fabricate an antenna system for the Nanosecond Radar Laboratory at the Rome Air Development Center, Floyd Test Annex. The antenna system is for use in high resolution radar experiments in support of TPO/5.

The antenna design selected was a folded conical horn with a reflector incorporated to focus the energy into a less than two degree main beam at a gain of 37 dB. The antenna delivered was an experimental model and it met all electrical and mechanical specifications. The electrical performance acceptance measurements were performed on a scaled model. All mechanical acceptance testing was carried out on the delivered device installed at the RADC Floyd Test Annex. Specifically, the antenna exhibited a beamwidth of 1.5 degrees in the E-plane and 1.85 degrees in the H-plane at a gain of over 40 dB at the design center frequency all well within the acceptance criteria. The very low dispersion of the antenna system over several hundred megacycles of bandwidth is of special significance to high resolution radar experiments. In addition, the oversized waveguide techniques used in designing the system allow peak power operation orders of magnitude above that of conventional antenna systems.

Frank E Welker

FRANK E. WELKER

TABLE OF CONTENTS

TABLE OF CONTENTS (Cont)

LIST OF ILLUSTRATIONS

LIST OF ILLUSTRATIONS (Cont)

SECTION 1

INTRODUCTION

The Nanosecond Pulse Antenna, known as NARHORN (NAnosecond Radar HORN antenna), was designed and fabricated for the Rome Air Development Center (RADC) Nanosecond Radar Laboratory (NARAL) by General Electric's Heavy Military Electronic Systems under contract F30602-70-C-0073. NARAL has had developed, under other contracts and in house, the transmitter, the waveguide run and the receiver. The waveguide run terminates in a conical horn section; NARHORN extends the horn to provide a larger (12-foot diameter) aperture and rotary joints to permit azimuth and elevation scanning. The resulting installation will demonstrate the radar capabilities which are the present objectives of the laboratory.

General Electric has participated in a number of studies which prepared the technology for the waveguide requirements of this program. These are identified in References 1 through 5. The waveguide has been developed in the High Power Oversize Waveguide contract F30602-69-C-0066, better known as NAROWS (NAnosecond Radar Oversize Waveguide System) by General Electric's Research and Development Center (R&DC) at Schenectady. The folded cone concept was recommended by R&DC as an effective antenna compatible with the waveguide requirements.

Several organizations have been active in the NARHORN program. It is one of several programs of the Nanosecond Radar Laboratory at RADC. Heavy Military Electronic Systems (HMES) of General Electric Company was the prime contractor. HMES has prepared and tested the RF design, and provided the positioning control subsystem. Consulting with HMES on the program was the group at R&DC who are producing the waveguide. The antenna structure was designed and fabricated by Fleet Manufacturing Limited of Fort Erie, Ontario.

This report is organized as follows. Section II describes the folded conical antenna as an equipment. The RF design, performed on a one-tenth scale model, is presented in Section III. The fundamental mechanical design is discussed in Section IV. The control system is described in Section V. The references for the body of the report are listed in Section VI. Special reference material is reproduced in Section VII as appendices. These include the RF design test plan and results; the structural specification placed on Fleet, and a technical discussion of the effects of the GFE NAROWS horn performance on the overall antenna performance, prepared by R&DC.

SECTION II

THE FOLDED CONICAL HORN ANTENNA

The folded conical horn antenna is a shielded, focused, reflector type antenna of very high efficiency and low sidelobes. It is shown installed on the roof of the Nanosecond Radar Laboratory in the photograph in Figure 1. The figure shows some of the mechanical detail, the conic waveguide, with the diagonal mirror which folds the cone and the paraboloidal mirror which collimates the beam.

The folded conical horn antenna was described by Bell Telephone Laboratories. (See Ref. 6, 7, and 8.) Model tests reported in the references and the unique, large size structure appeared to provide an excellent antenna for the nanosecond radar. The reported performance indicated low sidelobes and very high aperture efficiency. The single folded version permits simple azimuth and simple elevation rotary joints.

The specifications for this antenna are as follows:

Frequency	3350 MHz
Gain	37 dB minimum
Beamwidth	2 degrees nominal
Sidelobes	15-dB below main beam minimum 20-dB goal
Azimuth scan	450 degrees minimum
Elevation scan	0 to 70 degrees relative to the horizon
Position readout	nearest 0.1 degree within 0.1 degree
Operating wind	15 knots steady, 40 knots gusts
Stowed wind	50 knots steady, 80 knots gusts
Ice	1 inch maximum
Snow	40 pounds/ft^2
Weight	not over 13,200 pounds

(peak power and pulse data are classified and omitted here)

Figure 1. The Folded-Conical Horn Antenna

Electrically the antenna comprises a conic waveguide propagating a spherical wavefront wave to a phase correcting mirror which directs the resultant plane-wave at right-angles to the axis of the cone. The phase correcting mirror is a small portion of a paraboloid of revolution. The section is taken about the "latus rectum" of the generating parabola. The axis of the conic waveguide is along the parabola latus rectum. This relation of cone to parabola is shown in Figure 2.

The fold in the cone is essentially a miter bend in the conic waveguide. Because the miter is large compared to the wavelength it has been designed on an optical basis. The edge diffraction effects contribute to the sidelobe level far from the main beam. For the present application, the diffraction effects were not identified and are believed to be far below the level which would be detected in the pattern measurements made.

The antenna for the nanosecond pulse antenna utilizes the pressurized horn developed on the NAROWS (nanosecond oversize waveguide system) program, contract F30602-69-C-0066. This horn is pressurized to operate at the design peak power, and terminates in a 44-inch diameter radome. The NAROWS horn was developed to operate either as a direct radiator or as the initial section of the conical horn antenna. Some compensation of the mode conversion which occurs at a simple transition from rectangular oversize waveguide to conic waveguide was included. The effects of the remaining higher mode energy is discussed in Appendix III. The antenna was designed to meet the specifications with a fully compensated horn. There is a probability that with the NAROWS horn transition the sidelobe levels will exceed the specifications. The sidelobe levels will not affect the initial portions of the nanosecond radar demonstration program. The future program is likely to call for either dual polarization capability, tracking capability, or both. A new horn assembly should be considered to optimize these functions and can include mode control features.

The rotary joints are simple gaps with a minor choke action. The energy flowing into the gaps is small, and is absorbed by lossy material to avoid the generation of what would be effectively "sidelobes," or the occurrence of high-field regions outside the conic sections. Their structure is shown in Figures 3 and 4. The purpose of the absorber material is twofold. It absorbs the leaking power as noted above, and damps any ring resonances which might occur in the gap area.

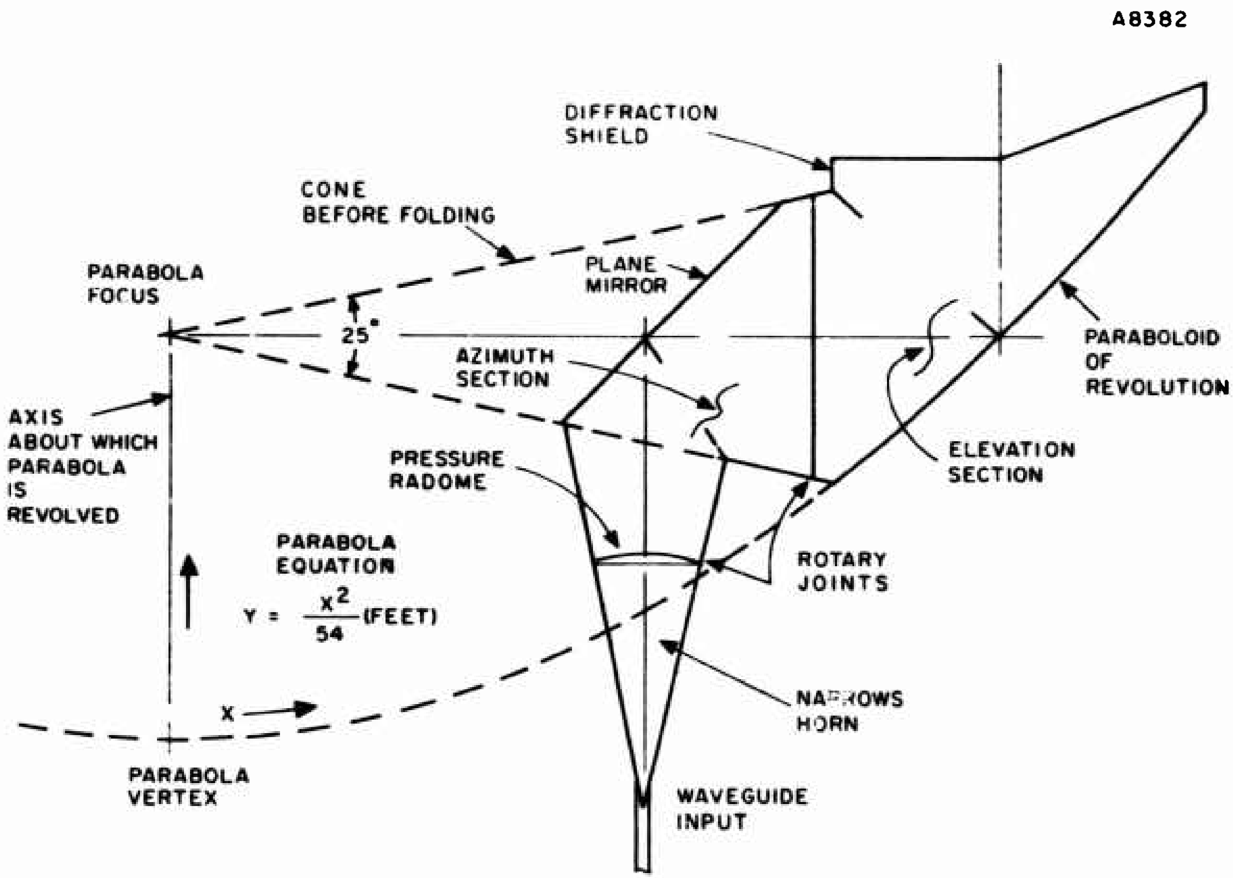

Figure 2. Folded Conical-Horn-Reflector Antenna Geometry

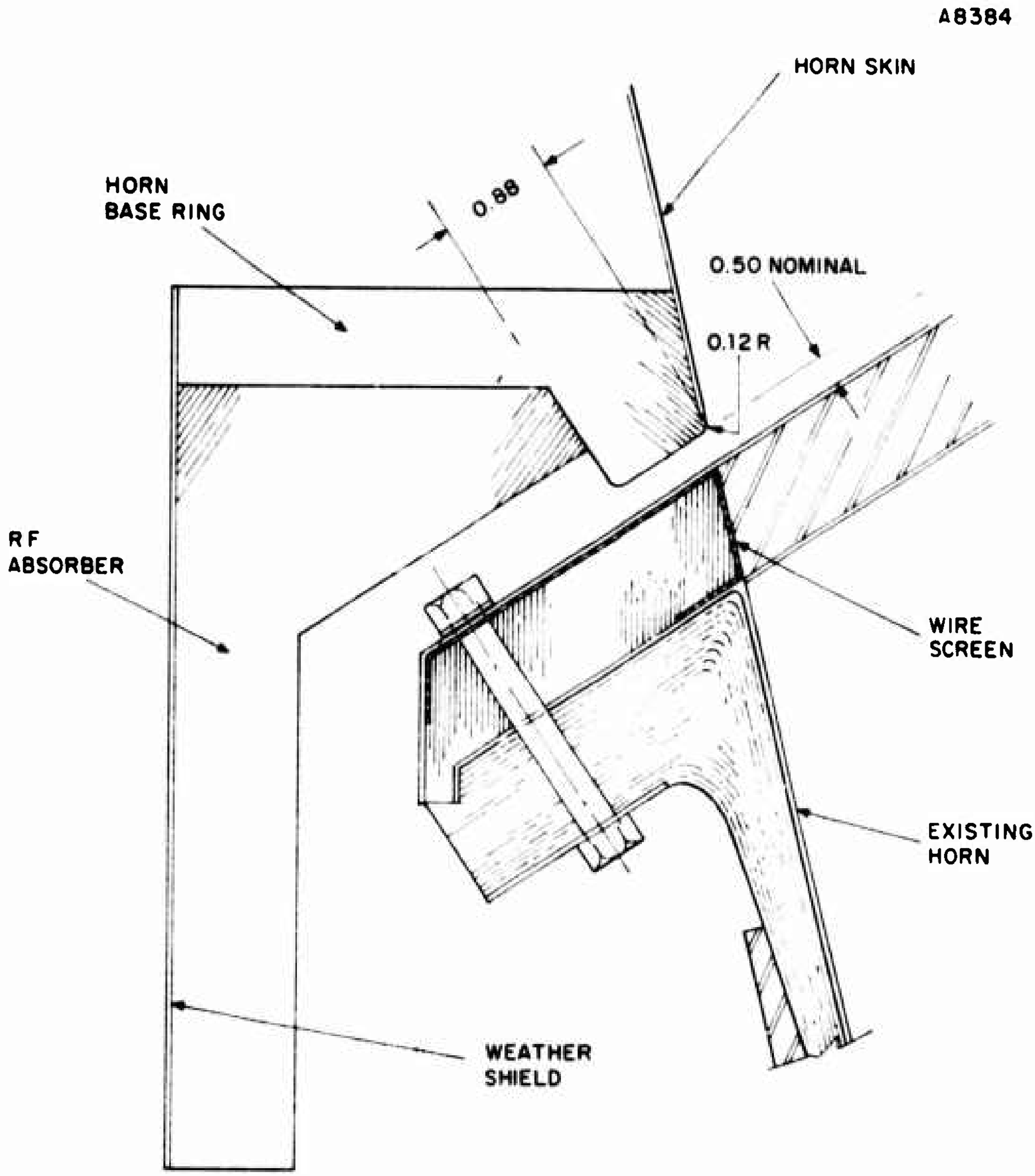

Figure 3. Azimuth Rotary Joint

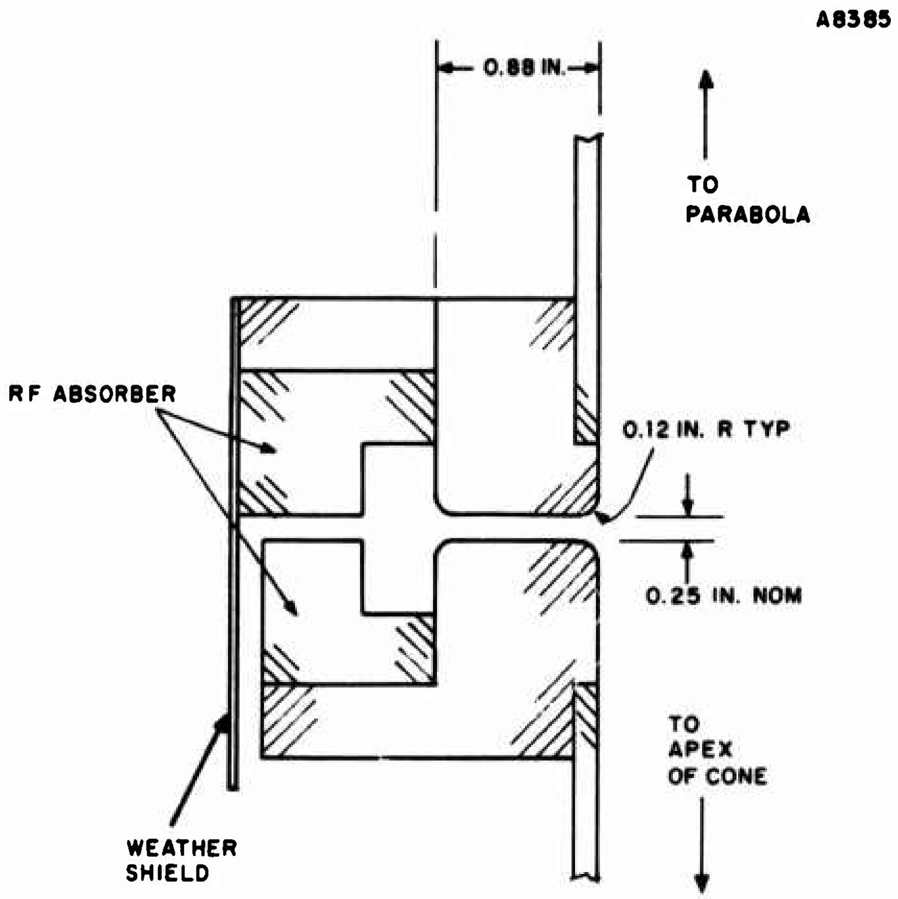

Figure 4. Elevation Rotary Joint

The proper RF performance of the antenna is very dependent on the mechanical structure of the antenna. The conic waveguide must match the nominal shape within one-quarter inch. The reflective surfaces must match the ideal within one-tenth inch. The structure in previous Figure 1 is designed to provide the support to preserve the tolerance. It is discussed in detail in Section IV.

The antenna will operate in either of two modes; slaved to a nearby radar or manually controlled. In addition, provisions were made for manual drive to permit stowing the antenna in case of power failure. In the manual control mode an operator can cause the antenna to move at selected speeds. In the slaved mode the antenna will follow binary position data.

The antenna position is read out digitally to 0.1 degree both in azimuth and in elevation. The position data which the antenna will follow is read out in the same manner. Thus, there will be provisions for the operator to position the antenna to match the incoming data before the control is transferred to the slaved condition. This is discussed in detail in Section V.

One major concern in the control system was the aerodynamically unbalanced load represented by the antenna. The large end of the conic section and the parabola section are offset from the azimuth axis. The large wind torque must countered by the drives. A balancing "sail" could have been installed, but this would have increased the overturning moment which appears as part of the roof load. A heavy duty drive was selected to counter the aerodynamic load.

An interesting structural effect produced a major upset during the antenna installation. The support structure alignment was found to change with time (one example was from before to after a break for lunch). The cause was deflection of the roof beams under thermal load. The upper flange of the roof beams are above the roof and were exposed to outdoor temperature and sun load. The lower flanges are below the roof and were exposed to the indoor temperature. The roof rests on angles near the midpoint of the webs of the 24-in. beams. Differential expansion produced bending of the beams which moved mounting points as much as 1/4 in. during the observation time, which did not include extreme temperatures. The temperature-related changes were reduced to an acceptable level by insulating the beams both above and below the roof, and by shading the roof with a wood platform which provides mechanical protection to the insulation.

Additional detailed documentation has been supplied under this contract. Included are a set of structural drawings of the antenna, an instruction book for the structure (both prepared by the structural subcontractor Fleet Manufacturing Limited), and a technical manual for the control subsystem. Structural and maintenance details are available in these documents.

SECTION III

RF DESIGN

The RF design of the Nanosecond radar antenna was based principally upon the data available in the Bell System Technical Journal. The fundamentals of the design were discussed in Section II.

The design was modeled to ensure that it would meet the contractual requirements. The oversize waveguide to conical horn transition which will be utilized in the first installation was not modeled. It is being Government furnished from the NAROWS program. The mode conversion which is expected to occur there can be corrected, and any future horn would be at least different and probably have much lower mode conversion. Therefore, the model was made with a simple single-mode guide-to-cone transition, with concurrence that this represented the condition under which the specifications should be met. The effects of the mode conversion were computed as discussed in Appendix III. There should be less than 1-dB gain loss, while the first sidelobes may rise as high as -11 dB.

The selection of the model scale was made so the model could be handled with ease, tolerances could be held with assurance, and the necessary test equipment could be assembled readily. The scale factor of one-tenth was selected. This permitted the model to be machined from aluminum. The model was about as large as could be conveniently handled, yet test equipment was available in the frequency range for the tests (31,000 to 36,000 MHz). The model range at the Syracuse Court Street Plant, between Buildings A and B, provided an excellent site for the tests.

The model antenna was built entirely from aluminum. Aluminum plates were welded to form pyramids and boxes as stock for the model. The aluminum was first rough machined (Figure 5) and then welded in place to obtain two assemblies, the folded cone (Figure 6) and the intersecting cone and cylinder. Then the finish machining was performed on each assembly, mostly on a vertical lathe (Figure 6). The parabola surface was machined in one inch aluminum plate stock by a tape controlled 3-D milling machine. The machine control tape was produced from a computer program using the equation for the desired parabaloid of revolution. The tool

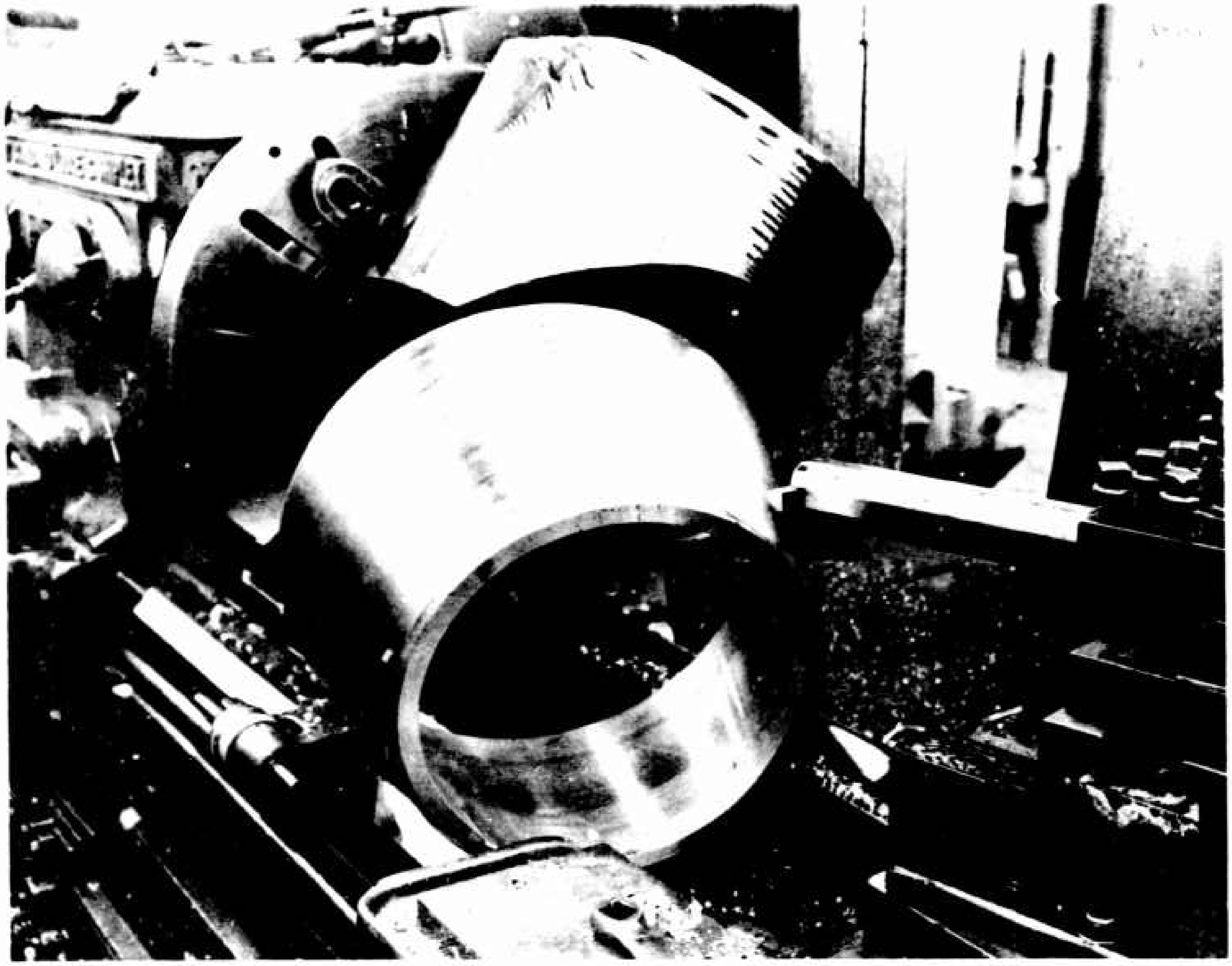

Figure 5. Rough Machining of Cone and Cylinder

Figure 6. Finish Machining of Folded Cone Assembly

employed was a large radius spherical end mill cutter. The machined surface had ridges which were 0.003-in. or 0.004-in. high located between the cutter paths (Figure 7). The ridges were removed by hand. The critical model dimensions are shown in Figure 8 on the cone axis. These dimensions are shown in inches and, of course, are one-tenth the dimensions of the full size antenna. The assembled model, ready for gain tests, appears in Figure 9.

As noted earlier, the model transition from the waveguide to the cone is not a model of the full scale transition. In the model this assembly was made in two parts. One part is an extension of the 25-degree cone from the location of the azimuth rotary joint at the 4.44 inch diameter to the one inch diameter. The second part starts at the mating one inch diameter and continues the 25-degree cone to the geometric intersection with rectangular waveguide. This part was made by turning the cone on a lathe and then using electron discharge milling to machine the rectangular waveguide concentric with the 25-degree cone. The rectangular waveguide is standard Ka band size, 0.280 x 0.140 inches. The apex of the cone is also the focus of the parabola.

The RF chokes necessary at the azimuth and elevation rotary joints were modeled and installed in the model antenna. The rings shown in Figure 10, an exploded view of the completed model, were replaced with model chokes. Both chokes have a gap around the inside wall of conical surface. The width of gaps was accurately modeled, 0.50 inch for the azimuth gap and 0.25 inch for the elevation gap. Each gap is $\lambda/4$ deep in metal, followed by a higher impedance section with one wall of microwave absorber. In the full scale antenna a weather shield is used adjacent to a continuation of the microwave absorber. It was not necessary to model the weather shield-attenuator portion of the joint since the diffraction and reradiation effects of the joints were adequately represented. Leakage levels through the joints will be tested on the full size antenna. The leakage energy has been computed to be far below the level which would affect the radiation performance of the antenna.

The model was pattern tested for the performance characteristics required by the specifications and for other characteristics not specified. Included were gain, beamwidth, sidelobe levels, cross-polarized signal levels and the effects of irregularities on performance.

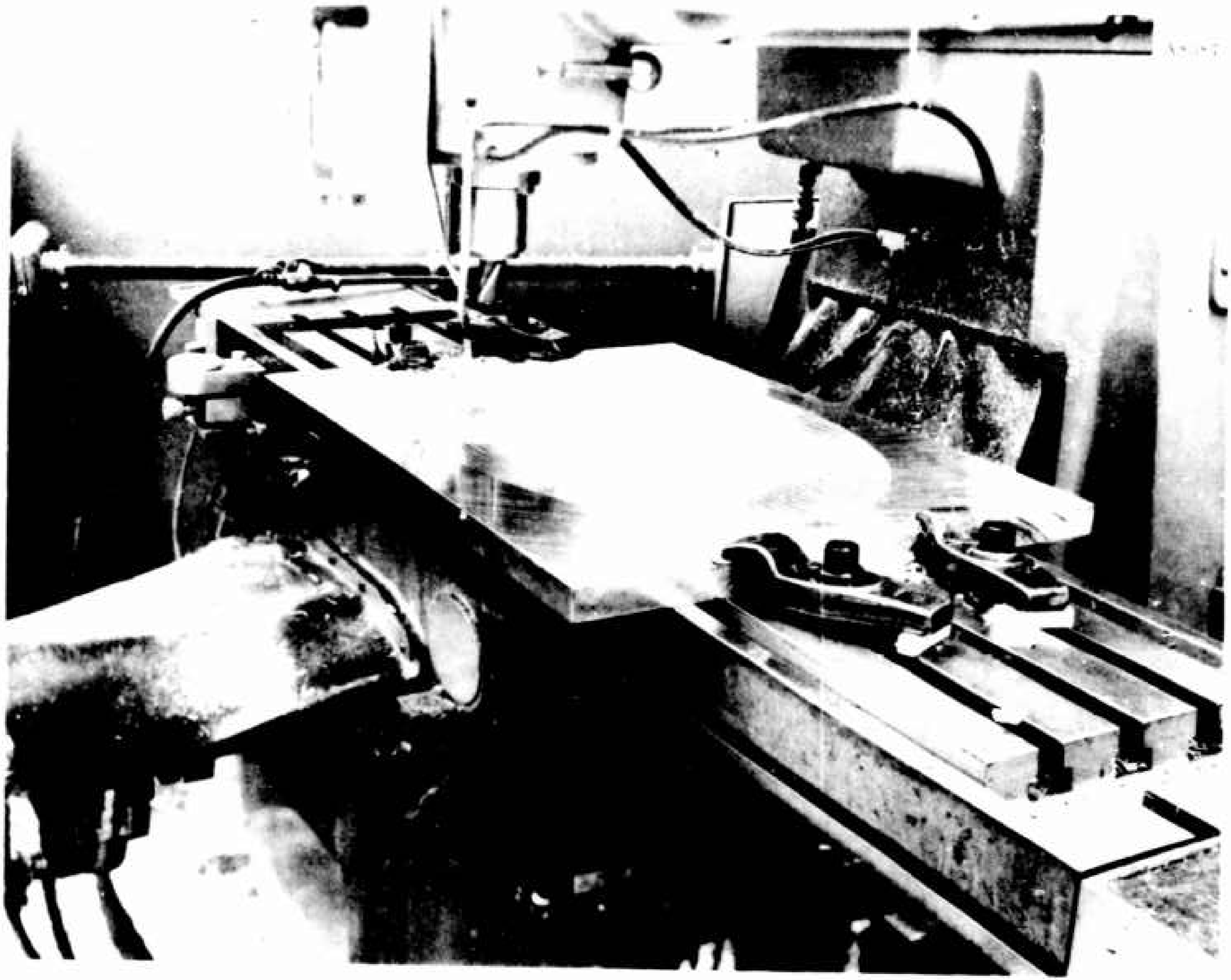

Figure 7. Photo Showing Parabola on 3-D Milling Machine

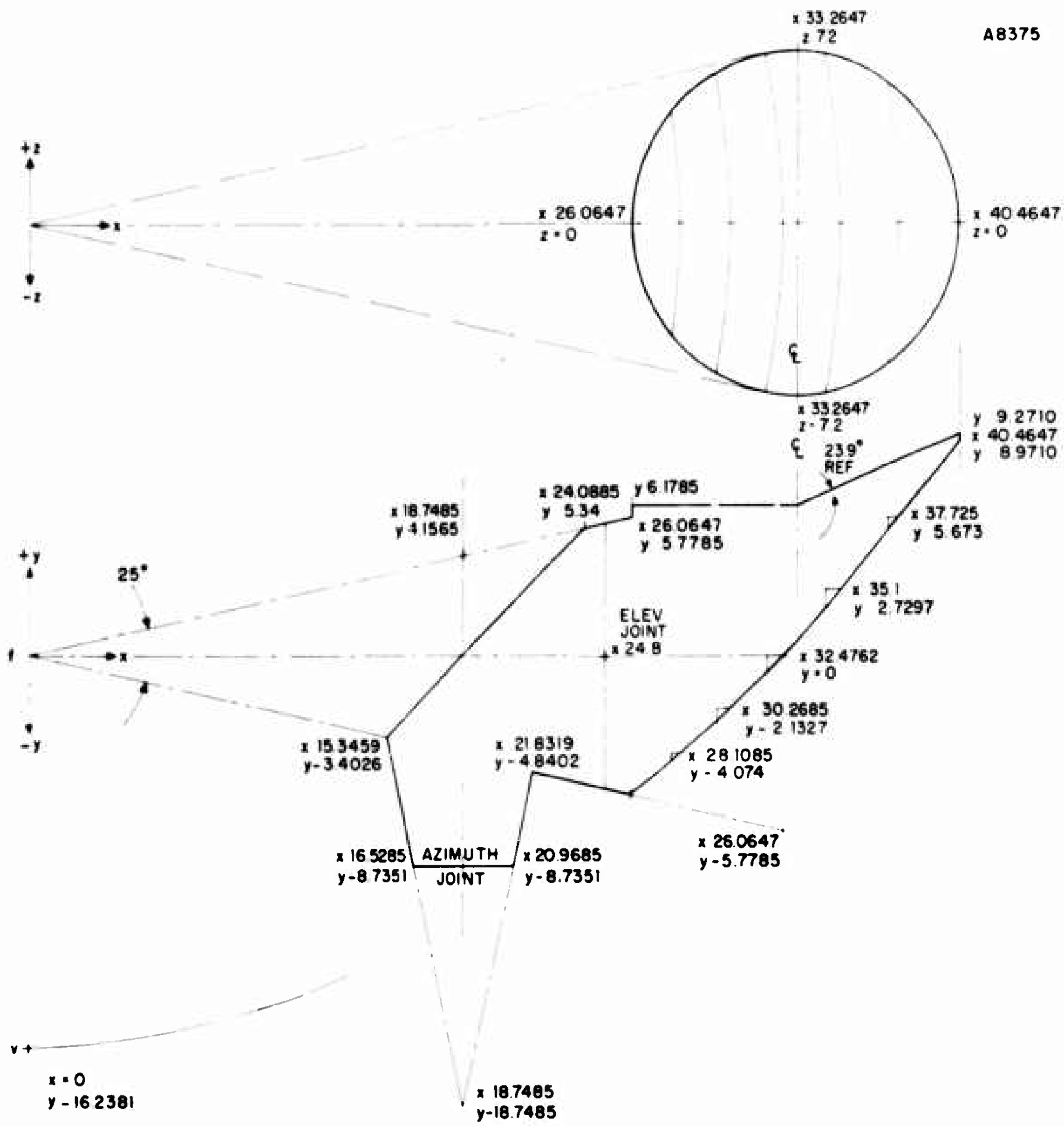

Figure 8. Scale Model Antenna Dimensions

A8388

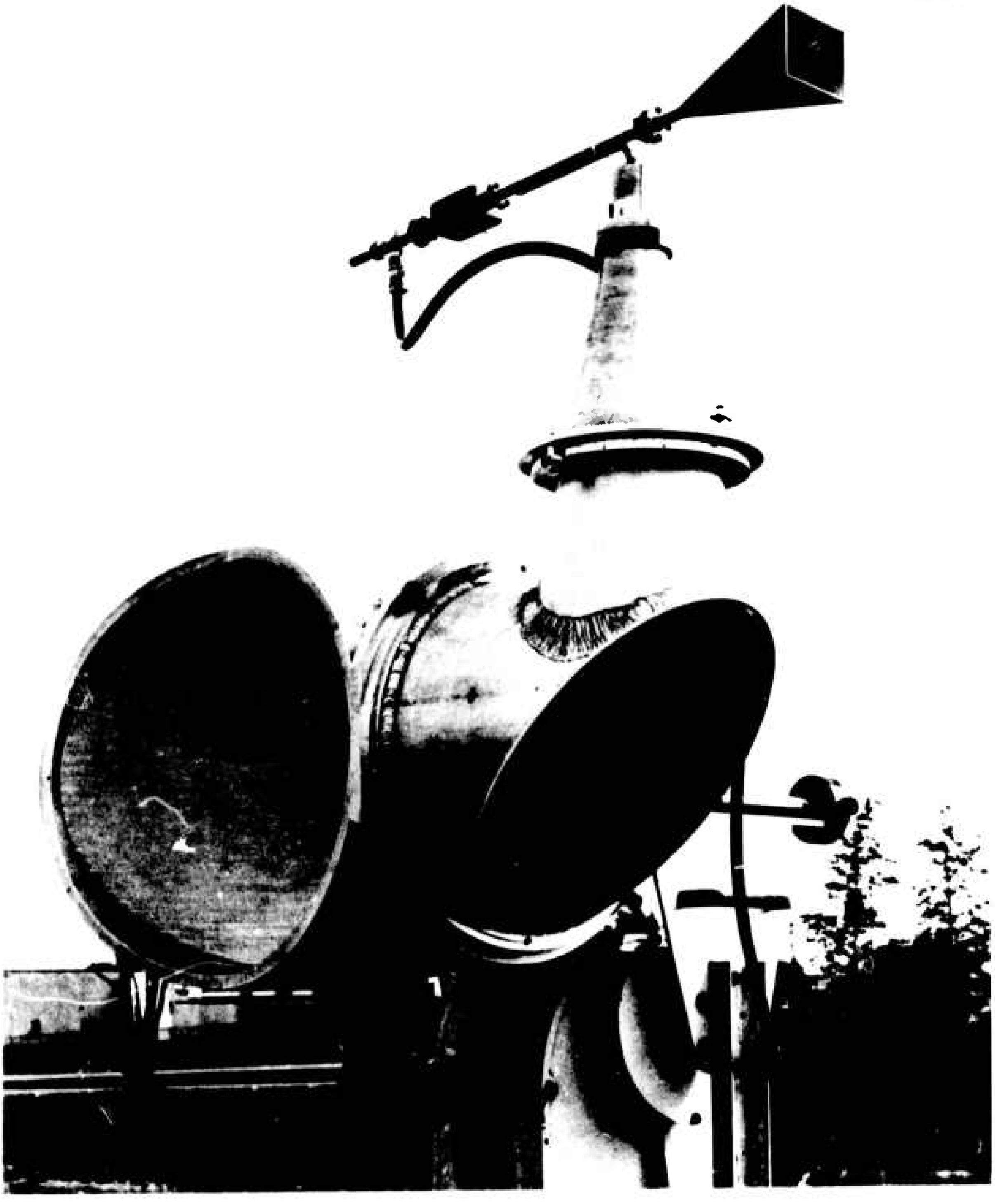

Figure 9. Model Setup for Gain Tests

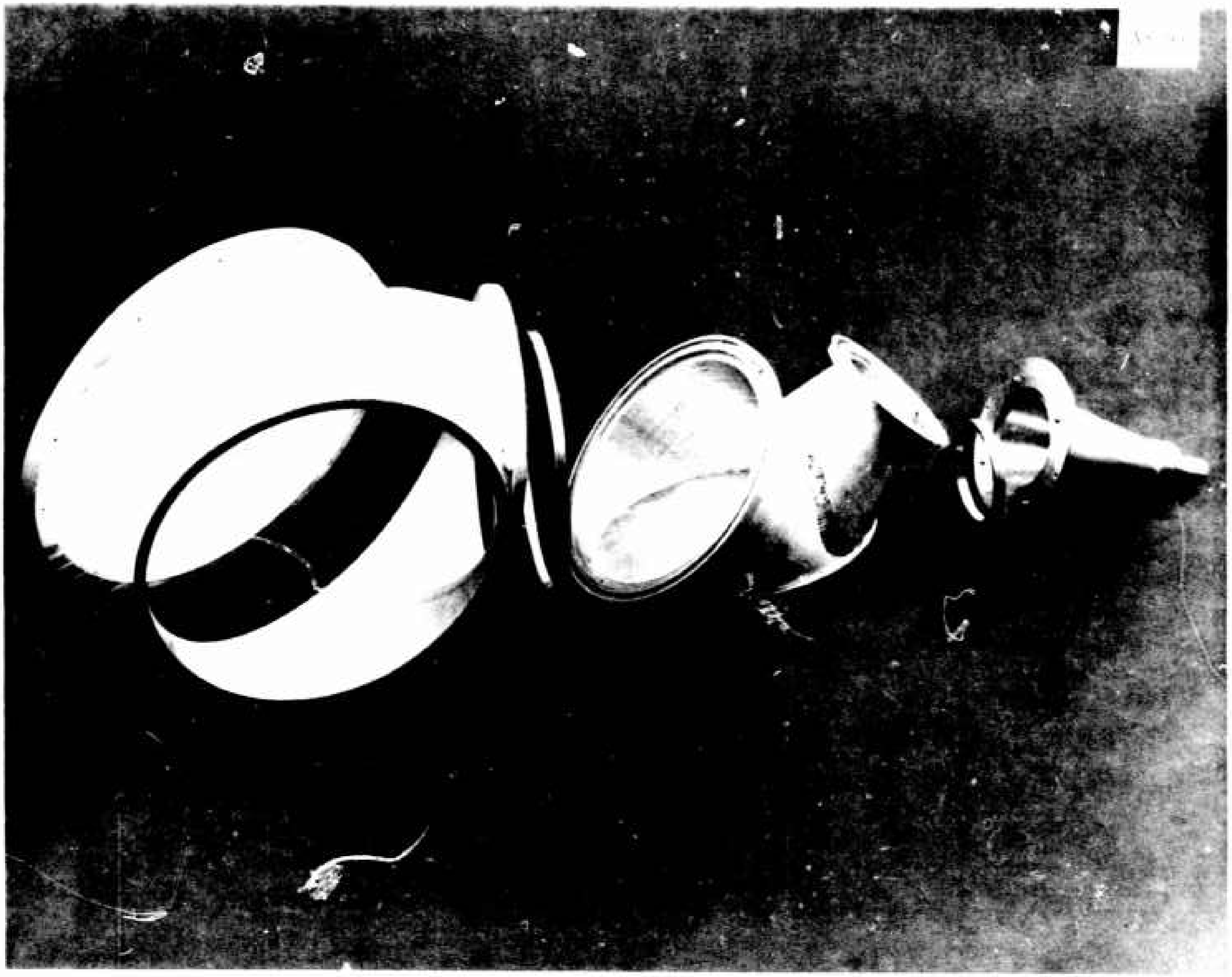

Figure 10. Exploded View of Finished Model

The test mount for the model appears in the photograph Figure 11. The antenna is aimed at the source on the building in the background. The standard gain horn and coupler arrangement on the antenna are arranged for the gain measurement. The pedestal provides elevation and azimuth motion and an additional axis is provided by the shaft mounting the antenna. This permits rotating the antenna to provide a desired polarization independent of the nominal antenna positions. That is, as the azimuth or elevation rotary joint positions on the model are changed, the polarization of the aperture illumination is changed. The polarization axis permits the antenna to be rotated for vertical or horizontal polarization of the aperture. Therefore, the pedestal azimuth motion can be employed for all patterns, either H plane or E-plane.

The model range exists from the roof of the building in the background to the pedestal. The pedestal is mounted on the roof of Building A at the Syracuse Court Street Plant; the source is on Building B. The range is about 140 feet from the source horn to the pedestal.

The Ka band equipment includes a Ku band oscillator in the trailer behind Building B, Ku band waveguide to the box mounted on the roof of Building B, and a frequency doubler feeding through a filter into the source horn, about 3.5 by 4.5 inches in aperture. Flexible waveguide in the Ku band run at the rear of the source housing permits the multiplier and source horn to be rotated through 180 degrees. Thus, any linear polarization may be radiated. At the receiving end an isolator was utilized ahead of the Scientific-Atlanta receiver mixer. A directional coupler permitted combining standard gain horn and antenna outputs so gain measurements could be made without disturbing the receiving equipment. More equipment detaii appears in the test plan, Appendix I.

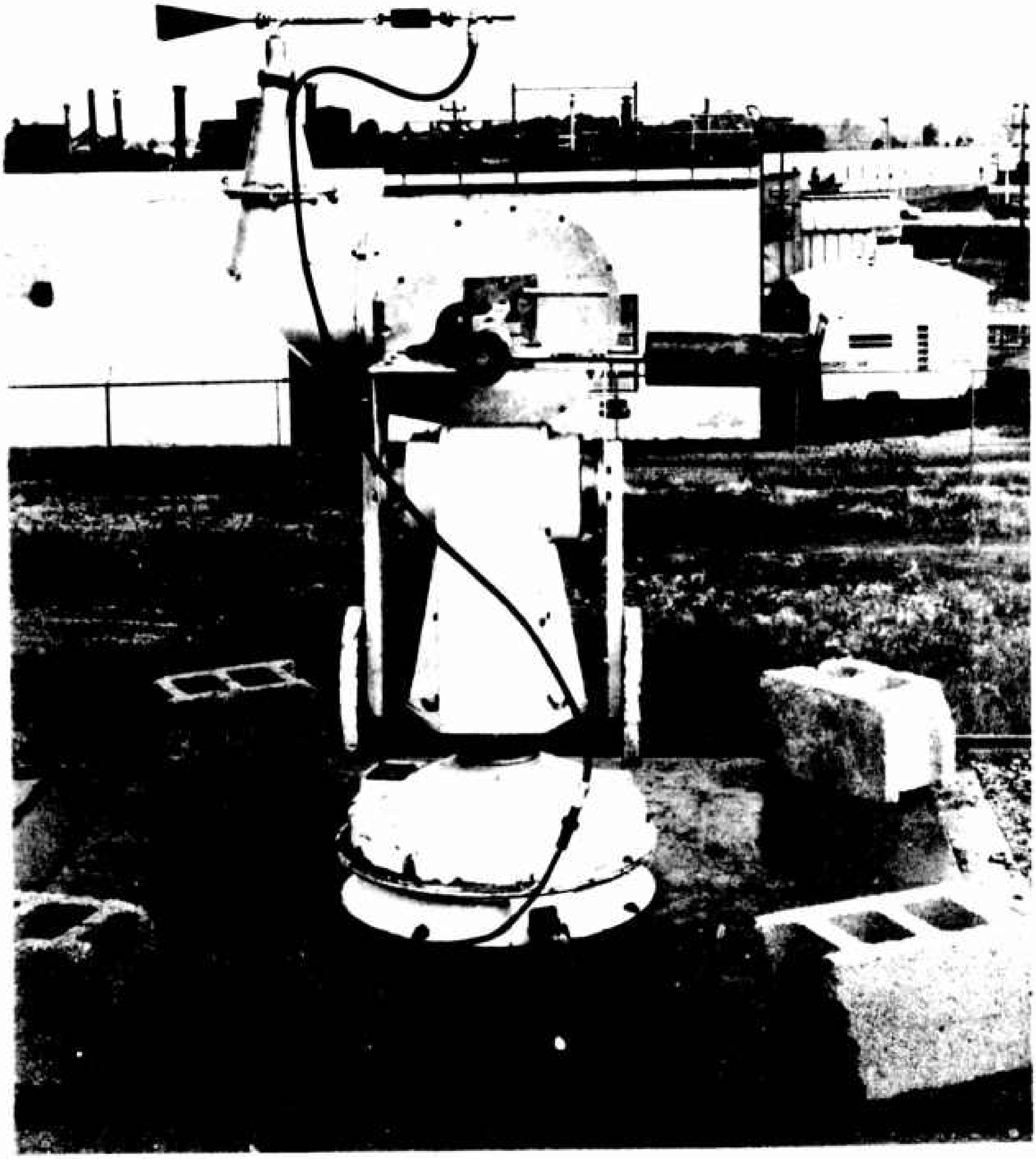

Figure 11. Model Range Setup

Typical pattern results are shown in Figures 12 through 18. A 360-degree E-plane pattern at the upper frequency end of the band is shown in Figure 12. The large returns at the left side of the figure are from the stairway and a chimney on the roof behind the antenna. Spillover past the parabolic reflector appears near the 70-degree point. The exact source of the response at 48 degrees is not known. This source may be the result of multiple reflections within the structure, but its low level, about 37-dB below the peak gain, indicates the potential difficulty of determining the cause. Figure 13 is another 360-degree E-plane pattern. In this case, the spillover is not in the path of the pattern cut. Again, the reflections from the surroundings are apparent.

Typical beamwidth measurement patterns appear in Figures 14 and 15. The expanded scale of the patterns makes beamwidth measurement easy.

The types of patterns taken for sidelobe measurements are shown in Figures 16 and 17. These are for the north-pointed antenna at zero elevation angle. Included are patterns taken in cross polarization, obtained by rotating the source. The low cross-polarized signal level is apparent. The merged sidelobe in the H-plane pattern is typical for this polarization cut in the direction of the cone axis, where the structure is asymmetric. The same effect can be observed in the patterns in the Bell Telephone Laboratories papers.

The typical gain measurement pattern is shown in Figure 18. The technique is described in detail in Appendix I. Briefly, two patterns are taken with a 10-dB coupler between the antennas and the receiver. In one case the direct feed is connected to the standard gain horn, with the 10-dB coupling in the antenna line. In the second case the antenna connections are reversed. The values of the coupling in the directional coupler drop out of the calculation, and the requirement is then only one of stability during the measurement. The values obtained during the acceptance test are higher than one would calculate, by almost one dB. Somewhat lower values were measured during the model test program. The exact cause of the variations are not known, but the variations are well within the range of typical measurement error. The gain readily exceeds the required value of 37 dB, being above 40 dB.

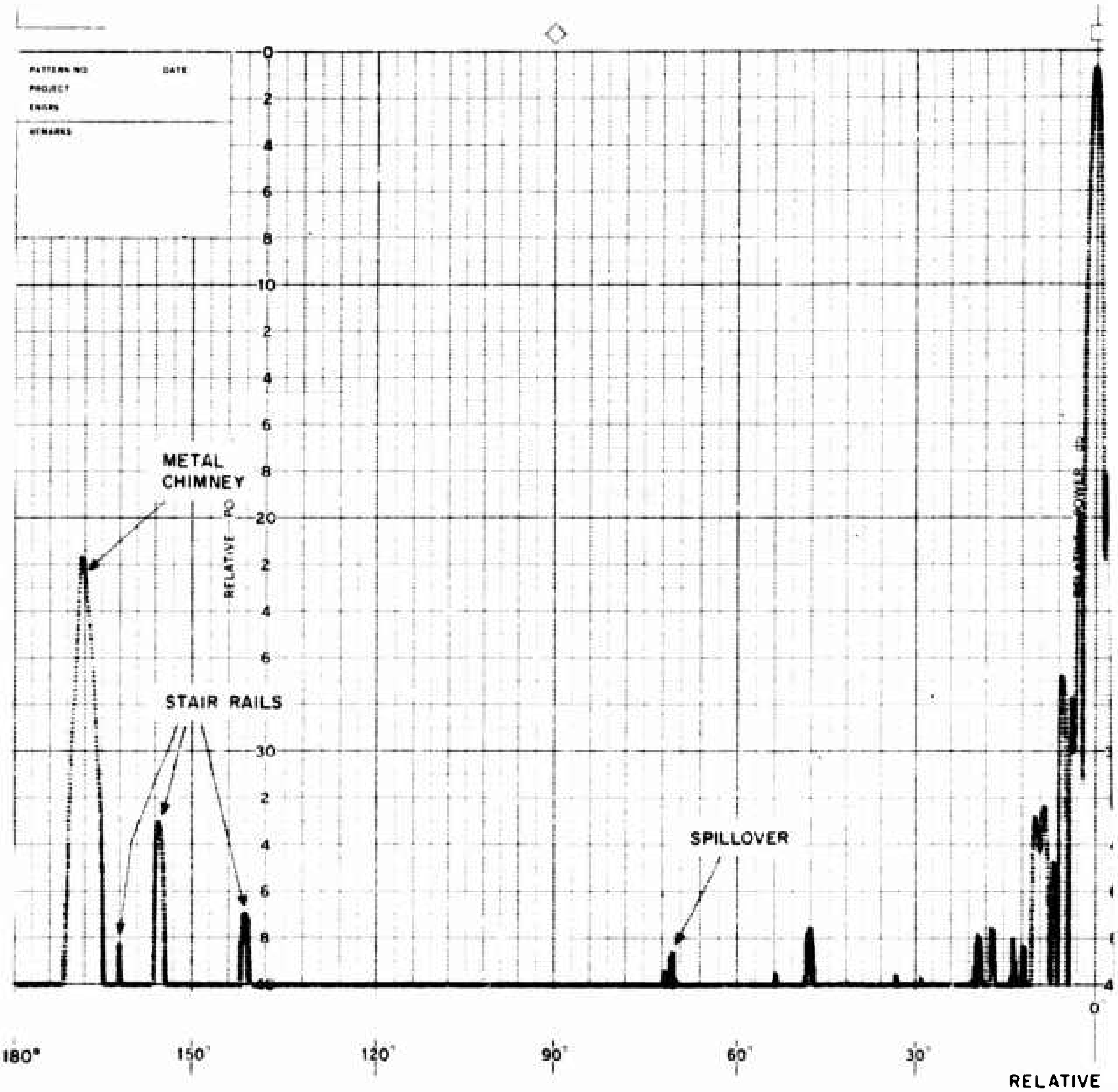

PATTERN NO
DATE
PROJECT
ENGRS
REMARKS
METAL CHIMNEY
STAIR RAILS
SPILLOVER
RELATIVE POWER dB
0
2
4
6
8
10
20
30
180°
150°
120°
90°
60°
30°
0
RELATIVE

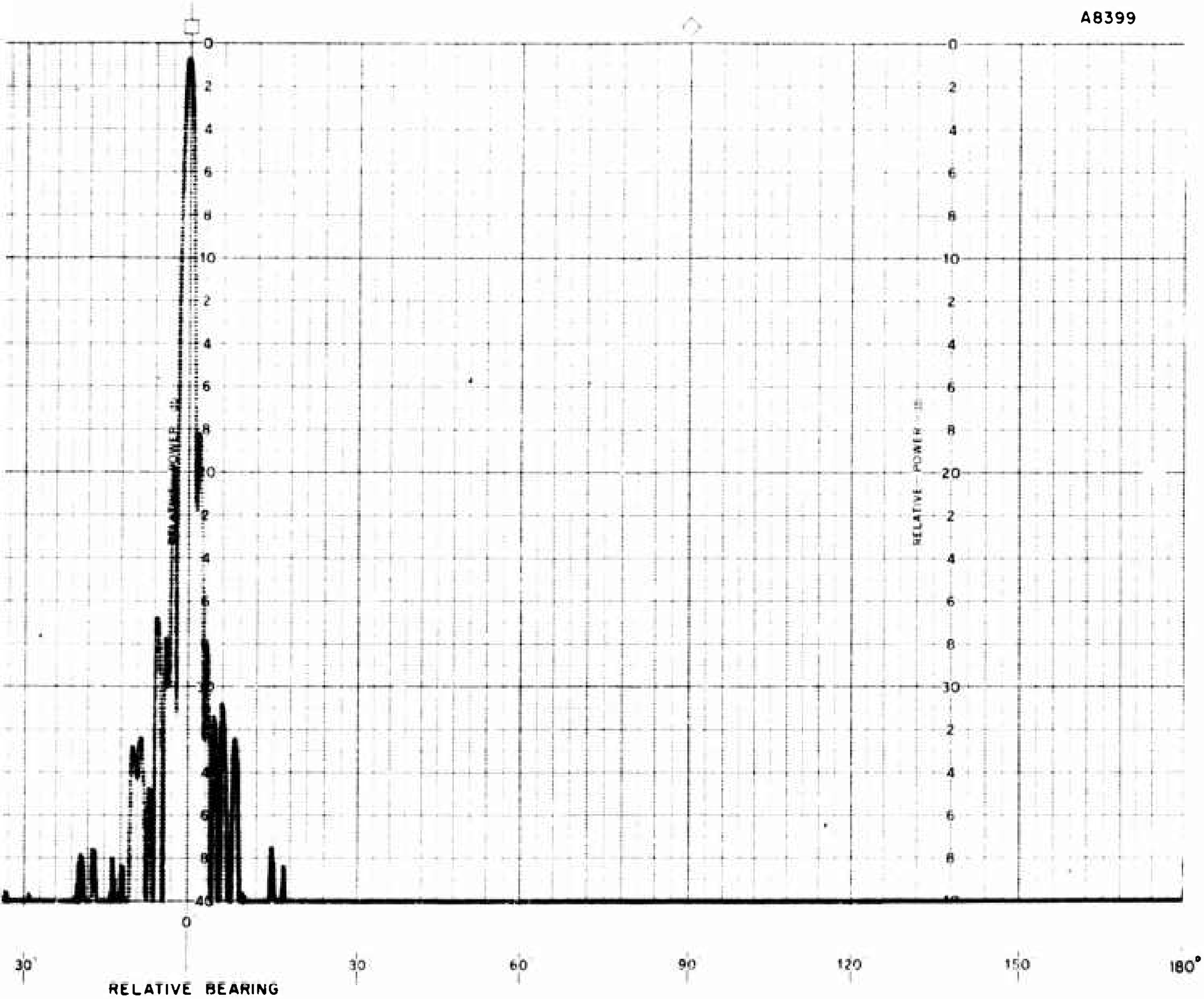

Figure 12. 360° E-Plane Patterns, Cone Axis Direction (E-90-0-EP-360)

A

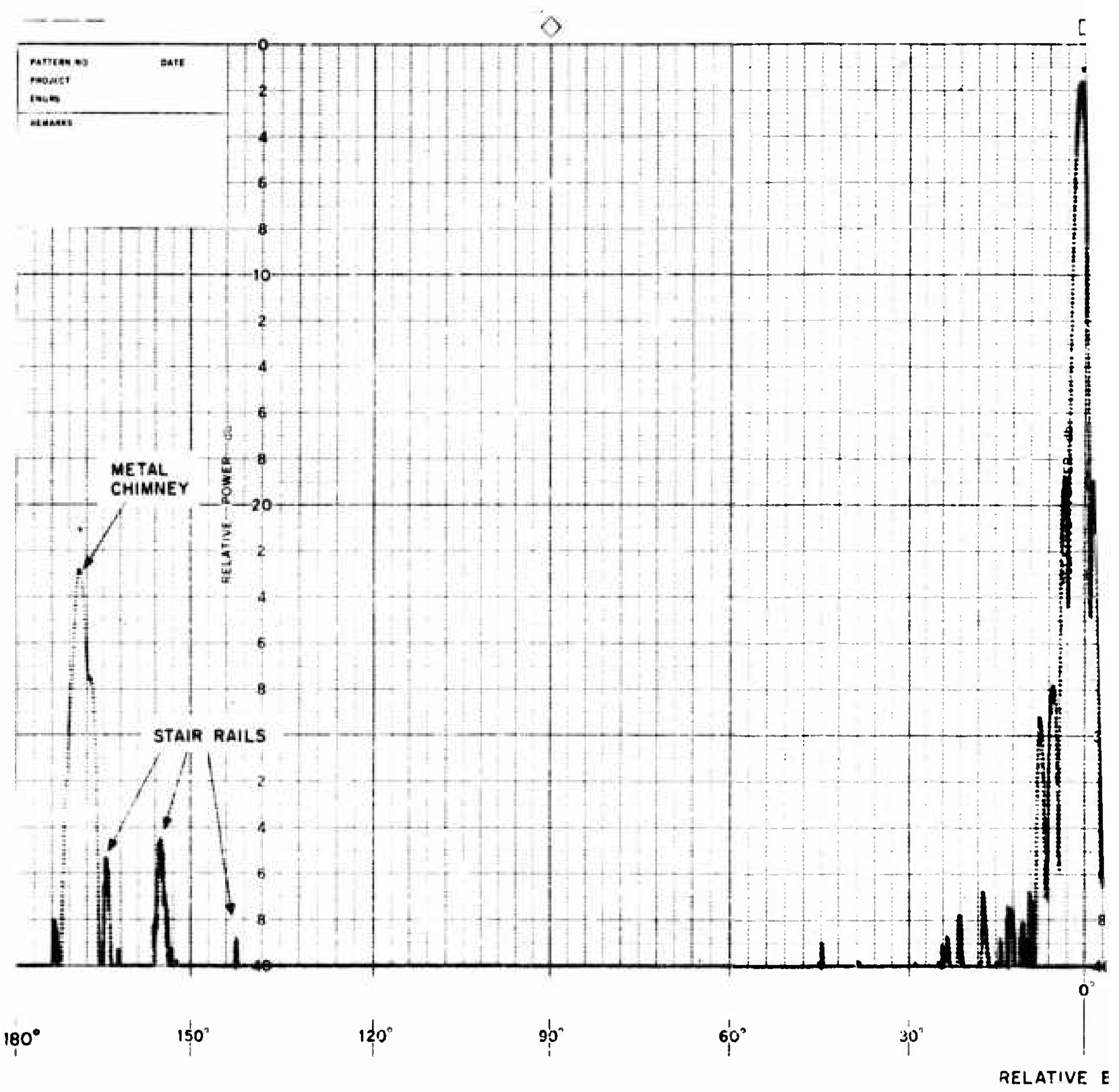
PATTERN NO
DATE
PROJECT
ENG'RS
REMARKS
METAL CHIMNEY
STAIR RAILS
RELATIVE POWER
180°
150°
120°
90°
60°
30°
0°
RELATIVE B

B

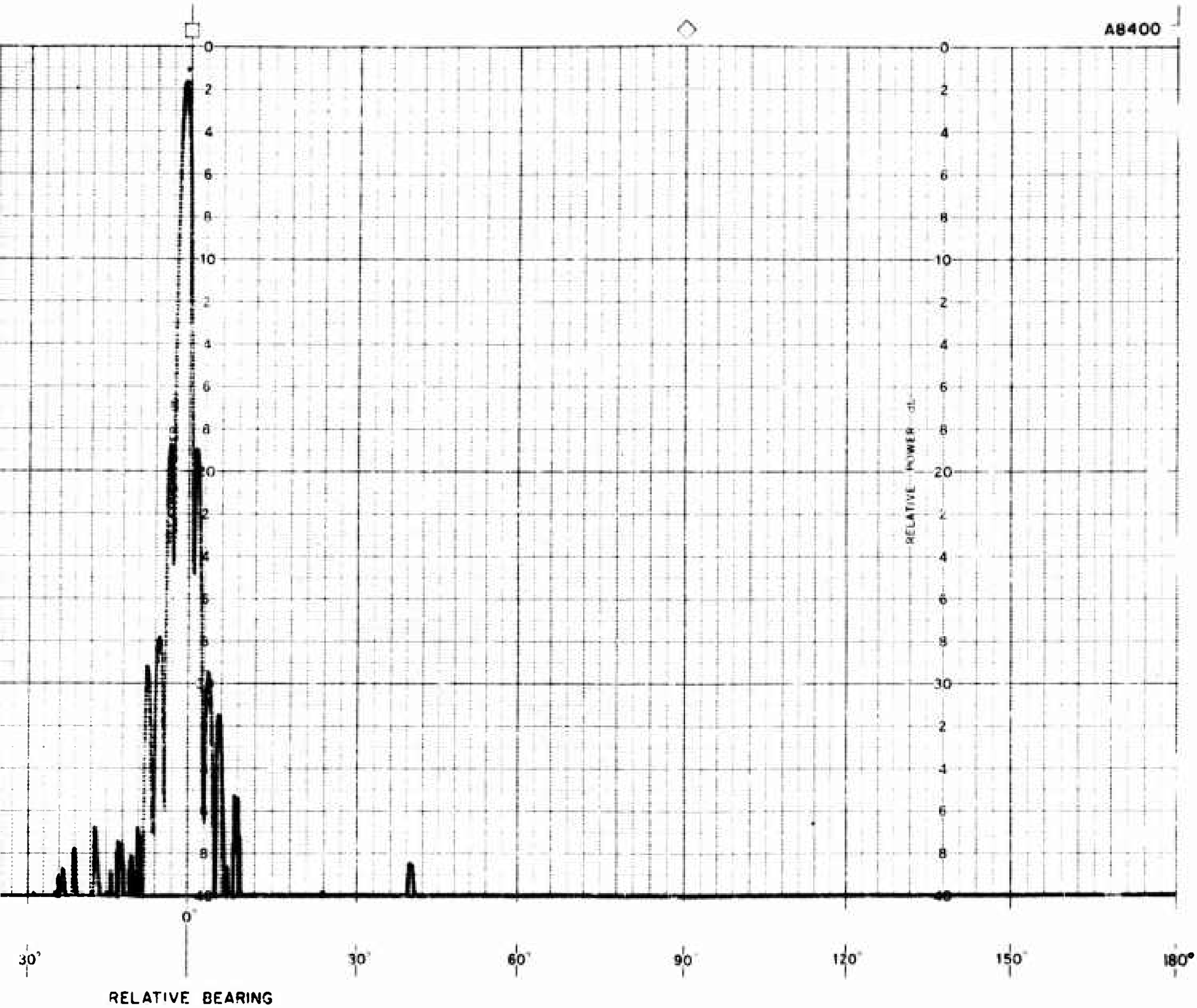

Figure 13. 360° E-Plane Patterns, Transverse to Parabola (C-0-0-EP-360)

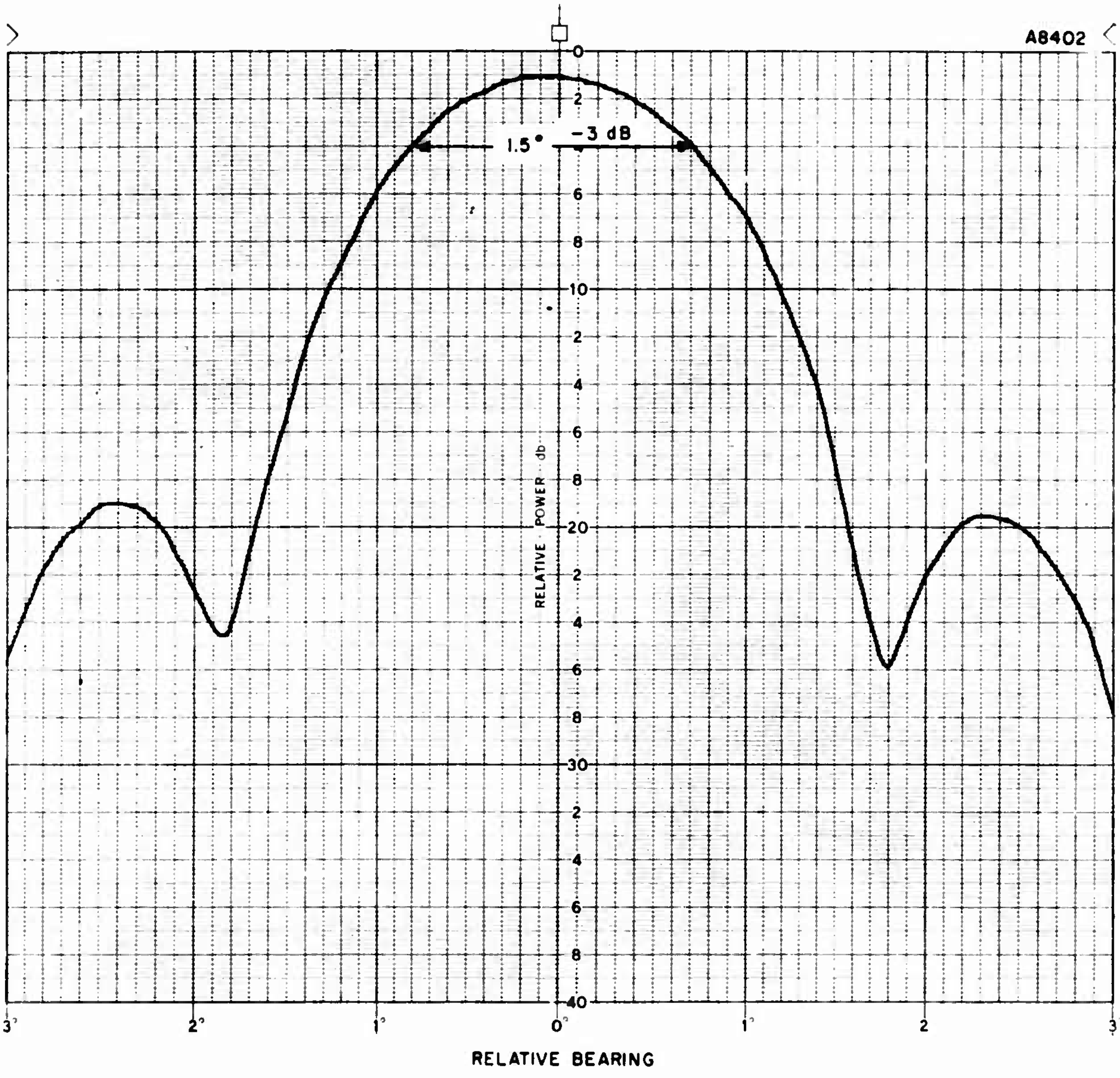

Figure 14. Beamwidth Pattern, E-Plane (C-90-70-EP-12)

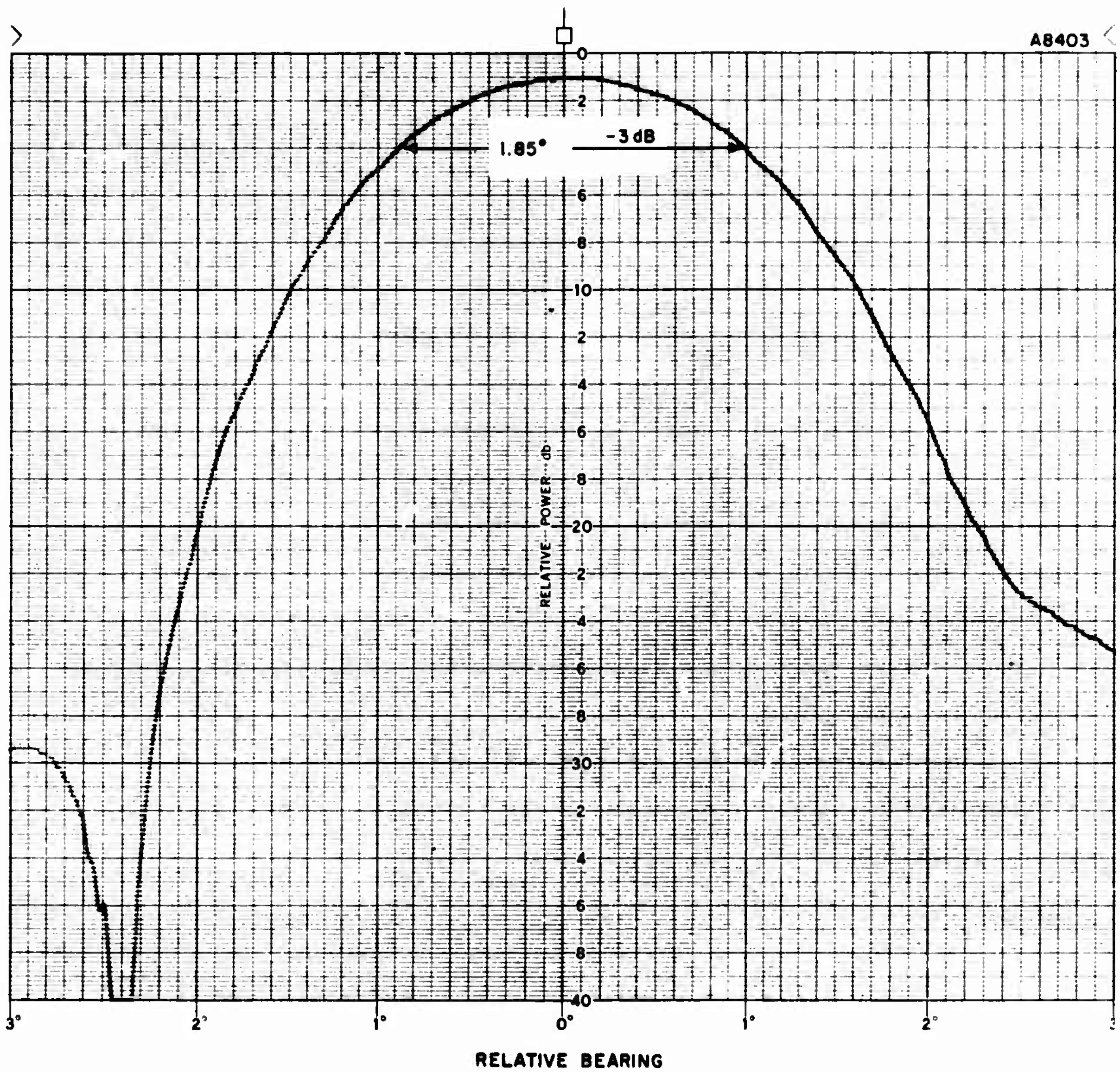

Figure 15. Beamwidth Pattern, H-Plane (C-90-70-HP-12)

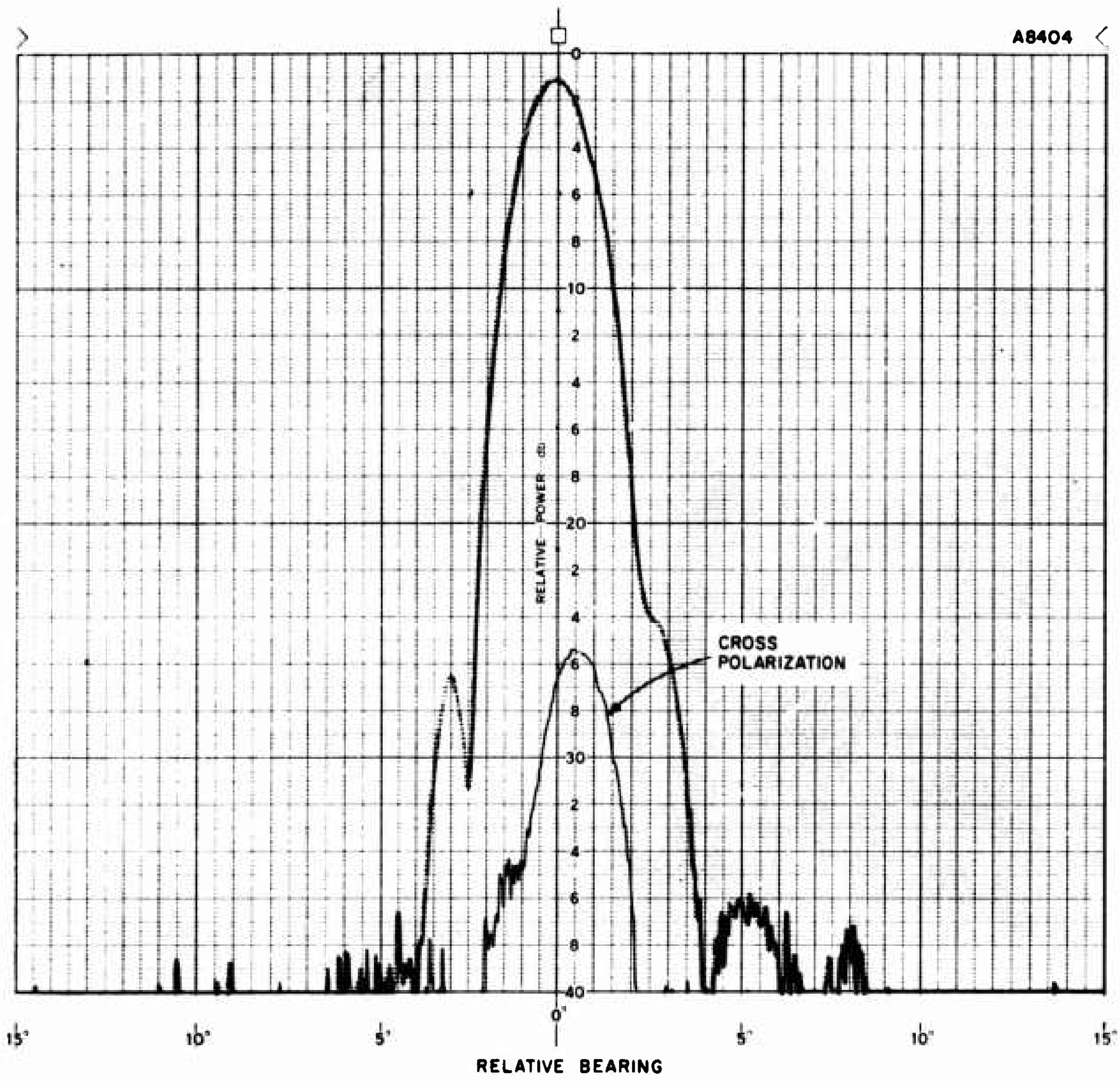

Figure 16. Sidelobe and Cross-Polarization Patterns (C-0-0-HP-60)

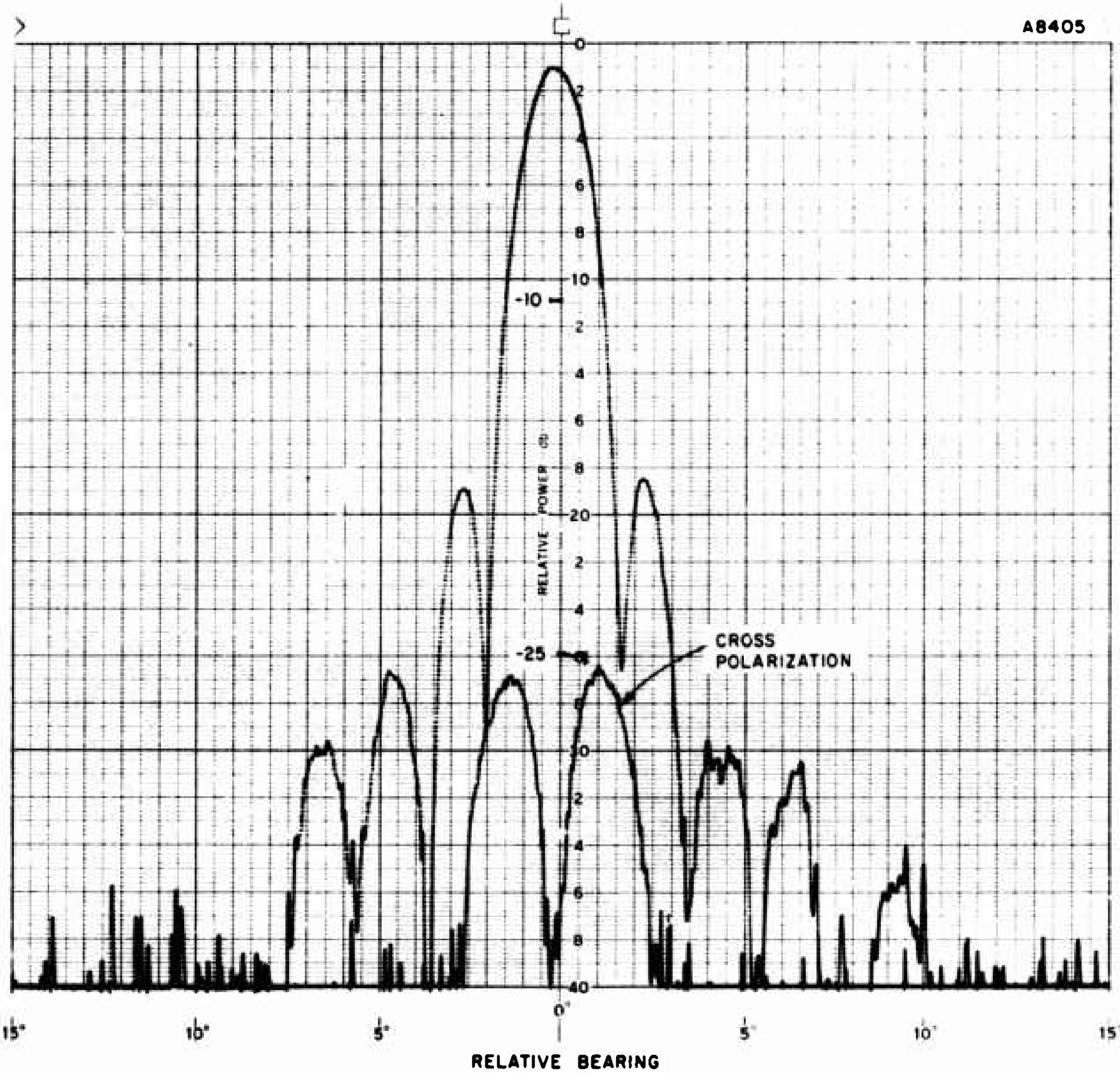

Figure 17. Sidelobe and Cross-Polarization Patterns (C-0-0-EP-60)

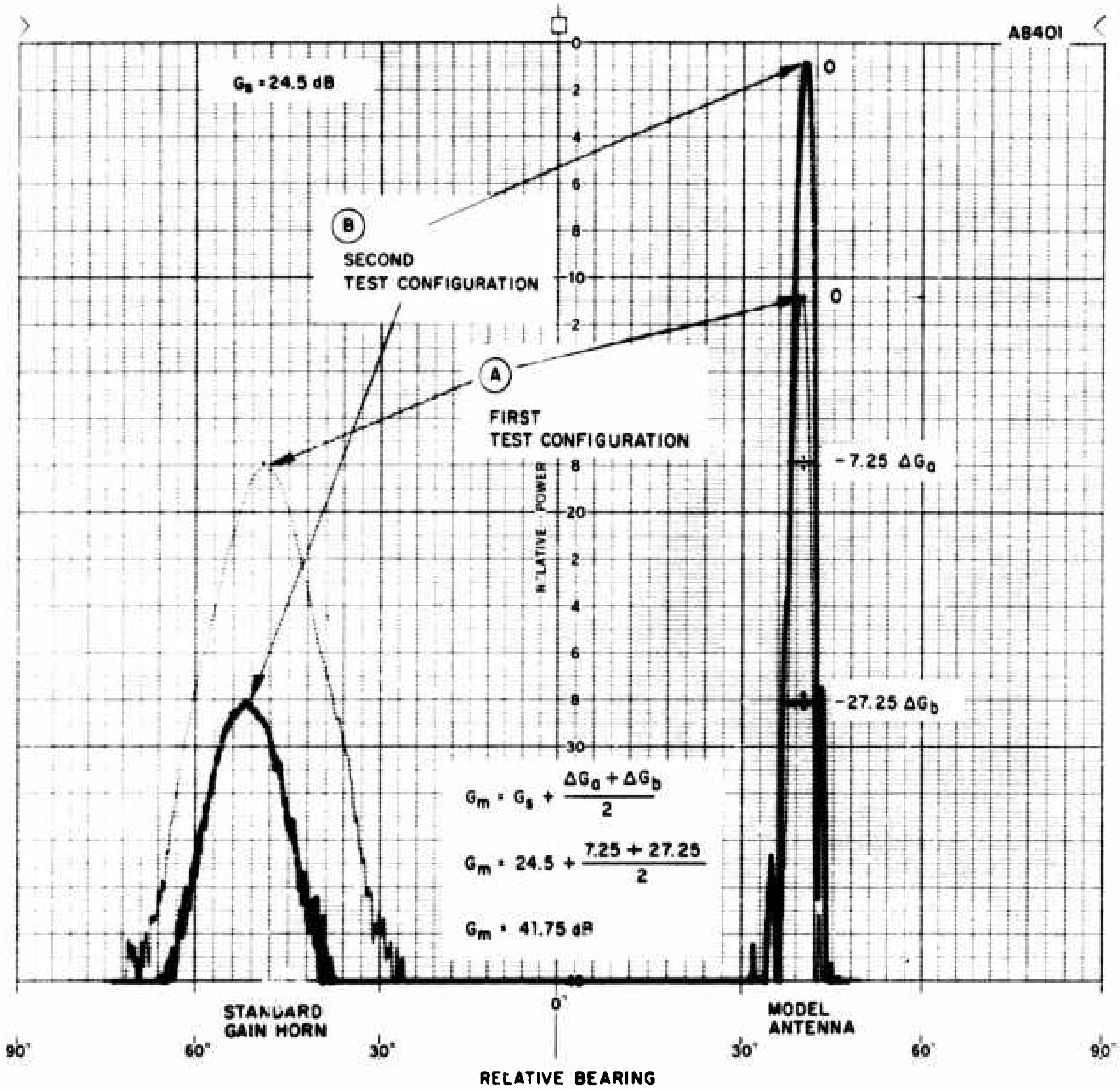

Figure 18. Gain Measurement Patterns

The data measured in the acceptance tests is summarized in Figure 19. The range of first sidelobe levels is indicated; the second sidelobe levels were always lower. It is interesting that the beamwidth and measured gains are compatible, when the product of the 3-dB beamwidths is compared to the area of a sphere.

One convenient way to visualize the antenna performance is an oblique view of patterns taken at close intervals. This approaches a three-dimensional picture of the response. Figure 20 is such a view, developed from patterns taken at 0.5 degree intervals in elevation, the H-plane from +5 to -5 degrees. The patterns run 15 degrees either side of the beam center.

The rotary joints have a minimal choke action. The very large diameter of the gap permits many resonances to occur within the operating band. The gap is backed by absorber material which will damp resonances. The energy flowing into the gap will be approximately equal to the ratio of the gap height to the guide height (joint diameter). In the model tests the insertion loss was not recognizable, nor were there signs of the scattered energy from the gap. Beyond the immediate gap region, the path to the antenna exterior will include absorber material to reduce the energy spilled.

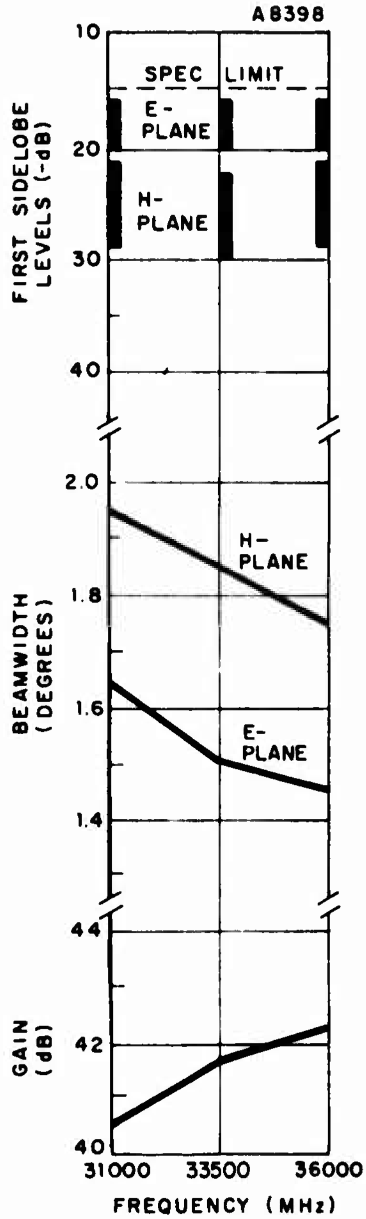

Figure 19. Acceptance Test Results

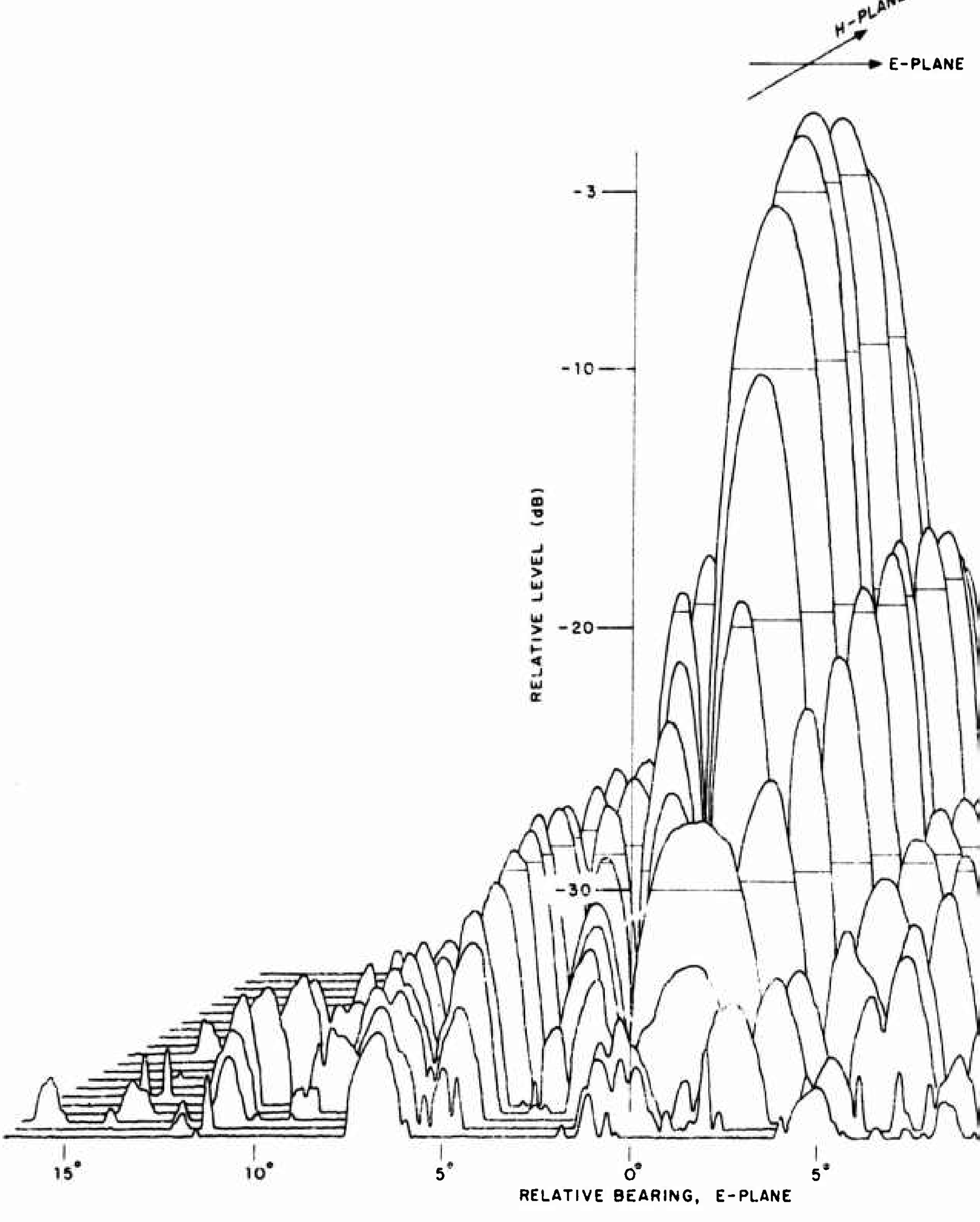

H-PLANE
E-PLANE
-3
-10
-20
-30
RELATIVE LEVEL (dB)
15°
10°
5°
0°
5°
RELATIVE BEARING, E-PLANE

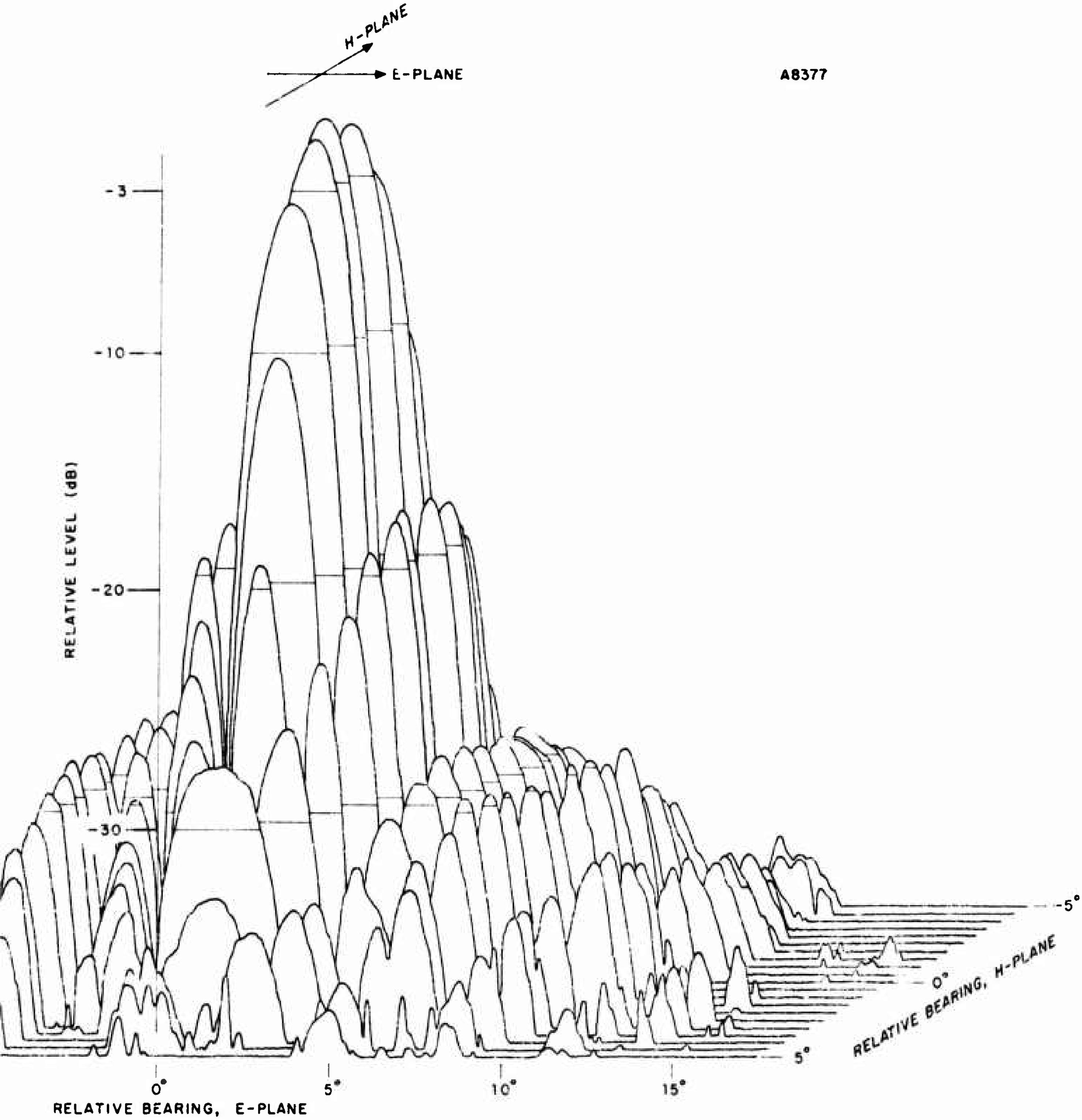

Figure 20. Three-D Model Antenna Pattern

SECTION IV

MECHANICAL DESIGN

1. GENERAL DESCRIPTION

The new antenna design consists of a double-fold conical horn with a planar reflector in the first fold and a parabolic reflector in the second fold as shown in Figure 21. The apex includes the feedhorn which is separated from the remainder of the cone by a horizontal rotary joint making it possible for the terminal equipment to be stationary. The horizontal portion of the cone terminates at a paraboloid reflector section with an intermediate rotary joint to permit rotation of the paraboloid reflector section in elevation.

The entire antenna is supported on an octagonal tower on the roof of the test building. The feedhorn is vertically coupled to the waveguide extending through the roof. The top of the tower supports a 20-ft diameter single rail track on which rotates the triangular turntable supporting a vertical triangular truss and elevation rotary joint. This makes possible the circular movement of the horn in azimuth. The vertical structural frame supports a cam roller assembly and captivates the parabolic reflector portion in its elevation motion about the antenna horizontal centerline.

2. THREE ANTENNA ELEMENTS

The three elements of the antenna are:

- The flat reflector
- The parabolic reflector
- The conical sections

a. The Flat Reflector

For the flat reflector, two alternatives were considered: a sandwich design of two aluminum skins and a honeycomb or foam core, or a single aluminum skin reinforced with aluminum hat sections.

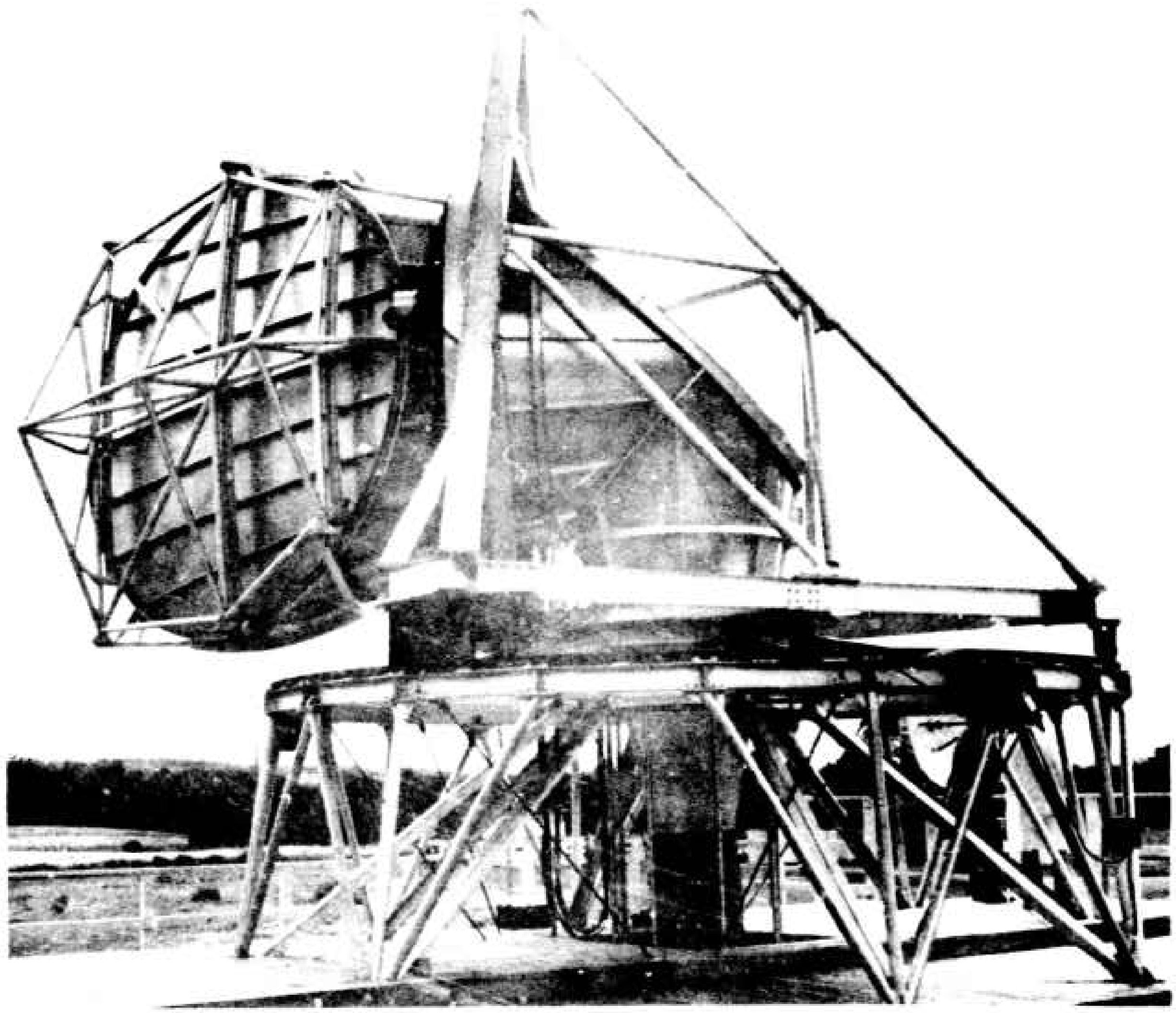

Figure 21. Folded-Conical Horn Antenna Structure

While the sandwich design met the windload stress and deflection requirements, there was fear that the polyurethane foam core would creep with time. Because of the insulation characteristics of the core, it developed that the two surfaces would have different expansions due to temperature differential. This results in a deflection or bowing of the reflector surface which, with sun loading producing a differential of 70°F, would be about 0.43 in. and above the acceptable limit.

The hat section reinforced aluminum plate design has an acceptable deflection under windload, and practically no "bowing" due to temperature differential. This is the type of construction chosen. The reflecting surface has a tolerance of plus or minus 0.100 in.

b. Parabolic Reflector

Three alternatives exist for the parabolic reflector: namely, the sandwich design, fiberglass skin with aluminum stiffeners and aluminum stretch formed skins with aluminum stiffeners. The sandwich design was eliminated because of bowing resulting from the large temperatute differential between the two faces. The fiberglass skin and the aluminum stretch formed skin with 3/8 in. x 3 in. rib stiffeners represent two fabrication techniques yielding similar performance.

While both of these latter alternatives had about the same minute deflection due to temperature and acceptable wind-load deflection, the final choice was stretch aluminum skins with rib stiffeners. The parabolic reflector tolerance is plus or minus 0.100 in.

c. The Conical Sections

The sandwich design was not considered for the cone sections due to thermal gradation problems. Also, aluminum stiffeners would be required whether the cone sections were made of reinforced fiberglass or aluminum sheets. Therefore, it was decided to make the sections of aluminum skin, reinforced with aluminum hat sections.

The vertical conical section from the azimuth rotary joint to the flat reflector and horizontal-portion transition flange is made of 0.062 in. aluminum skin axially reinforced with 2 in. x 4 in. hat sections riveted to the cone at an average of 2 ft apart. The cone is stiffened by a 3 in. channel around the circumference and held by an angle bracket and a 1/2 in. thick, 56 in. inside diameter aluminum flange.

The second and horizontal cone portion up to the elevation rotary joint was built in similar fashion.

The final elbow from the rotary joint to the exit aperture, which includes the parabolic reflector, was also made of 0.062 in. skin reinforced by 2 in. x 4 in. hat sections. The exit flange is 2 in. x 3/8 in. flange and 2 x 2-1/2 x 1/4 in. angle section around the circumference; the 45° transition has 3 in. x 0.375 in. flanges. The hat sections are anchored to the flanges. The contour tolerance on the conical surfaces is 0.250 in.

3. FRAMING FOR SURFACES

The hat section method for stiffening the skin of the various conical sections has already been described.

The parabolic reflector is stiffened by 0.375 in. aluminum ribs 3 in. to 5.57 in. wide, spaced 15 in. to 18 in. apart and mounted normal to the reflector.

The flat reflector is stiffened by extruded aluminum hat sections on 12 in. centerlines.

4. SUPPORT STRUCTURE

a. Substructure (Tower)

The tower in plan has an octagonal configuration resting on the roof beams on eight pads. Each supports a vertical leg of 3 in. standard aluminum pipe. The top cord elements are 6 in. x 6 in. wide flange I-sections. The diagonal braces are also 3-in. standard aluminum pipe.

The center is open to allow for the bottom vertical portion of the antenna conical section.

b. Antenna Support Truss

The rotating antenna-support truss has a triangular-shaped base with one supporting crane-type wheel in each corner on the 20-ft diameter track. Two of these wheels are power driven and one is an idler. The power driven wheels are more heavily loaded than the idler wheel and include the drive gear.

One leg of this horizontal triangular base is also the bottom portion of a vertical triangular truss. This envelopes the horizontal portion of the cone approximately in the plane of the elevation rotary joint and supports that portion of the antenna that rotates in elevation.

The other two sides each become the bottom portion of two triangular structures having a common point at the idler wheel corner and another common point at the top apex of the previously described vertical truss.

5. DRIVING MOTION

a. Azimuth

The antenna rotates in azimuth supported within the previously described triangular base truss structure with a flanged wheel on each of the three corners. Two of these wheels are in the vertical plane of the vertical truss supporting the elevation rotating portion of the antenna. These two power driven wheels carry 3200 lbs each. The remaining 800 lbs is carried by the idler wheel. The two drive wheels are driven from two separate motors, and are gear-and-shaft connected for purposes of adhesion.

Overturning moments resulting from wind forces will produce weight transfer from one driving wheel to the other. Reference to the accompanying curve (Figure 22) illustrates the relation between percent adhesion on the lightest driving axle and wind load in knots in a direction of worst weight transfer. Railroad experience permits an evaluation of the required adhesion.

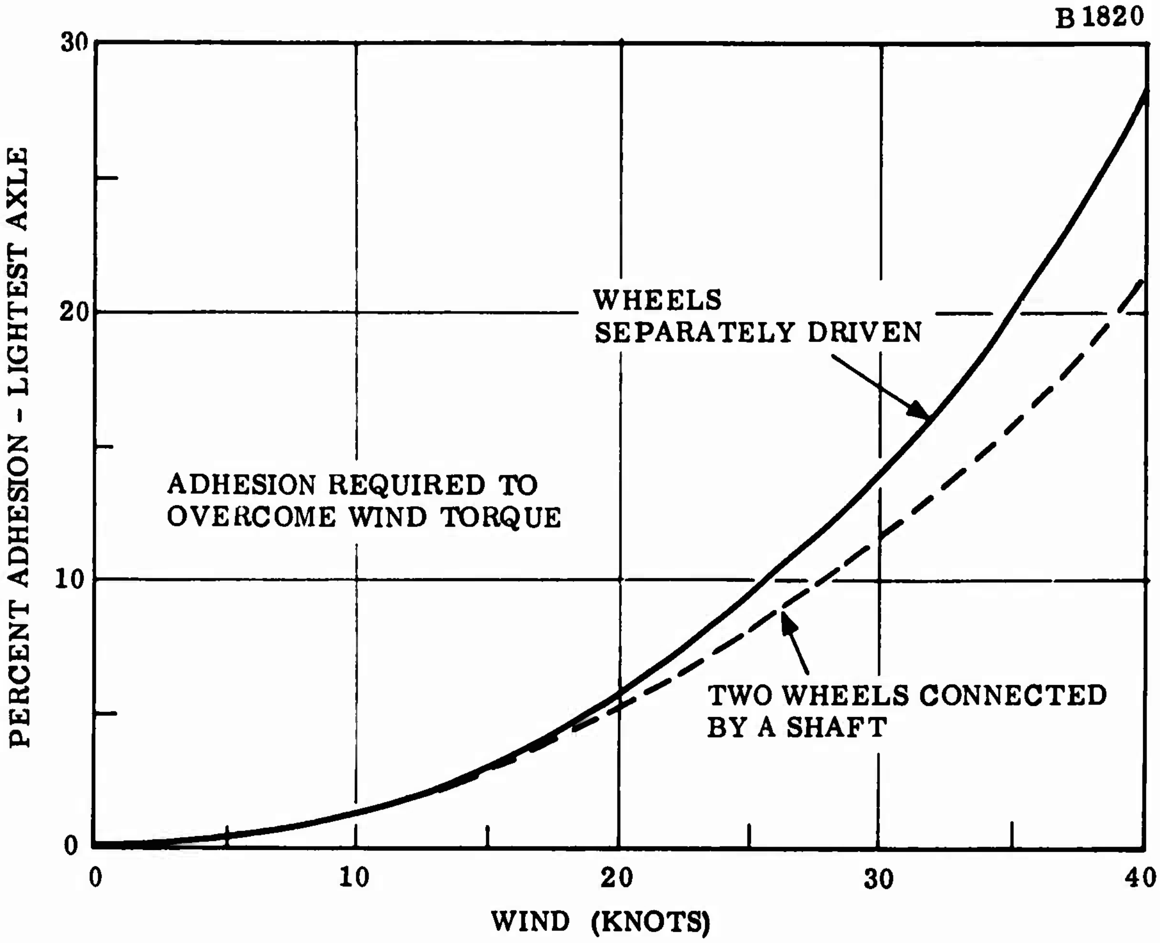

Figure 22. Relation Between Wheel-Rail Adhesion and Wind Velocity

For railway locomotive propulsion purposes, 24 percent is considered to be a good adhesion figure to use at low speeds. In the antenna, this adhesion occurs at 37.5 knots wind speed. In other words, with the 40-knot wind requirement and 28 percent adhesion, the equipment is just borderline on requiring - or not requiring - a connecting shaft to compensate adhesion to weight transfer. However, the connecting shaft was used with a resulting conservative 21.3 percent adhesion at 40 knots wind speed.

The superstructure is centered in azimuth by a ring and guide wheels around the azimuth rotary joint. These guide wheels have an eccentric center adjustment for the purpose of changing their center location and guide ring clearance.

b. Elevation

The elevation drive is from a gear rack enveloping 360° of the cone on the rotating side of the rotary joint. The outlet aperture can be moved from approximately the top to bottom center. The bottom center is the weather protected "out-of-service" position. The reduction to the low two r/min rotational requirement from standard motor speeds places quite a burden on the gear reduction facility. This has been resolved by the application of a harmonic-drive type gear assembly with a 180 to 1 reduction which combined with the ring-gear pinion drive results in a reduction of 2500 to 1.

Centering and support of the elevation section of the antenna is accomplished by rollers riding on the edge of a radial flange mounted to the rotating side of the elevation joint.

6. CHOKE AREAS

The azimuth and elevation choke joints were described in Section II. Radite 75 was cemented into place as the absorber.

7. LOAD ANALYSIS

The following briefly summarizes the load analysis. More detail appears in Appendix D.

a. Total Weight

The total weight of the antenna is less than 13,000 lbs using aluminum construction for the tower and eight support feet or pads.

b. Roof Loading

With an 80-knot wind speed, one pad could have a load of 7200 lbs and with a different wind direction there could be a lifting force of 1083 lbs.

c. Track Loading

With an 80-knot wind speed, the maximum track single-wheel load could be 7025 lbs. The under-rail-head stow clamp will prevent the idler wheel from leaving the rail under another 80-knot wind speed where there could be a lift of 2610 lbs from certain azimuth angles.

d. Drag Coefficient

For purposes of calculating wind loading, the following drag coefficients were used from Hoerner's book on Fluid Drag (Reference 9):

Conical Section	$C_D = 1.3$ (Endwise)
Structure Members	$C_D = 2.0$
Flat Plate	$C_D = 1.5$
Cylinder	$C_D = 1.17$

e. Roof Beam Deflection

The maximum roof-beam deflection at the point of maximum load with an 80-knot wind is 0.29 in. The maximum at a 40-knot wind is 0.1 in. or less.

SECTION V

CONTROL SYSTEM DESIGN

1. DESCRIPTION

The NARHORN antenna controls provide several methods for directing the antenna. The antenna may be positioned about the azimuth and elevation axes by position servos. These servos normally follow a tracking antenna located some distance away. There is also an optional velocity mode, in which the operator can position the antenna by slewing it to any desired position using manual controls. Finally, there is a completely manual mode, permitting hand cranking the antenna at the mount, independent of the servos.

The two servos are similar. Each contains digital processing circuitry, which compares the command signal from the remote antenna with the local antenna's response signal and converts the difference from binary form to an analog voltage. The associated power circuitry takes the analog output of the digital processing circuitry and produces the power needed to drive the servomotors, their associated gearing and the mechanical drives. Each also contains readout circuitry, which converts and displays the directed and actual position information in both azimuth and elevation in decimal number format. There are separate power supplies for the output stages of the power amplifiers. The power requirements for the azimuth motion are high; there is a motor-generator (M-G) set driving the azimuth servomotors. In elevation, the motor is driven directly from the power amplifier.

The main power input to the antenna positioning system is four-wire 208 V ac 3 PH 60 Hz. Control circuitry distributes power to the various supplies and the azimuth M-G set. This circuitry also contains various interlocks and overload protection.

All of the electronic circuitry is mounted in a six-foot cabinet. The azimuth M-G set is located separately. The electromechanical components such as motor-tachometers, position encoders, limit pots and switches, are located on the antenna.

Figure 23 illustrates the general configuration of the antenna positioning system.

2. SERVO DESIGN

The two servomechanisms are Type 1, tachometer-stabilized, using dc motors as the power elements. In elevation, the motor is a 1/4 hp, 1700 r/min unit geared at 2500 to 1 and providing slew capability up to 0.6 r/min (3.5°/s). For azimuth, a total of 3 hp is required to provide slew velocities up to 18°/s. Sufficient torque is available about each axis to operate continuously in winds up to 15 knots, with gusts up to 40 knots.

Figure 24 is the block diagram for the azimuth drive system and Figure 25 the block diagram for the elevation drive system. The two are similar. The major difference is that the azimuth system has the M-G set mentioned previously and operates over a larger range (450° versus -90° to +70° in elevation).

The input commands are received from the remote antenna on a single Alpha Wire No. 4050 cable which contains 50 pairs of No. 19 conductors. The form of the commands is binary, positive, up-logic with 8 V dc representing a logic "one" and 0 V dc representing a logic "zero". The 13 most significant bits of 14 sent over is used for each axis. In addition to the azimuth and elevation command signals, a "servo flag" signal is received. This is an 8 V dc, 20 μs pulse occurring 10 times per second which indicates when the source information is being updated. The input commands are buffered and converted to a 5 V dc logic level.

The servos operate by comparing binary signals and driving the antenna to null the difference. The position of the antenna (in both azimuth and elevation) is fed back as the output of a 13-bit binary encoder. This output is compared with the buffered input command and subtracted to produce a digital error signal. The error is converted to an analog signal, amplified, mixed with the various feedbacks and used to drive the power amplifiers. In elevation, the power amplifier feeds a dc motor-tachometer directly. In azimuth, the power amplifier supplies the field current for the M-G set which in turn feeds the azimuth motor-tachometers. The tach signals are used as stabilizing feedbacks. The motors turn the antenna through appropriate gearboxes and drive systems.

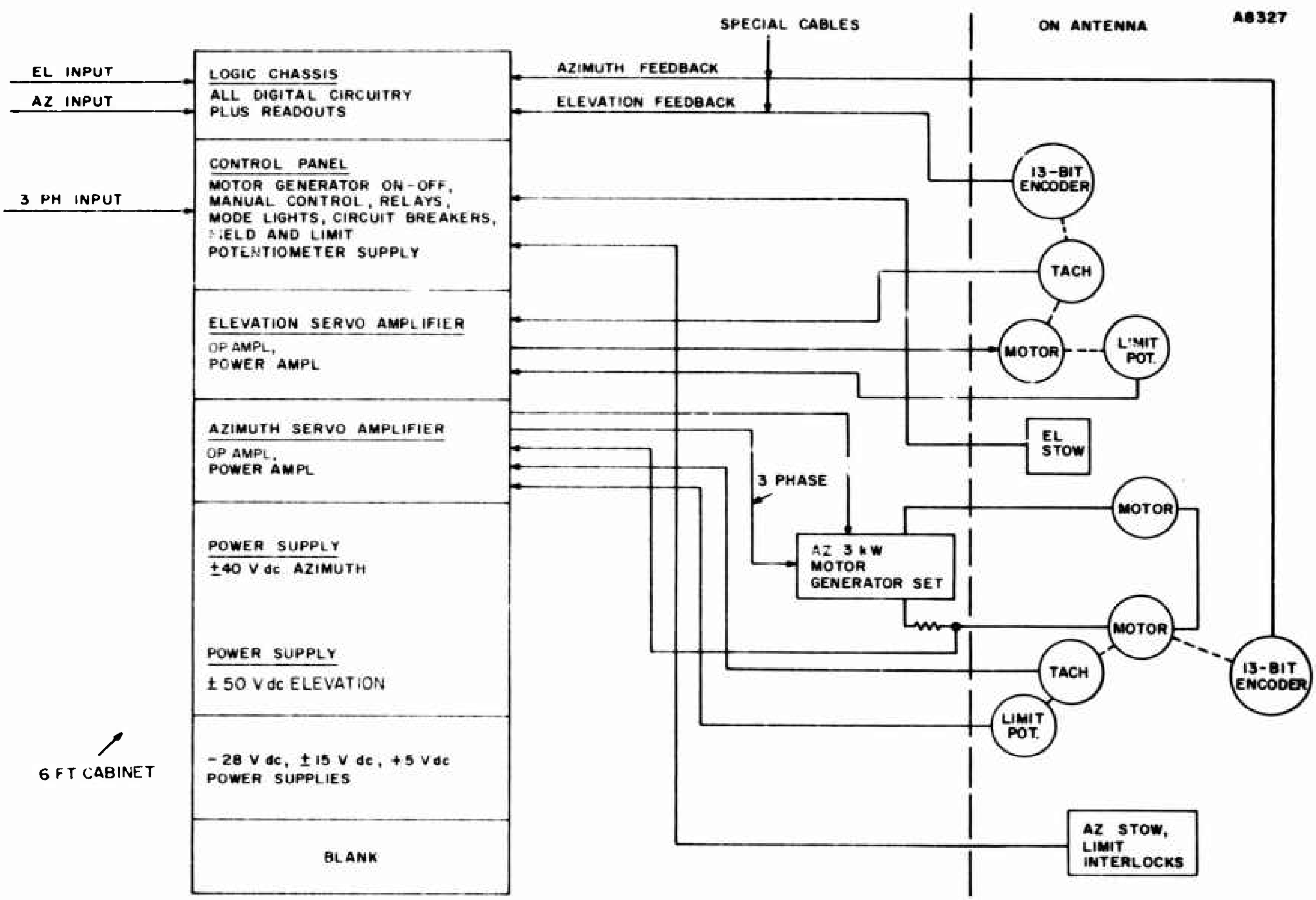

Figure 23. Antenna Positioning System

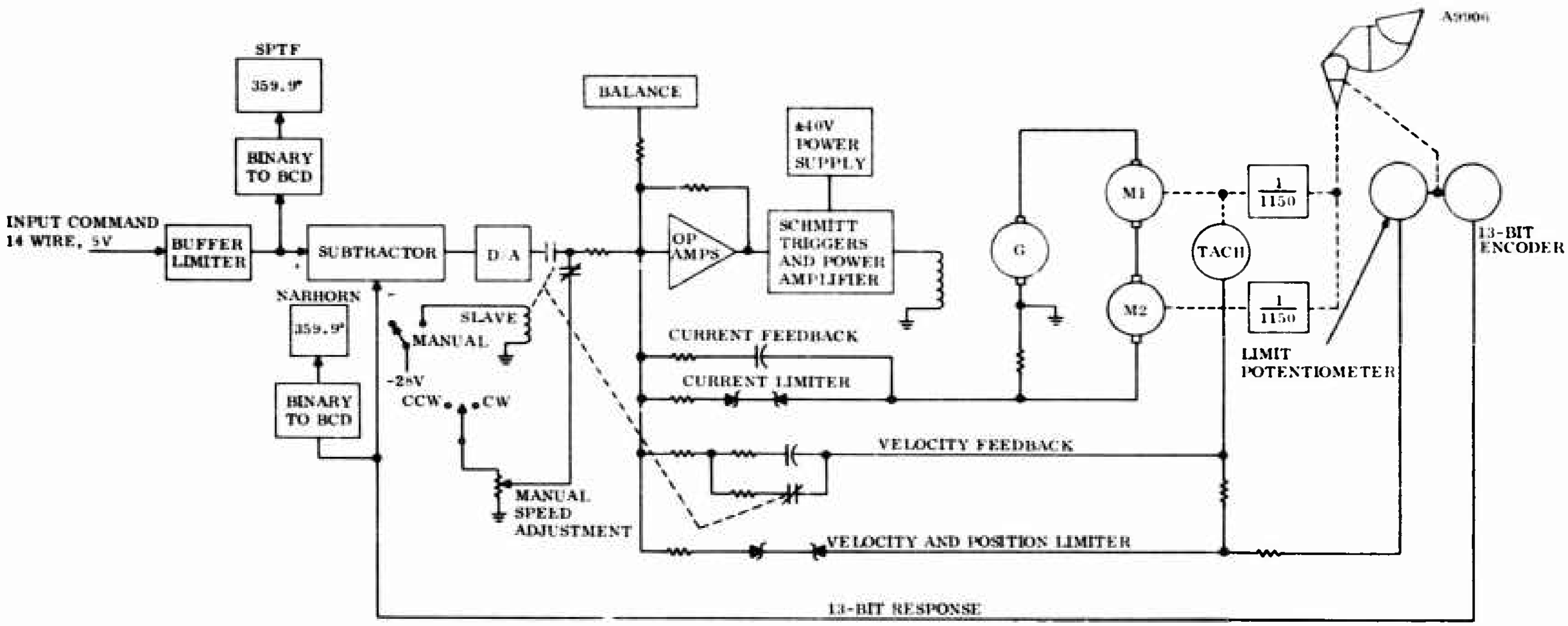

Figure 24. Azimuth Drive Block Diagram

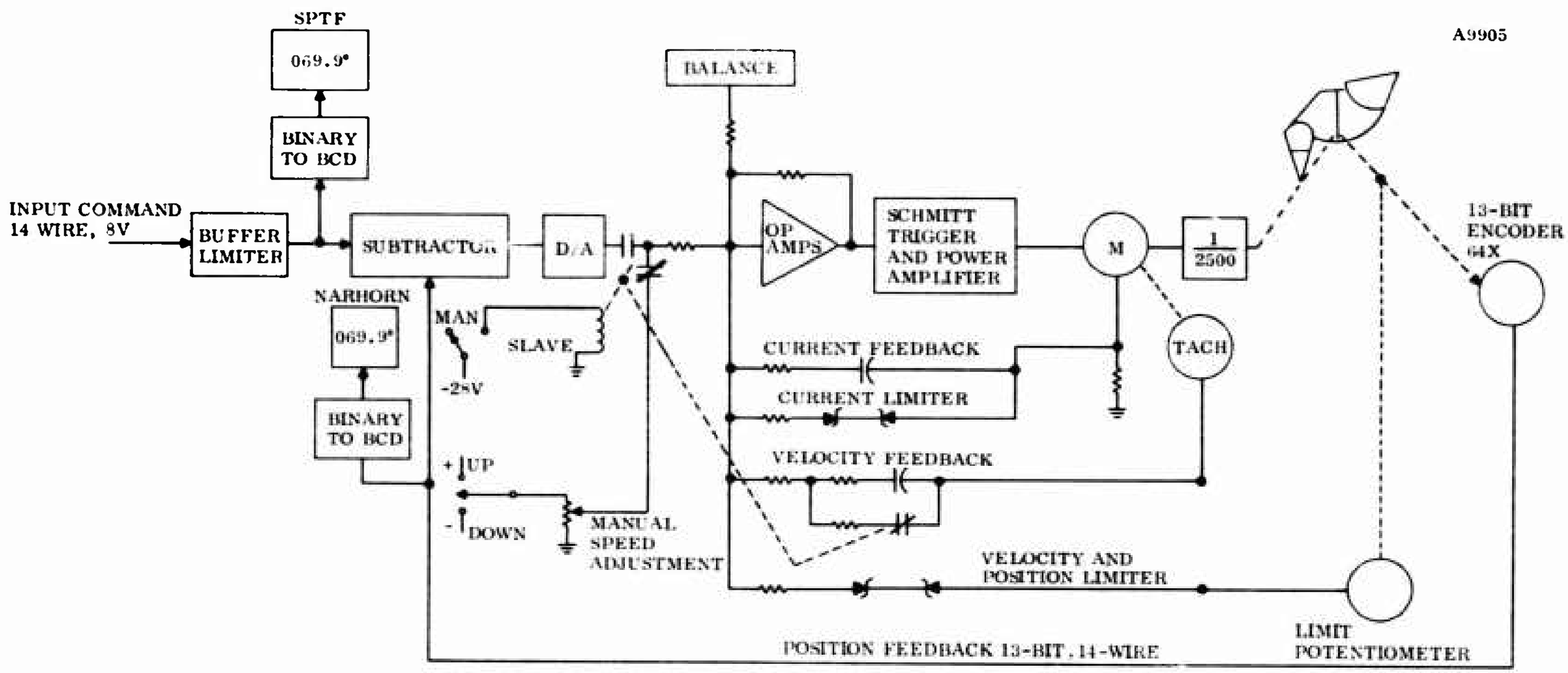

Figure 25. Elevation Drive Block Diagram

The input command and the position feedback from the encoder are converted and displayed as decimal digits for both azimuth and elevation by the readout circuitry.

In the velocity mode, the position loops are opened and an analog drive signal is fed directly into the amplifiers. This causes the motors to run at a velocity as set on the manual speed potentiometers. The tachometer is the principal feedback in this mode.

3. DIGITAL PROCESSING CIRCUITRY

This circuitry accepts a 13-bit "desired position" digital signal from the SPTF remote site, and a 13-bit "actual position" digital signal from the encoder on the antenna, subtracts one from the other, and converts the digital error signal to a dc analog error signal. A more detailed block diagram for this portion of the circuitry as well as the readout circuitry is shown in Figure 26. All this is mounted on one chassis. Figure 27 is a sketch of that chassis illustrating the location of the boards, connectors, etc., with the azimuth and elevation command and response position readouts. Figure 28 depicts the grouping of the circuitry on printed circuit (PC) boards.

Since the command signals have logic levels of 0 V dc and 8 V dc, a buffer circuit (Figure 29) is used to convert these levels to 0 V dc and 5 V dc and to provide noise immunity. There are a total of 28 of these circuits used, mounted with 18 on each of two printed circuit boards (PCB) (4 spare on each PCB). These buffer each of the 13 bits of the azimuth and elevation inputs and the servo flag for each channel. The data outputs of the buffers then go to the subtractors. The comparison of the desired and actual positions is accomplished by subtracting the two. This is done by adding the "twos complement" of the actual position to the command signal. The "twos complement" is derived by using the inverted output of the encoder and hardwiring an additional bit into the carry input of the least significant bit (LSB) adder. On the same PCB with the subtractors is a divide-by-8 counter which reduces the frequency of the servo flag from 10 times per second to 1.25 times per second.

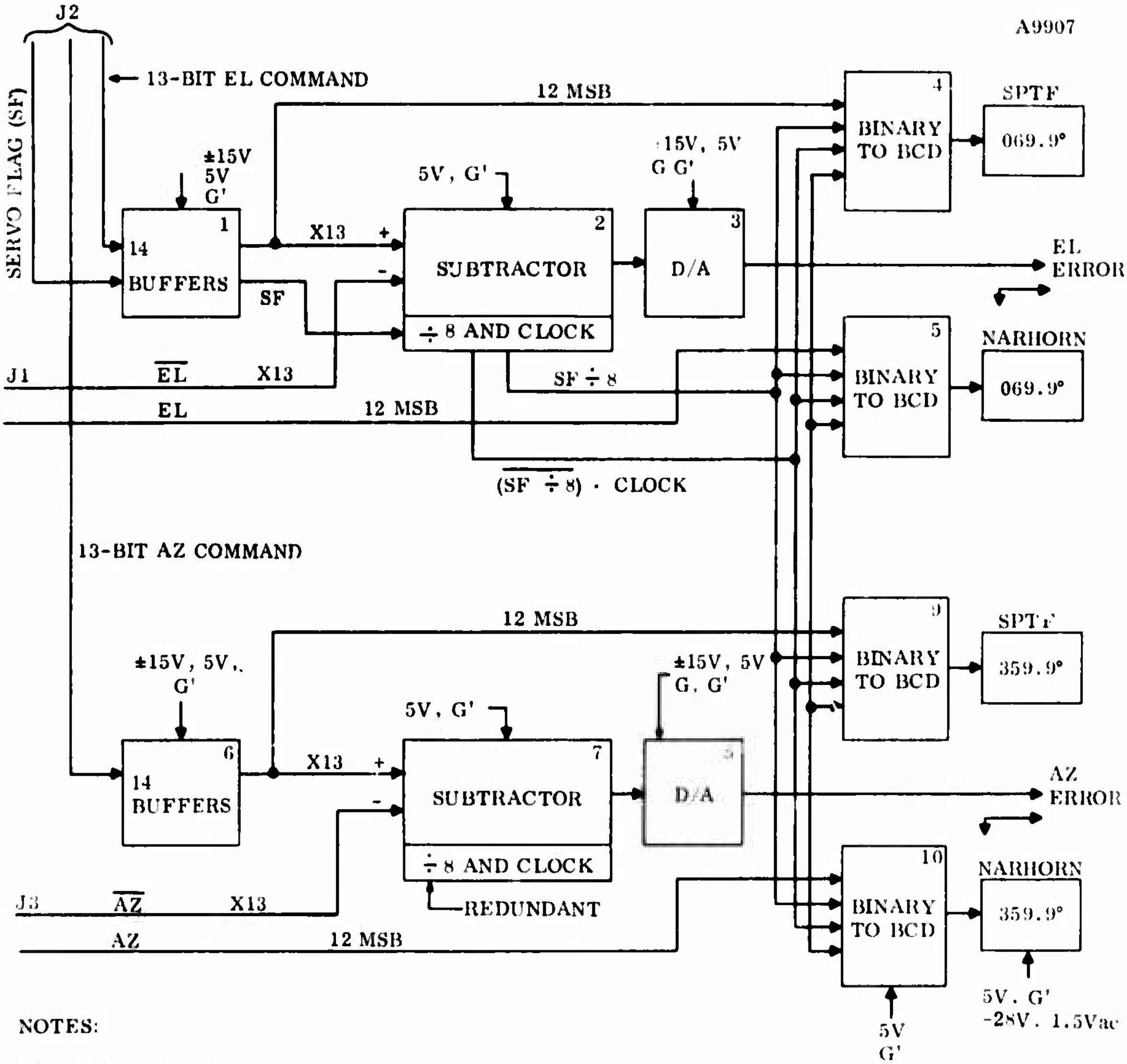

NOTES:

G' - DIGITAL GRD
(- OF 5V POWER SUPPLY,
+ OF 28V POWER SUPPLY
AND ONE SIDE OF 2.5Vac).
G - ANALOG GRD
(COMMON OF ±15V
POWER SUPPLY).
EACH BLOCK ABOVE
REPRESENTS 1 PC BOARD
EXCEPT FOR THE FOUR
READOUTS (10 PC BOARDS
IN ALL).

Figure 26. Error Signal and Display Logic

B1821

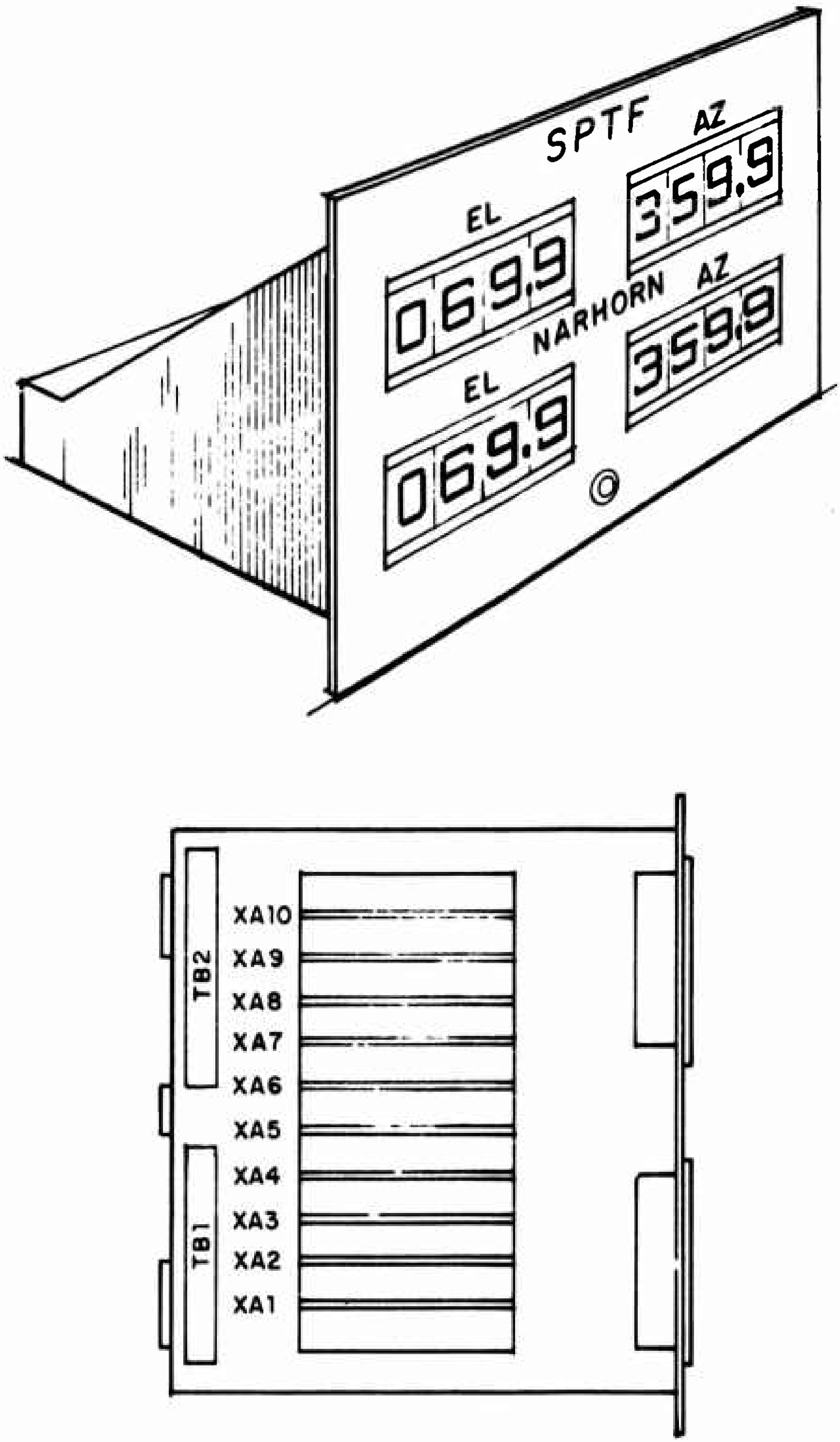

Figure 27. Digital Processing and Display Chassis

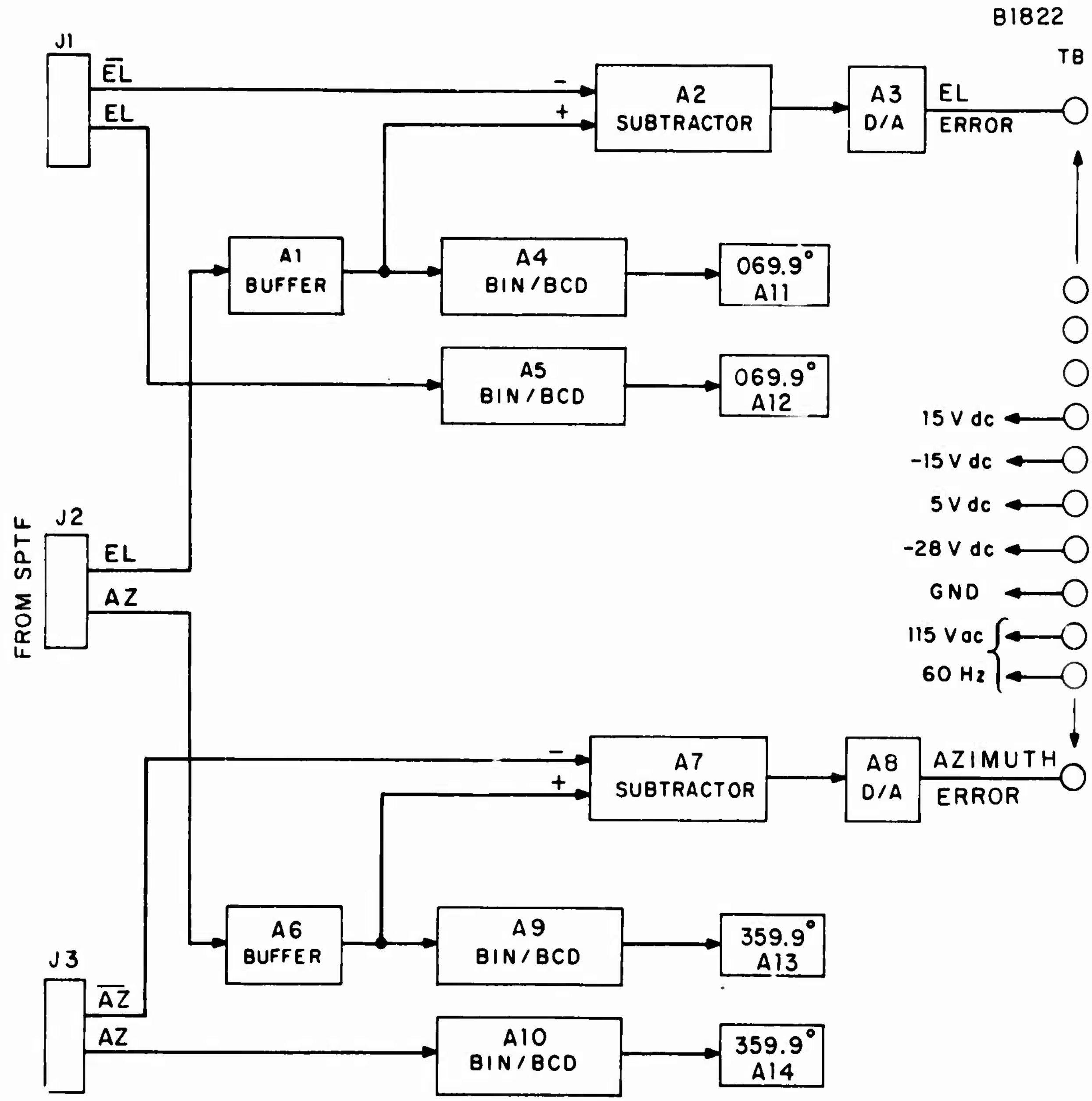

Figure 28. Circuitry Grouping

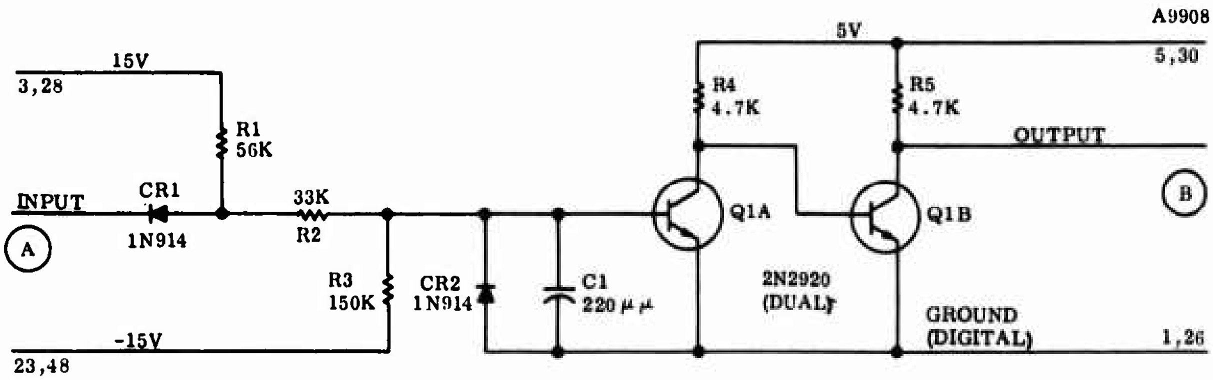

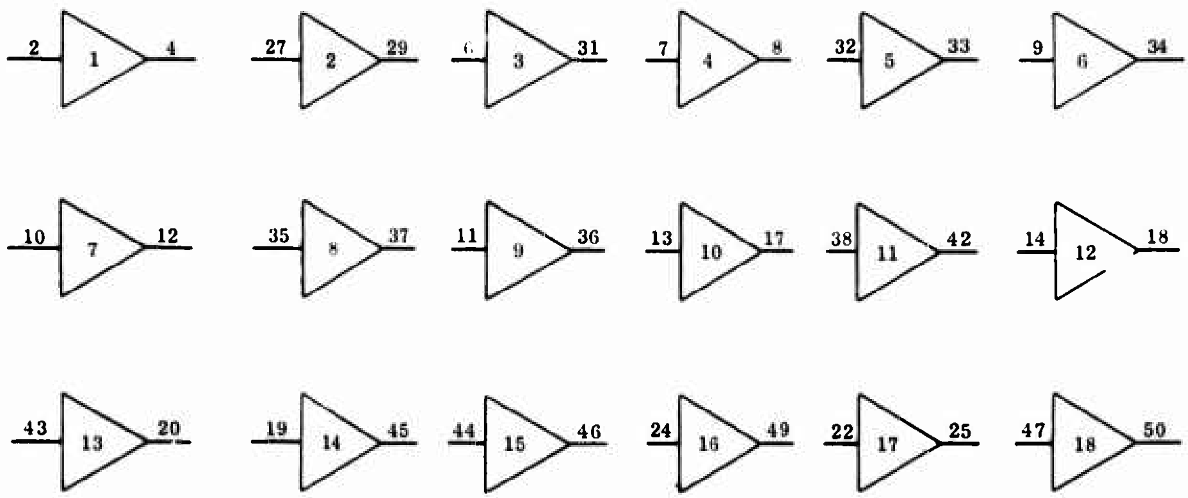

NOTES:

18 CIRCUITS PER BOARD,
14 ACTIVE, 4 SPARE.
ALL RESISTORS 1/8 W.

A AND B REPRESENT THE INPUT AND OUTPUT, NUMBERED IN THE LOWER BLOCKS.

Figure 29. Buffer Circuit

The outputs of the two subtractors are digital signals representing the error between the desired and actual antenna positions. The D/A converters change these into dc analog voltages. Since a linear error output is required for only plus or minus 45°, the digital bits weighted ≥45° are gated to the D/A converter to provide a slewing signal ≥ 5 V dc. The polarity of the 5 V dc is determined by the most significant bit, and represents the direction of rotation required to obtain a null of the error.

Figure 30 is a more detailed diagram for one channel of the digital processing circuitry. The 14 buffer circuits are used for 13 bits representing the "desired position," and the servo flag. The buffered servo flag line then goes through an arrangement of J-K flip-flops and gates which produce a servo flag signal, and its complement, reduced in frequency by a factor of 8 down to 1.25 pulses per second. Both of these are used in the readout circuitry.

The buffered "desired position" bits are routed to four SN7483N four-bit binary adders. The other inputs to the adders are the complement outputs of the encoders on the antenna. This is made into a "twos complement" by permanently running 5 V dc into the "13" input of the lower SN7483N. The output of the adders are thus 13 weighted lines representing the difference between the desired and actual antenna positions. The output from the top-most SN7483N in the previous Figure 29 represents 180°. This is used to determine the polarity of the analog error. The next two MSB's down represent 90° and 45°. These, along with the 180° line, are combined by logic circuits to indicate an error of 45° or greater. This results in a slew voltage out of the D/A converter (i.e., no longer a linear control). The 10 remaining lines (22.5° through 2.636') go directly into the D/A converter. This is an Analog Devices DAC-12Q unit. The output is used by the power circuitry and is an analog dc voltage representing servo error. The output range is plus or minus 10 V dc with plus or minus 5 V dc being the linear range for plus or minus 45° error.

4. READOUT CIRCUITRY

This portion of the electronics takes the binary information for the azimuth, elevation, desired, and actual antenna positions. These four sets are converted into BCD form and displayed as decimal readouts. Figure 26 shows the four binary-to-BCD converters and the four sets of readouts required. The inputs to this circuitry are the 12 MSB's of the buffered "desired position" information and the 12 MSB's out

A

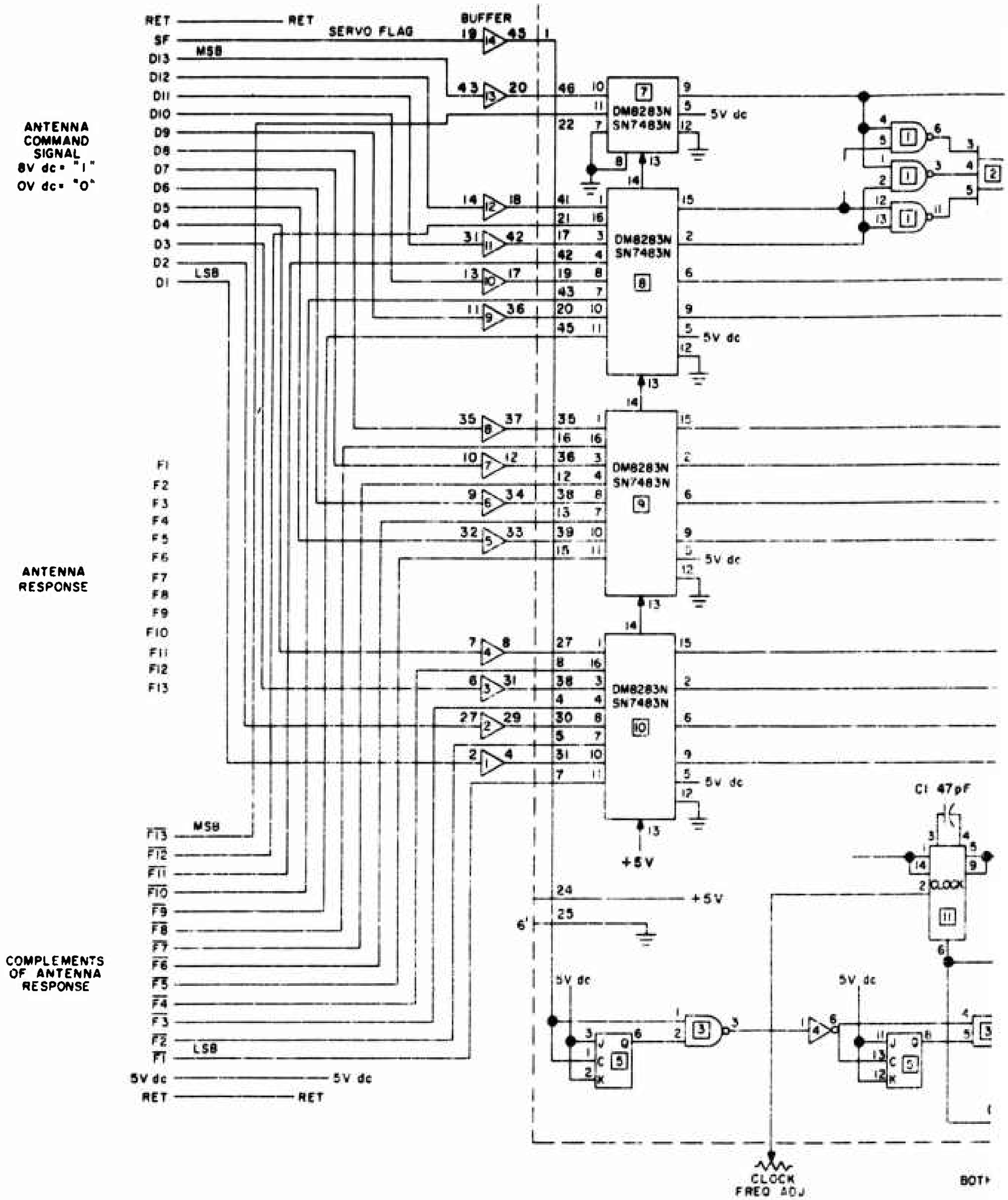

RET
SF
SERVO FLAG
BUFFER
MSB
LSB
ANTENNA COMMAND SIGNAL 8V dc= "1" OV dc= "0"
D13
D12
D11
D10
D9
D8
D7
D6
D5
D4
D3
D2
D1
DM8283N SN7483N
5V dc
ANTENNA RESPONSE
F1
F2
F3
F4
F5
F6
F7
F8
F9
F10
F11
F12
F13
COMPLEMENTS OF ANTENNA RESPONSE
+5V
C1 47pF
CLOCK
CLOCK FREQ ADJ

B

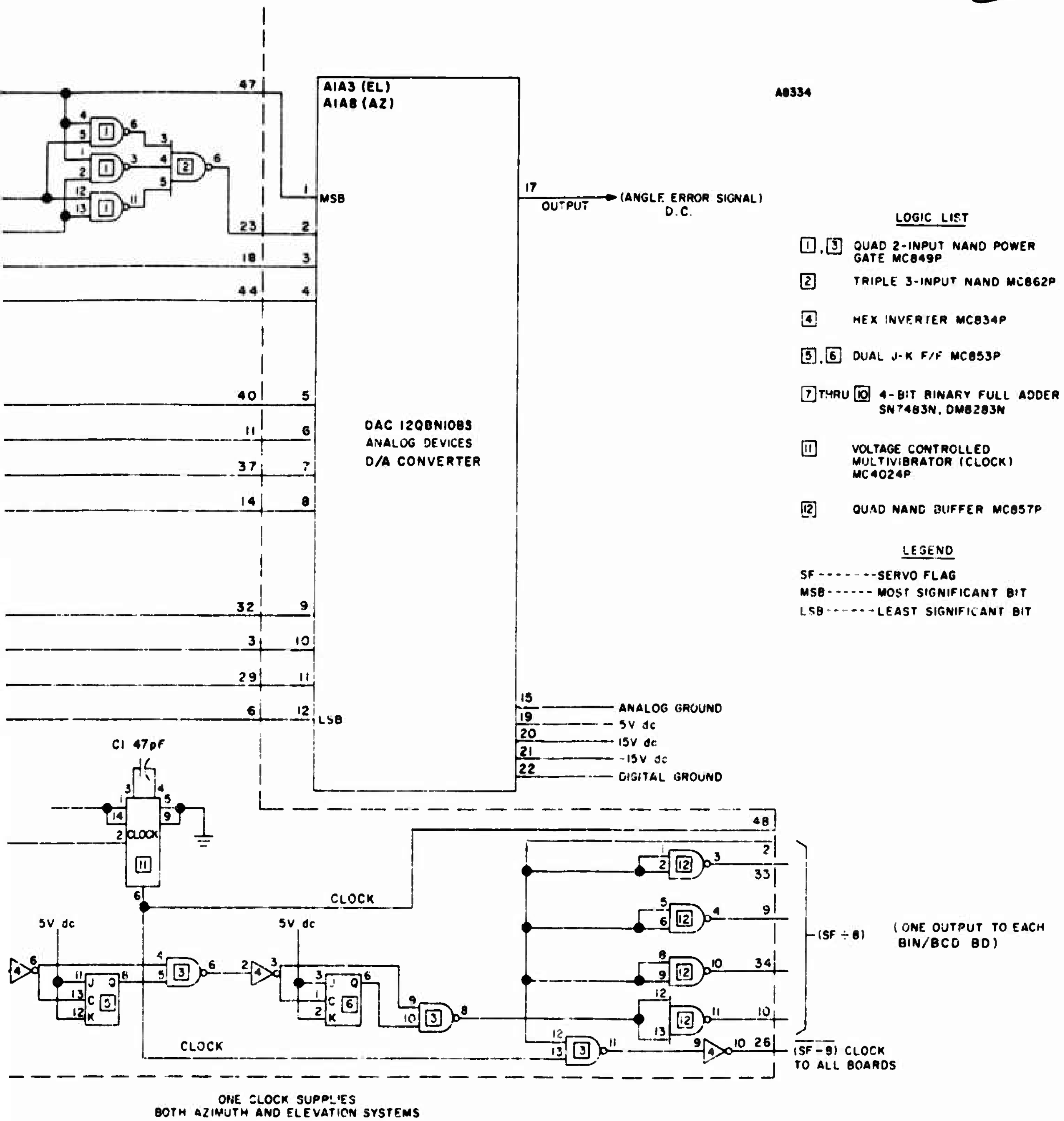

Figure 30. One Channel of Digital Processing

of 13 bits from the encoders on the antenna. There is a 2-MHz clock for system timing on each subtractor board (one is a spare). The divided servo flag signals described previously are also used. Each of the four sets of inputs is converted separately and displayed on decimal readouts. The resolution of the displays is 0.1°.

Figure 27 illustrates the placement of the readouts on the front panel of the logic chassis. The diagram of Figure 28 shows that each binary-to-BCD conversion is done on a separate PCB.

Figure 31 is a more detailed block diagram for the readout circuitry. There are two displays in azimuth, one indicating the "desired position" angle called for by the remote site, and the second indicating the "actual position" of the HARHORN antenna. Each is a set of digital decimal readouts, displaying 000.0 to 359.9 degrees in increments of 0.1 degree, with a static accuracy of plus or minus 0.1 degree. Each readout will be updated every 8 servo flags (0.8 s). Thus, its maximum error when following a moving input equals the angle the input changes in 0.8 s, plus the static error.

All display processing is separate from servo processing and will not interact in any way. The 12 most significant bits (MSB's) of the 13 buffered command bits are inputs of the command display and the 12 MSB's of the 13 response bits from the binary shaft encoder on the antenna are inputs of the response display. Therefore, 360 degrees is divided into 4096 steps. As the binary input increases from 0 to 360 degrees in 4096 steps, the readout increases from 0 to 360 degrees in 3600 steps. This is done as follows: an internal clock free runs at 2 MHz and is fed through a gate into two countdown circuits, one by 225 and one by 256. The f/225 clock then feeds a count-by-4096 circuit. The f/256 clock feeds a count-by-3600 circuit. Both circuits reach full count at the same time (every 0.46 s). The count-by-4096 circuit resets the count-by-3600 circuit (with no reset it would count to 10,000). The state-of-the-count-by-4096 circuit is continually compared with the binary input by the coincidence detector (exclusive OR's). Without the coincidence detector the counter would cycle from 0 to 4095 once every 0.46 s. With the coincidence detector, when the counter number matches the input number, the clock is disconnected from all count down circuits.

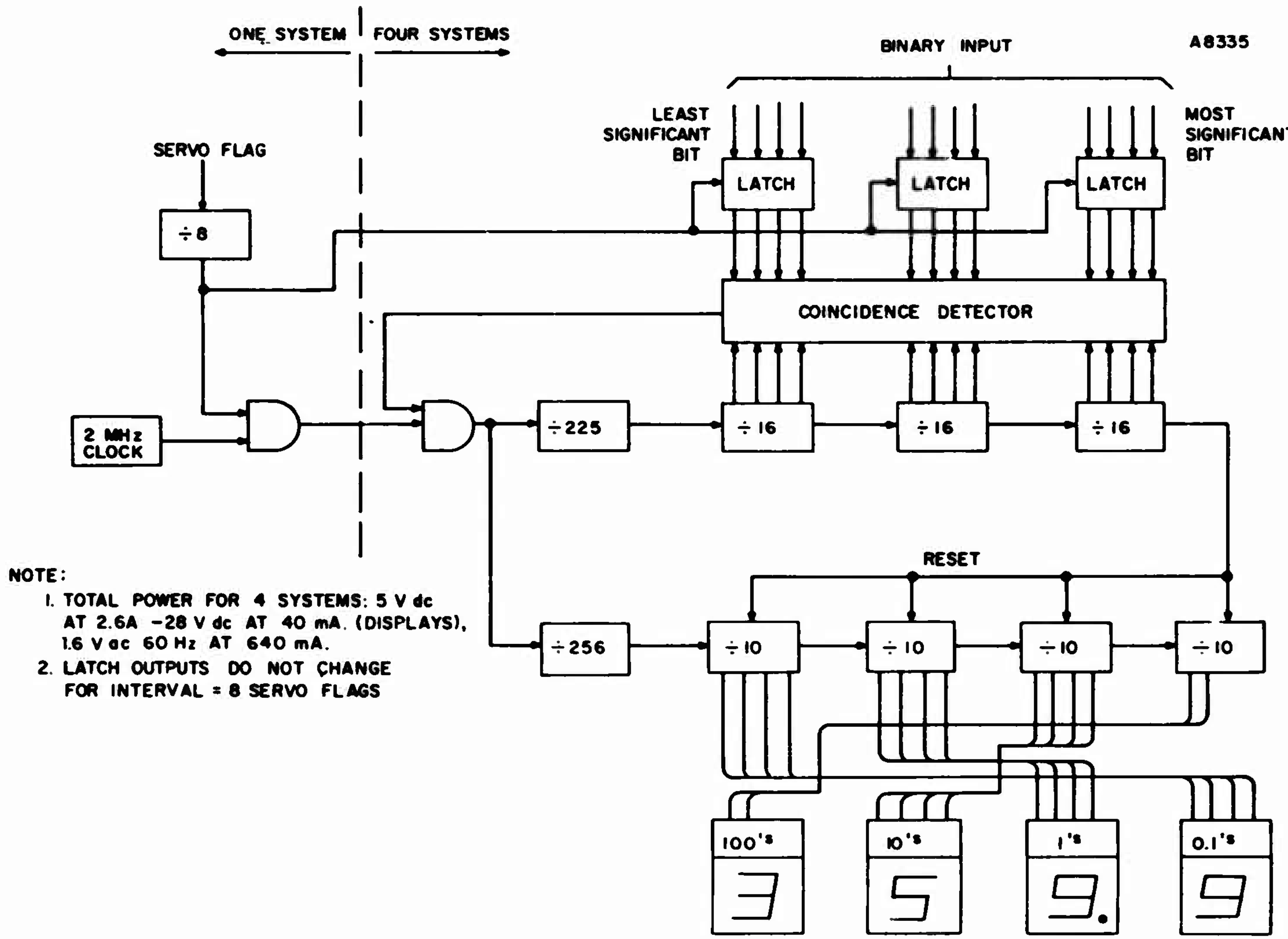

Figure 31. Readout Circuitry

Between the 12 binary input bits and the coincidence detectors are 12 latch flip-flops, all triggered by a strobe pulse which is the counted down servo flag. The state-of-the-binary input bits which exists at the end of the strobe pulse is held until the next strobe pulse. If the binary input increases, the display circuit will acquire each new number in 112 μs. If the binary input decreases, a complete cycle of 4096 counts must go by until the next number is matched, since the counters count in the direction of increasing numbers only. Hence, it will take 0.46 s to acquire each new number. The period between strobe pulses is 0.8 s. Thus, if the input is continually decreasing, the display will be erratic for 0.46 s and steady for 0.34 s. This is the "worst-case" dynamic situation.

The display device is an integral assembly of decoder/driver and display. Each of the 4 digits is generated by a 7-segment fluorescent readout tube. Character size is 0.57 in. x 0.36 in. The decimal point is displayed.

The command and response azimuth display logic systems is contained on two 4.5 in. x 6 in. printed circuit cards. The cards are identical, each having 12-wire (plus one return) binary inputs, and 14 wire outputs to its respective display module, 4 wires per digit except 2 wires to the 'hundreds' digit. Both systems are fed from the common clock and strobe pulse which also feed the two elevation displays. The power required is 5 V dc for the logic, and -28 V dc and 1.5 V ac 60 Hz for the readout tubes.

The elevation circuitry is identical to that of the azimuth displays. The only difference is in the interpretation of the displayed angles. They are to be interpreted as follows:

BINARY INPUT	TRUE ANGLE	DISPLAYED ANGLE
001100011011	69.9°	69.9°
000000000000	0	00.0°
111111111111	-0.1°	359.9°
110000000000	-90.0°	270.0°

The hundreds digit is only used to indicate depression angle when the antenna is below zero degree. A more detailed logic diagram is shown in Figure 32.

A

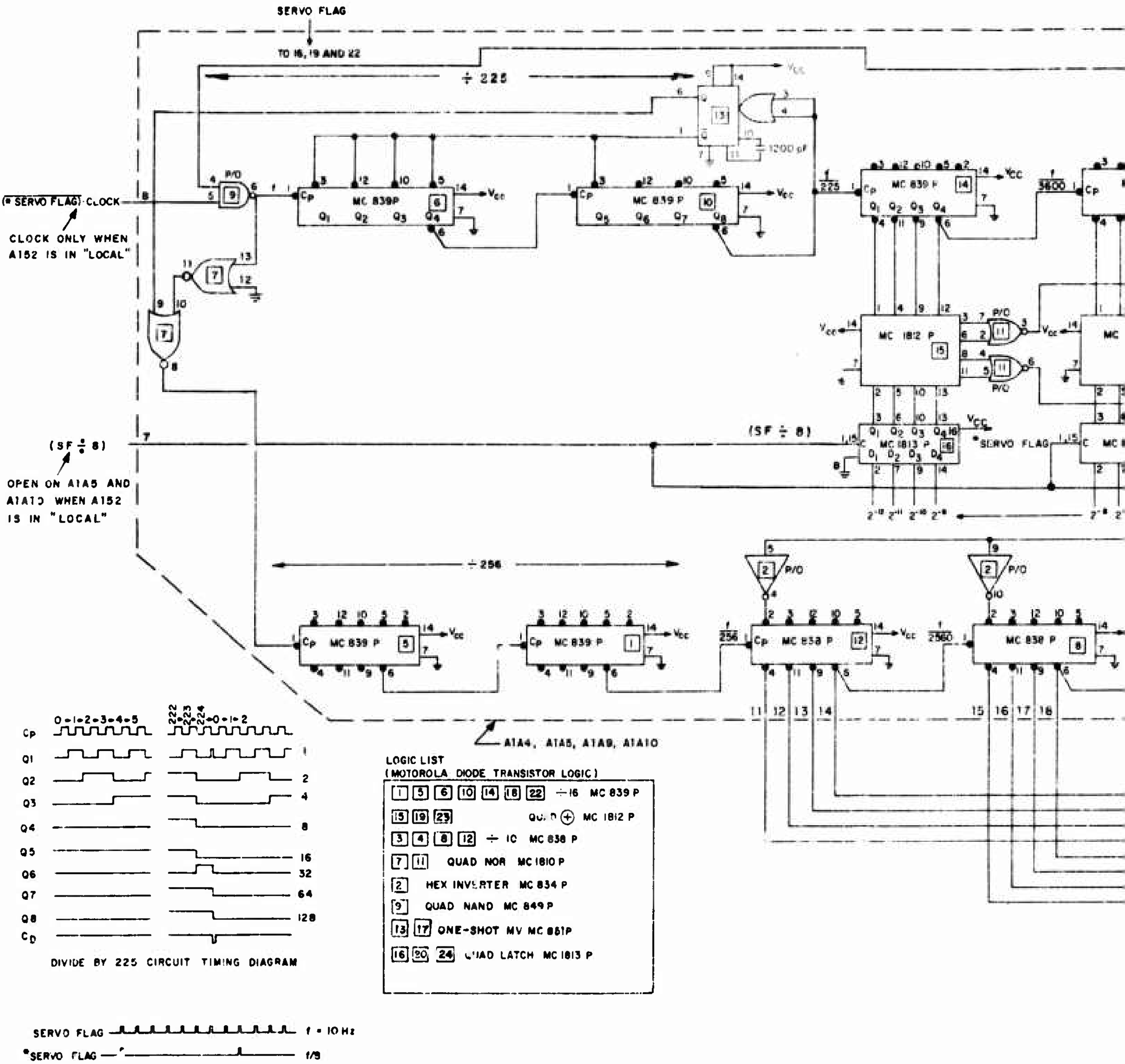

SERVO FLAG
TO 16, 19 AND 22
÷ 225
1200 pF
(* SERVO FLAG) · CLOCK
CLOCK ONLY WHEN A1S2 IS IN "LOCAL"
MC 839P
MC 839 P
MC 839 P
MC 1812 P
MC 1813 P
(SF ÷ 8)
*SERVO FLAG
OPEN ON A1A5 AND A1A10 WHEN A1S2 IS IN "LOCAL"
÷ 256
MC 839 P
MC 839 P
MC 838 P
MC 838 P
A1A4, A1A5, A1A9, A1A10
LOGIC LIST
(MOTOROLA DIODE TRANSISTOR LOGIC)
1 5 6 10 14 18 22 ÷16 MC 839 P
15 19 23 QUAD ⊕ MC 1812 P
3 4 8 12 ÷ 10 MC 838 P
7 11 QUAD NOR MC 1810 P
2 HEX INVERTER MC 834 P
9 QUAD NAND MC 849 P
13 17 ONE-SHOT MV MC 851P
16 20 24 QUAD LATCH MC 1813 P
DIVIDE BY 225 CIRCUIT TIMING DIAGRAM
SERVO FLAG f = 10 Hz
*SERVO FLAG f/8

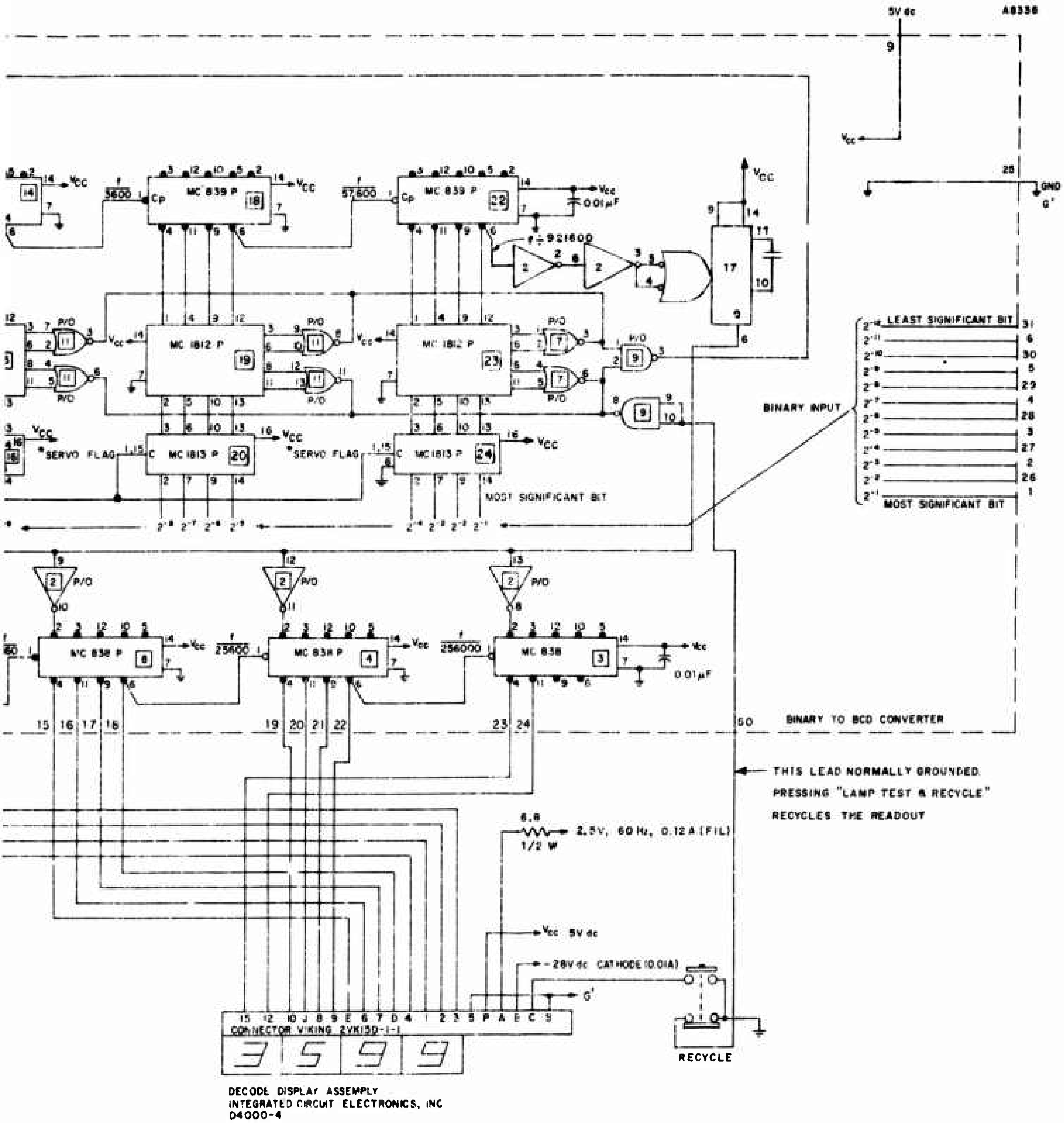

Figure 32. Display Logic

5. POWER CIRCUITRY

This circuitry takes the dc analog voltage which represents azimuth (or elevation) error and amplifies it to provide the power required by the servomotors to reduce the error to zero. Figures 33 and 34 are the schematics for the elevation and azimuth servo amplifiers. Each consists of a mixing network, operational amplifiers, sawtooth oscillator, a pair of complementary Schmitt triggers and an output stage. The elevation output stage feeds the single elevation motor directly. In azimuth, it supplies the field to a dc generator to drive the two azimuth motors. The azimuth motors drive wheels on a circular track to position the antenna. Tachometers provide stabilizing feedback signals for both servos. In azimuth, there is an additional feedback proportional to the motor current. This is for stabilization and current limiting.

The servo amplifiers are of the pulse-width modulation type with very low dissipation in the output stage. This is accomplished by adding the dc error signal to the output of a sawtooth oscillator to raise or lower the inputs to the complementary Schmitt triggers. If the error goes positive, the positive trigger will be turned on for a proportionately longer time and the negative trigger for a proportionately shorter time. This continues until saturation, at which time the positive trigger will be on all the time and the negative trigger will not be on at all. Quiescently, without any error signal, the plus and minus triggers will be on for equal periods of time to produce a net zero dc. Operational amplifiers are used for signal mixing and providing gain adjustment.

Each servo amplifier is housed in its own chassis and fed by its own power supply for the output stages. The azimuth supply is plus and minus 40 V dc at 5A while the elevation supply is plus and minus 50 V dc at 6A. Each amplifier contains 2 PCB's, one for the mixing/amplifying section and the other for the Schmitt triggers.

The schematic for the plus or minus 40 V dc and 50 V dc power supplies is shown on Figure 35. The -28 V dc, plus or minus 15 V dc, and 5 V dc power required for the antenna positioning system is supplied by commercial power supplies. The connection for these is shown in Figure 36.

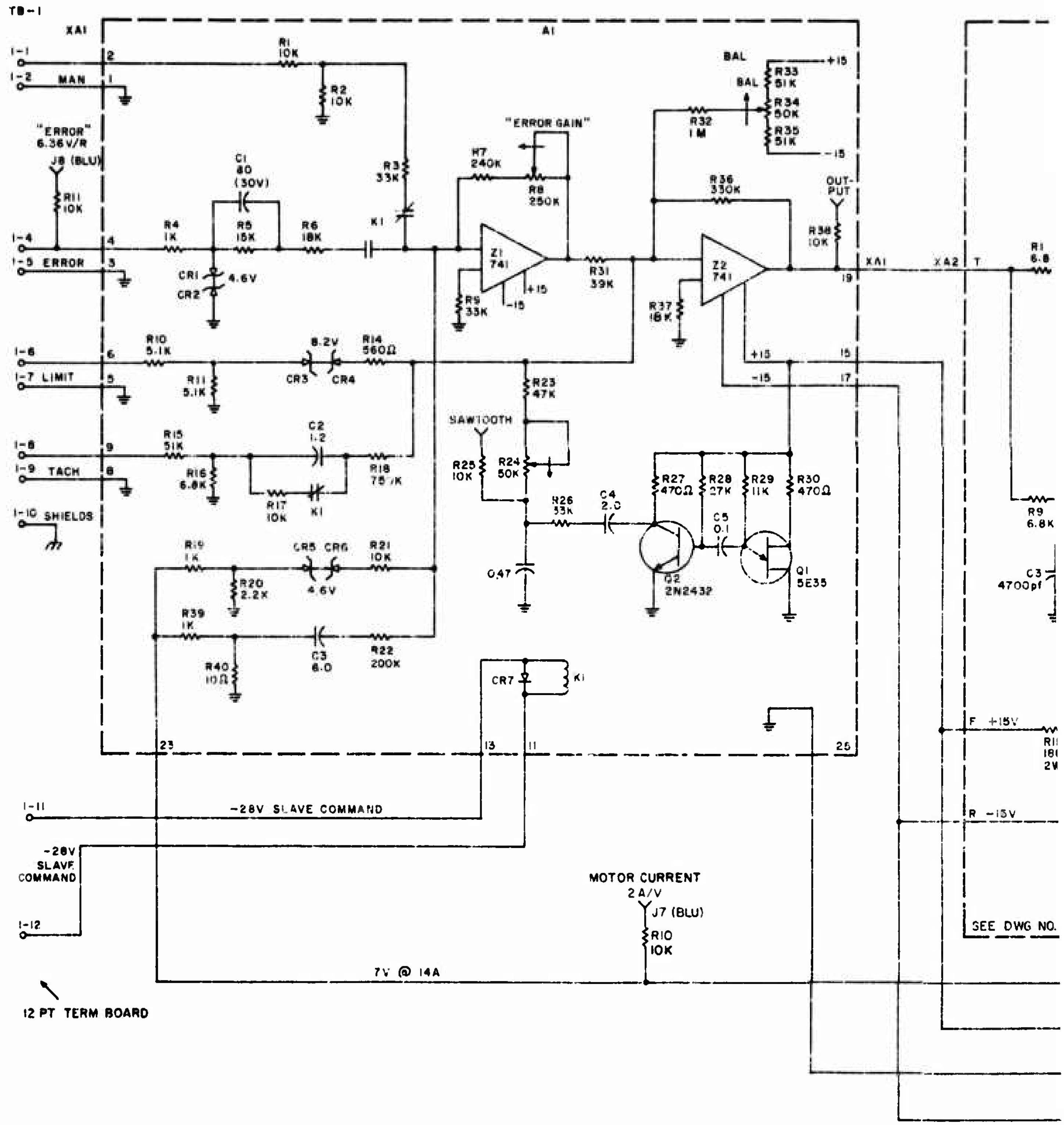
TB-1
XA1
A1
"ERROR" 6.36 V/R
J8 (BLU)
MAN
ERROR
LIMIT
TACH
SHIELDS
"ERROR GAIN"
BAL
OUT-PUT
Z1 741
Z2 741
SAWTOOTH
Q2 2N2432
Q1 5E35
-28V SLAVE COMMAND
MOTOR CURRENT 2 A/V
J7 (BLU)
7V @ 14A
12 PT TERM BOARD
SEE DWG NO.

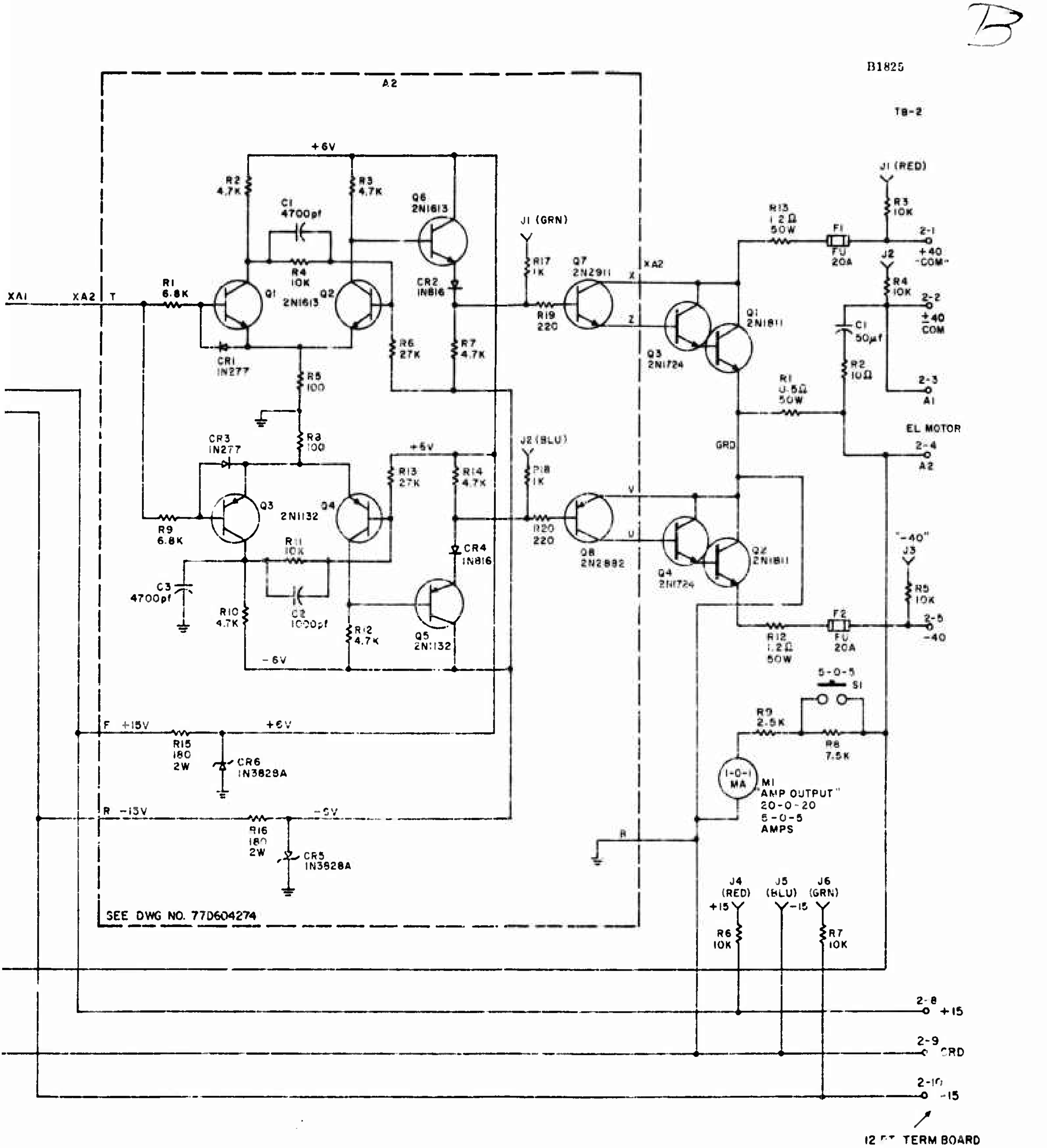

Figure 33. Elevation Servo Amplifier

A

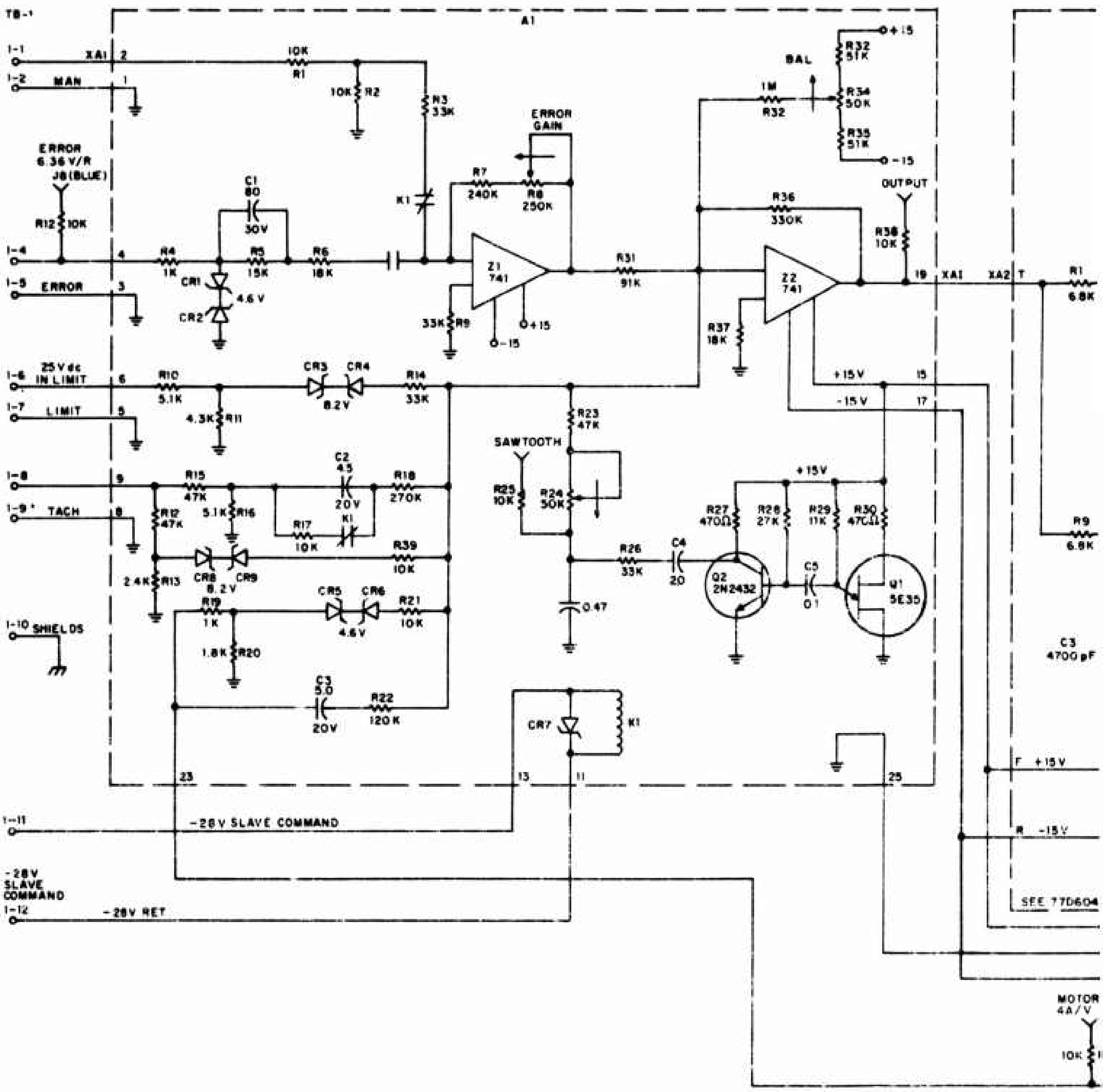
TB-1
A1
1-1
XA1
1-2
MAN
ERROR
6.36 V/R
J8 (BLUE)
R12 10K
1-4
1-5
ERROR
1-6
25 V dc
IN LIMIT
1-7
LIMIT
1-8
1-9
TACH
1-10 SHIELDS
10K
R1
10K R2
R3
33K
ERROR
GAIN
K1
R7
240K
R8
250K
C1
80
30V
R4
1K
R5
15K
R6
18K
CR1
CR2
4.6 V
Z1
741
33K R9
-15
+15
R10
5.1K
4.3K R11
CR3
CR4
8.2V
R14
33K
R15
47K
5.1K R16
C2
4.5
20V
R18
270K
R17
10K
K1
R39
10K
R12
47K
2.4K R13
CR8
CR9
8.2V
CR5
CR6
4.6V
R19
1K
R21
10K
1.8K R20
C3
5.0
20V
R22
120K
BAL
+15
R32
51K
1M
R32
R34
50K
R35
51K
-15
R36
330K
OUTPUT
R38
10K
R31
91K
Z2
741
R37
18K
+15V
-15V
15
17
19
XA1
XA2
T
R1
6.8K
R23
47K
SAWTOOTH
R25
10K
R24
50K
+15V
R27
470Ω
R28
27K
R29
11K
R30
470Ω
R26
33K
C4
20
C5
.01
Q2
2N2432
Q1
5E35
0.47
R9
6.8K
C3
4700 pF
CR7
K1
23
13
11
25
F +15V
R -15V
1-11
-28V SLAVE COMMAND
-28V
SLAVE
COMMAND
1-12
-28V RET
SEE 77D604
MOTOR
4A/V
10K

B1836

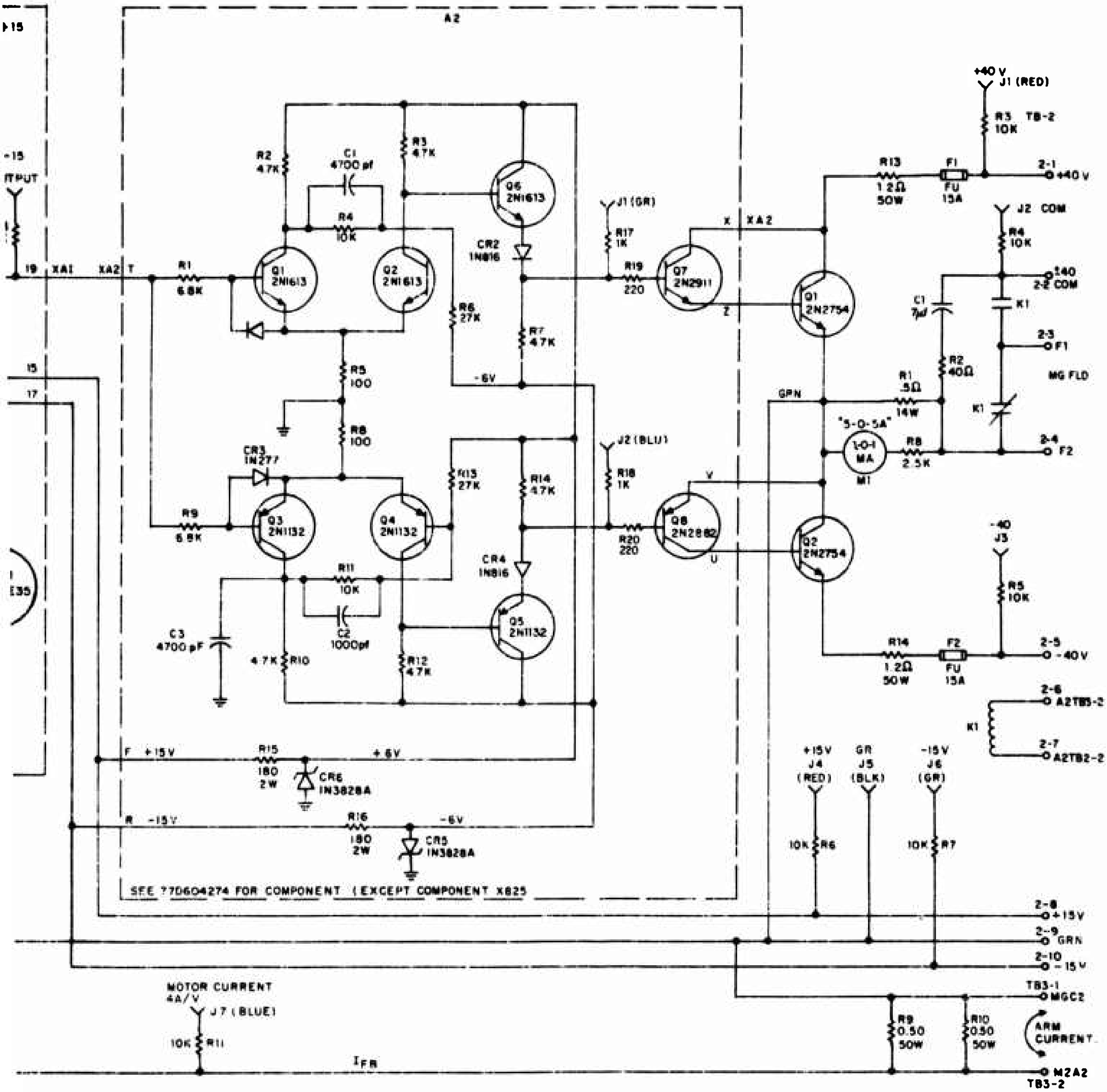

Figure 34. Azimuth Servo

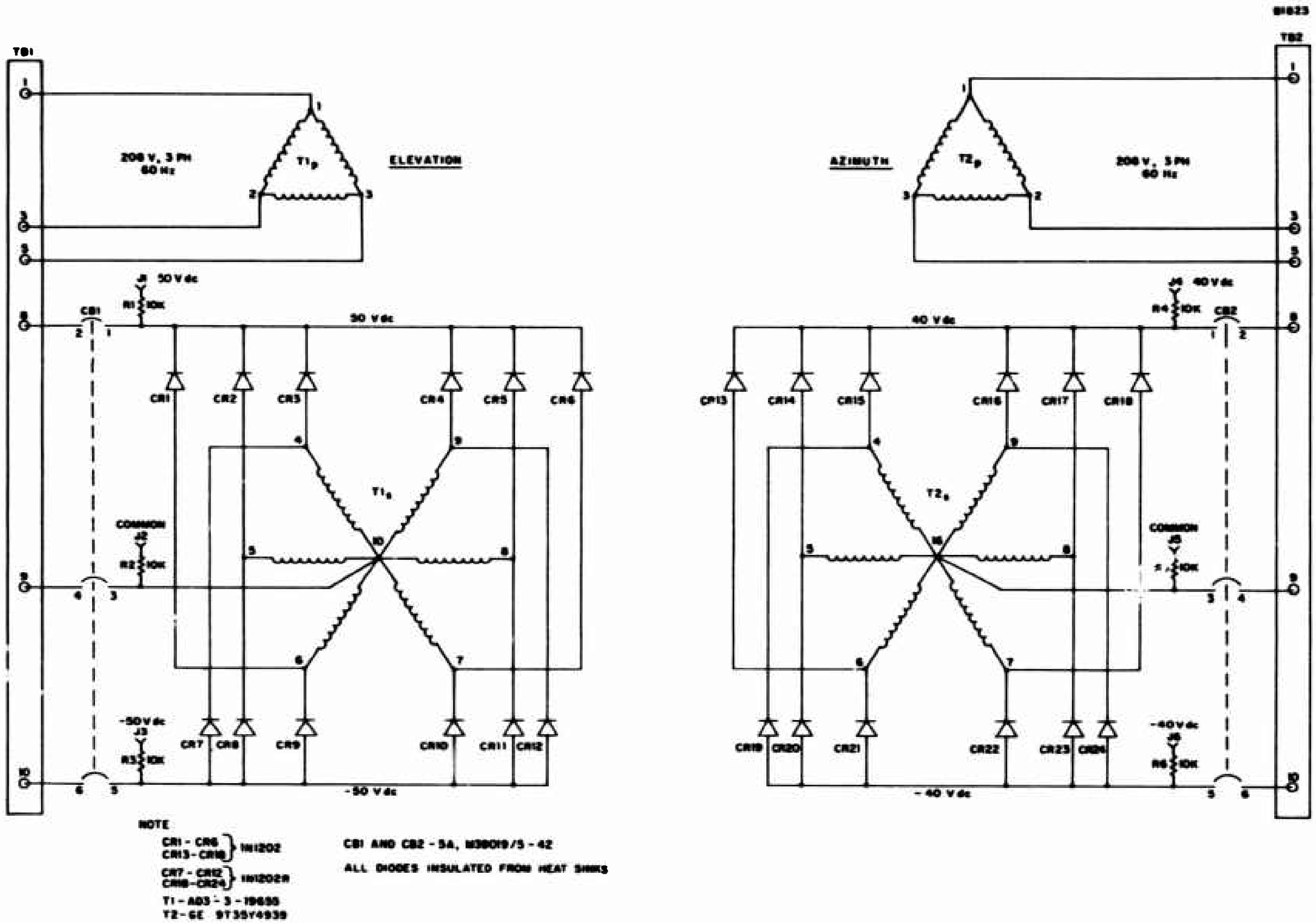

Figure 35. 40 Volt and 50 Volt Power Supplies

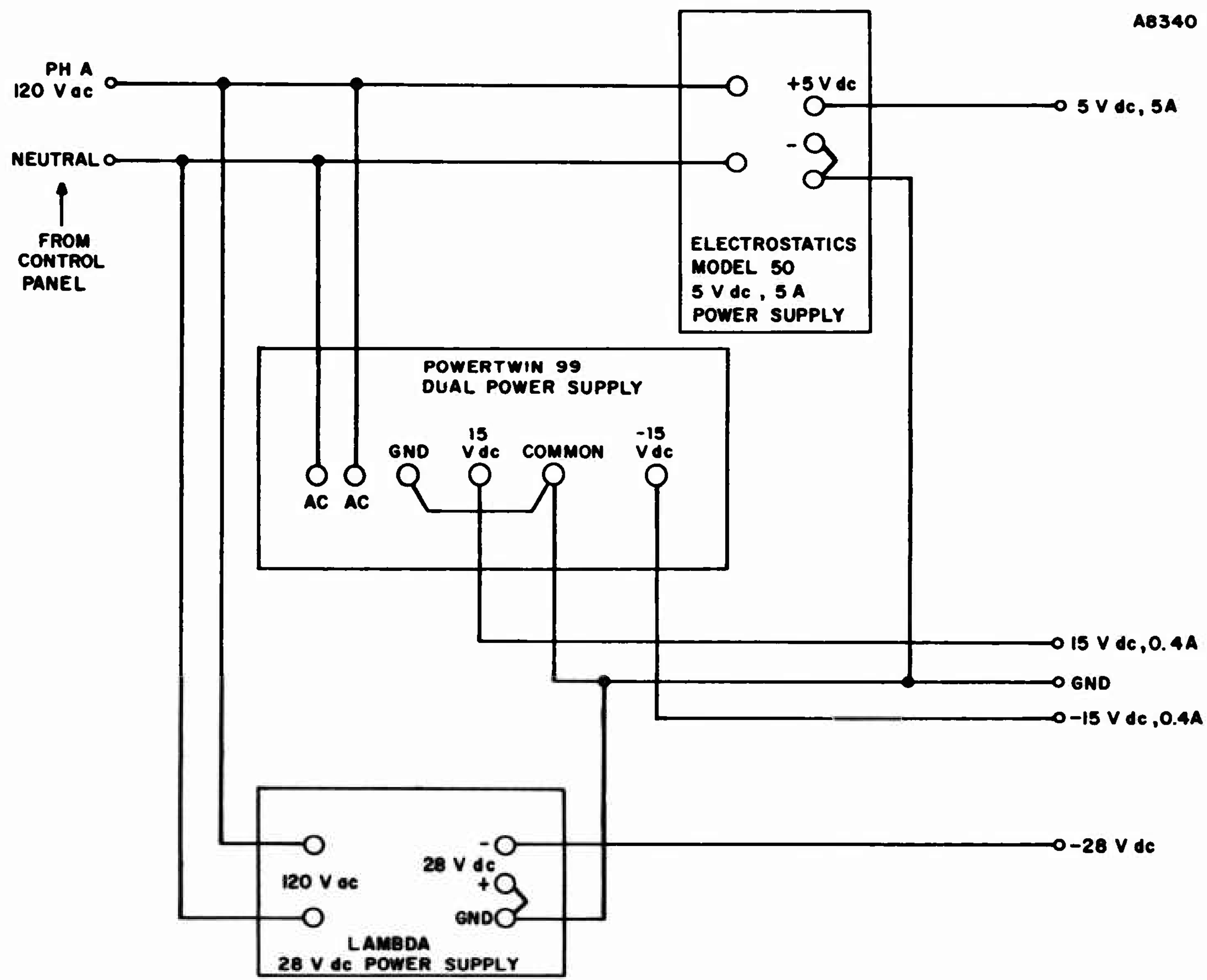

Figure 36. Low Voltage Power Supplies

6. MOTORS/DRIVE METHOD

In elevation, the motor drive combination is straightforward with a wound-field dc servomotor driving a ring gear through a gearbox to position the antenna from 70° down to -90°. The data pickoff is through gearing off the ring gear. A steady-state torque of 2000 lbs ft is available to overcome friction, unbalance and winds up to 15 knots. 5700 ft is available transiently for 40 knot gusts. The plus or minus 50 V dc power supply which supplies the motor power has a 6A continuous rating and can provide peaks up to 15 A. The stabilizing tachometer is direct-mounted to the motor. A 100 V dc power source excites the field on the motor through a loss-of-field relay interlocked to the start circuitry.

The azimuth drive is not as straightforward. There are two drive wheels, each providing half the required torque to rotate the antenna on a circular track. With two motors and two gear boxes a mechanical coupling between them is provided to prevent one motor from grabbing load in the event the wind unloads one wheel. A total of 3 hp in azimuth allows a steady-state torque of 5300 lbs ft and transients of about 14, 500 lbs ft. They are 3450 r/min machines geared at 1150:1 with a peak-to-average torque ratio of 2. 75:1, typical of industrial machines.

7. SYSTEMS CONTROLS AND OPERATION

Figure 37 shows the control circuitry for the antenna positioning system. It consists of a 5 hp motor-starter for the azimuth M-G set and various interlocking switches and relays to prevent inadvertent damage to personnel or equipment during operation. Azimuth stow interlocks, azimuth and elevation limit switches and a key-safe switch prevent operation of any part of the servo. The elevation stow interlock allows operation of the azimuth function even with the elevation stowed. During elevation stow, the elevation function is deactivated. This feature permits the antenna to be stowed in elevation but still be powered in azimuth either to its stow position or any other position. Ac overloads protect the azimuth M-G set against long term overloads. The "slave" mode is not possible in elevation stow.

A

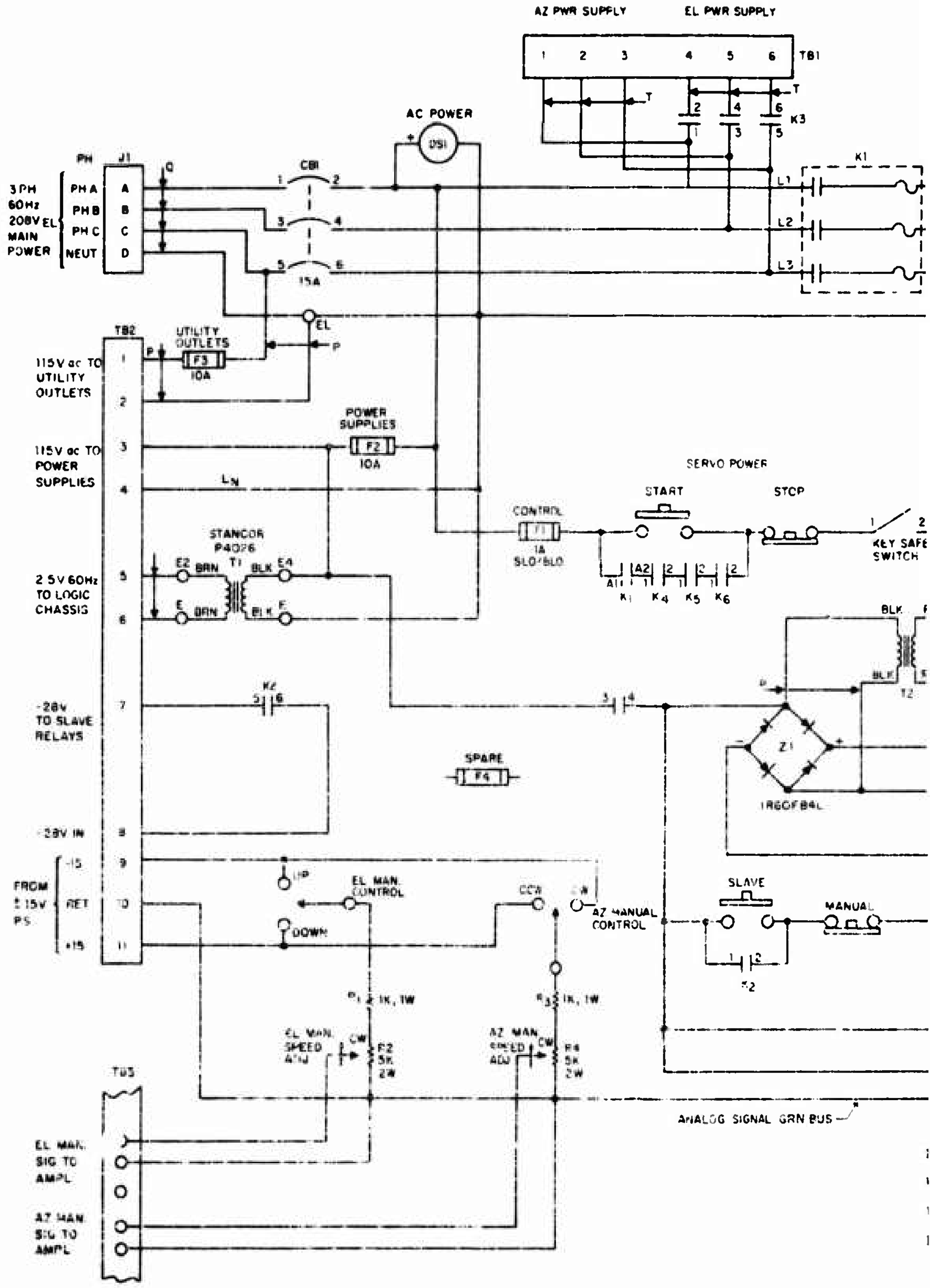
AZ PWR SUPPLY
EL PWR SUPPLY
TB1
K3
K1
AC POWER
DS1
CB1
15A
PH
J1
3 PH 60Hz 208V EL MAIN POWER
PH A
PH B
PH C
NEUT
TB2
UTILITY OUTLETS
F3
10A
115V ac TO UTILITY OUTLETS
POWER SUPPLIES
F2
10A
115V ac TO POWER SUPPLIES
SERVO POWER
START
STOP
CONTROL
F1
1A SLO-BLO
KEY SAFE SWITCH
STANCOR P4026
T1
2.5V 60Hz TO LOGIC CHASSIS
-28V TO SLAVE RELAYS
SPARE
F4
Z1
1R60F84L
-28V IN
FROM ±15V PS
EL MAN. CONTROL
UP
DOWN
AZ MANUAL CONTROL
SLAVE
MANUAL
R1 1K, 1W
R3 1K, 1W
EL MAN. SPEED ADJ
R2 5K 2W
AZ MAN. SPEED ADJ
R4 5K 2W
TB3
ANALOG SIGNAL GRN BUS
EL MAN. SIG TO AMPL
AZ MAN. SIG TO AMPL

13

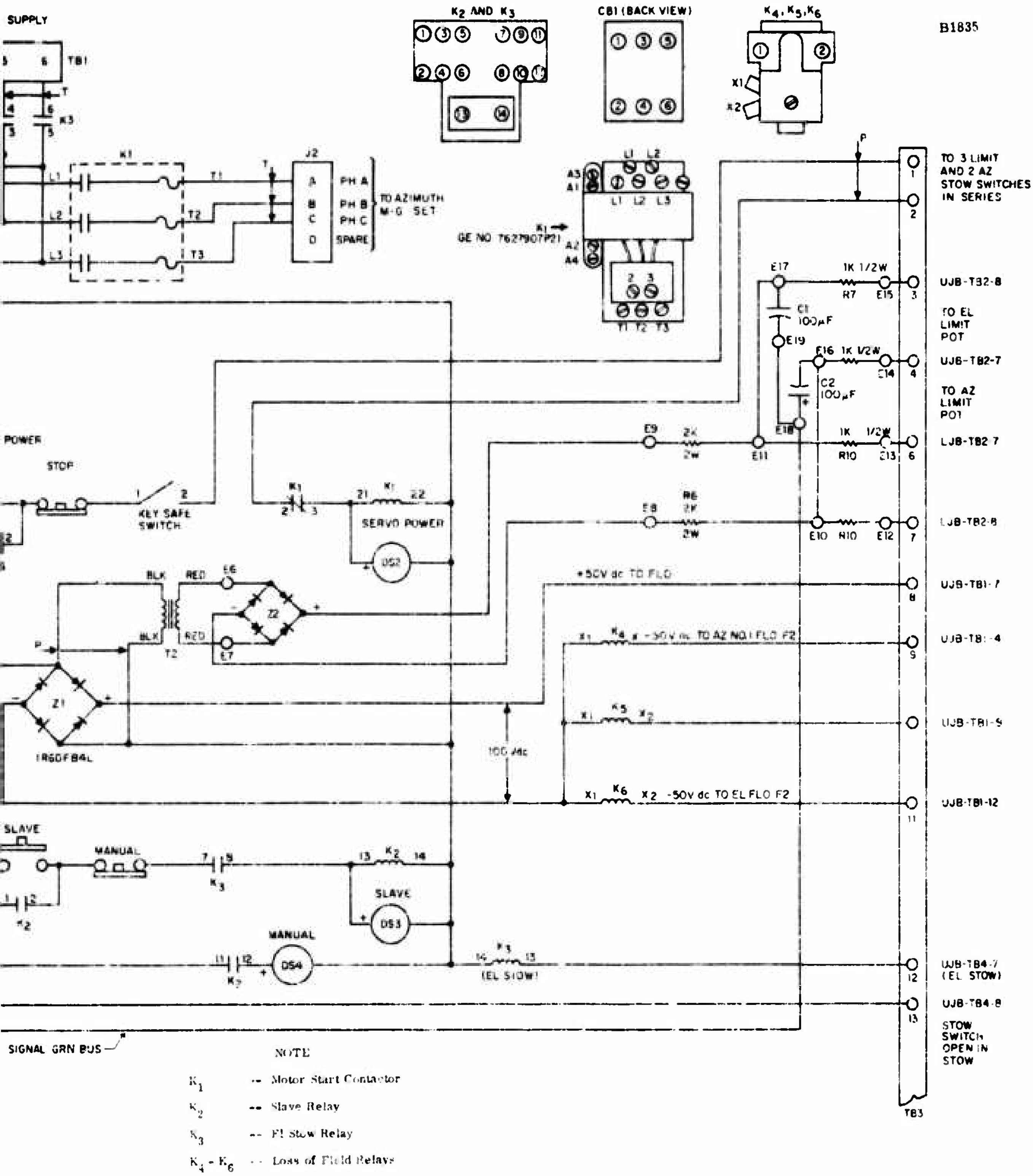

Figure 37. Antenna Positioning Control Circuitry

The operation of the system consists of depressing the START pushbutton and then manually positioning the antenna about its axes (each with a different potentiometer and set of switches) in a velocity mode. The system will automatically start up in the MANUAL mode. To enable the SLAVE mode (slaved to the remote tracker) the operator will have to depress a SLAVE pushbutton. A return to MANUAL can be made at any time by depressing the MANUAL pushbutton.

The operator may compare the commanded input with the antenna response by observing the readout. The antenna may then be directed into correspondence with the command. Spring-centered lever switches select up/down or left/right. Azimuth and elevation potentiometers determine the manual speed; each is independently adjustable.

Special limit potentiometers in the data takeoff units provide "soft" limiting at plus or minus 225° in azimuth and at 70° and -90° in elevation. The limit pots prevent travel past the desired limit points but will not prevent backing out.

APPENDIX I

RF DESIGN ACCEPTANCE TESTS

The following pages are a reproduction of the acceptance test procedure for the RF design. The addendum was submitted to clarify points in the test plan. The report pages include the results of the tests made in accordance with the test plan.

ACCEPTANCE TEST PLAN

NARHORN

RF DESIGN

Submitted to

Rome Air Development Center
as part of
Contract F30602-70-C-0073
GE Requisition EH-61777
Project No. 4506

Prepared by

Heavy Military Electronic Systems
General Electric Company
Syracuse, New York

CONTENTS

I INTRODUCTION AND SCOPE

This document is the RF Design Acceptance Test Plan, submitted as partial completion of item B006 of the Nanosecond Pulse Antenna (NARHORN) contract F30602-70-C-0073. The final acceptance test plan, applying to the deliverable antenna, will be prepared and submitted, as required, in advance of the completion of the antenna, early in 1971. The RF design is best tested on a model, and in fact the RF design checks have been made on such a model. The design model is available for the acceptance tests.

The scope of these tests is limited to the fundamental RF design characteristics, determined by the nominal shape of the antenna. These are the antenna gain, including the losses of the rotary joints, the beamwidth, and the sidelobe levels.

It must be noted that the model of the initial portion of the horn, which in the full-size antenna is Government Furnished, is a simple transition from single-mode waveguide to a uniform conic taper. As recommended in the General Electric proposal, and reviewed with the Project Engineer, this is the RF design condition to which the specifications apply. The effects of the actual horn transition have been computed. The results were presented as an appendix to a monthly status report and were reviewed with the RADC project team. It was was determined that the specifications would apply to the RF design with the low-mode-conversion transition and horn. The actual horn and transition could be modified to reduce mode conversion at a future date.

The data to be acquired is taken by one basic type of test — the pattern test. The tests will be made by engineering personnel, and are not of a type to be repeated in the future. Therefore, the basic test equipment and procedure are described in Sections III and IV of this plan, and the applicable documents in Section II. The test reports are referenced and any additional details are given in the individual specification test plan in Section V.

II APPLICABLE DOCUMENTS

A Statement of Work for Nanosecond Pulse Antenna PR A-0-1000, 1969 April 10.

III BASIC TEST EQUIPMENT

The following is a list of test equipment for radiating a CW signal of about 3 dBm power level directed to the antenna under test. This signal source is located about 20 feet above ground, on a flat roof. The signal is tunable over the frequency band of interest and the polarization is remote controlled from the receiver site.

Make, Model or Equivalent.

HP 8690B Sweep Oscillator

HP 8695A BWO Plugin 12.4 — 18 GHz

HP P752D WR62 Directional Coupler 20-dB

HP P532A Frequency Meter 12.4 — 18 GHz

HP P424A WR62 Crystal Detector

Miscellaneous WR62 waveguide (40 ft) and bends

HP 940A-59A Frequency Doubler

GE WR28 Waveguide Horn with polarization rotation

The following is a list of test equipment at the receive site, located 140 feet from the transmitter horn. The pedestal used to mount the antenna under test is located on a flat roof about 20 feet above ground.

Make, Model or Equivalent.

Antlab Antenna Pedestal Elevation over Azimuth

Antlab Pattern Recorder

Scientific Atlanta SA1710 Receiver

Scientific Atlanta SA13-26 Crystal Mixer

Scientific Atlanta SA12-26 Standard Gain Horn

FXR U610CF WR28 10-dB Directional Coupler

Sperry D41V5 Isolator

HP 608 VHF Signal Generator

Telonic TG-950 VHF Attenuator

IV PATTERN TEST PROCEDURE

The model antenna will be mounted on the pedestal, with control of azimuth and elevation positions. The receiver is a superheterodyne type, with the first mixer connected to the model antenna. The tunable LO in the receiver is fed to the mixer by coaxial cable. The IF is returned to the receiver by the same cable. The bolometer output of the receiver is used to drive the 40-dB logarithmic pen amplifier of the pattern recorder. The pattern recorder chart is controlled by synchros located in the pedestal. Before taking a pattern the receiver will be tuned to the transmitter frequency. The pedestal will be adjusted to the position of the main beam, and the gain will be set to position the recorder pen at the 1-dB position on the 40-dB paper. The pattern will be taken by rotation of the antenna pedestal. This will give an X-Y plot of the model antenna pattern; (angle of rotation versus signal level). Calibration will be accomplished by a substitution method because the

measurements are relative (sidelobe level to main beam level, antenna to gain standard, or beamwidth). Both the receiver and the pattern recorder can be calibrated by inserting a signal at the receiver from a signal generator operating at the intermediate frequency. The level is then adjusted, by means of a calibrated step attenuator, to any point in the recorder range. This method will calibrate the system, with the exception of the first mixer. The maximum RF signal input to the 1N53C crystal mixer is extremely low (less than -35 dBm), with ample local oscillator injection. It will be considered to be linear.

Model antenna gain measurements will be taken by using a standard gain horn. By using a WR28 waveguide 10-dB coupler, both the model antenna and the standard gain horn can be connected to the receiver. In this configuration the antennas will face 90° apart. An antenna pattern in this configuration will measure the difference in gain and coupler loss. When a second pattern is taken with the coupler waveguide ports reversed, the coupler loss becomes known and the model antenna gain above an isotropic source is measured. The gain measurements will be recorded on the test report summary sheet.

The model antenna beamwidth measurements are made by taking a pattern of the main beam on the expanded 12-degree scale and reading the angle at the half-power (3-dB) points. The E and H plane beamwidths will be recorded on the test summary sheet.

The model antenna sidelobe measurements will be made by taking a wide angle pattern of the main beam and sidelobes through an angle of 15° on either side of the mainlobe. These patterns will be E and H plane, at combinations of model elevation positions of 0, 35, and 70 degrees, and azimuth positions of 0, 45 and 90 degrees. The first and second sidelobes on both sides of the main beam will be read on each pattern in dB down from the peak of the main beam, and recorded on the test summary sheet.

All tests (gain, beamwidth, and sidelobes) will be taken at three frequencies — Fo, Fo -7.5 percent, and Fo +7.5 percent.

It is desirable not to test during inclement weather, both to protect the model and the equipment and to avoid any changing path loss from rain. While the path is short, heavy rain could cause a noticeable change in level.

V TEST REPORTS AND REQUIREMENTS

The test reports for the RF design acceptance will be on the forms appended to this plan.

A. Gain

The model antenna gain is to be 37 dB minimum, with a goal of 39 dB above an isotropic source, per work statement PRA-0-1000 RADC 1969 Apr. 10.

B. Beamwidth

The model antenna beamwidth is to be 2° x 2° nominal at half-power main beamwidth points, per work statement PRA-0-1000 RADC 1969 Apr. 10. Note that this has no tolerance (the proposal suggested a beamwidth of 2 ± 0.5 degrees).

C. Sidelobes

The model antenna sidelobe level is to be -15 dB minimum, -20 dB goal, in reference to the main beam in both E and H planes, per work statement PRA-0-1000 1969 Apr. 10.

GENERAL ELECTRIC

REV NO.	TITLE	
CONT ON SHEET 2 SH NO. 1	Acceptance Test Report	CONT ON SHEET 2 SH NO 1
	FIRST MADE FOR NARHORN Model Antenna	

REVISIONS

SIDELOBE LEVEL

There were no sidelobes observed that exceeded the specification level.

Witnessed: John L Stapleton - RADC Certified: S. W. Kenyon G.E.

-dB From Peak of Beam

Antenna Position		Polarization	31 GHz				33.5 GHz				36 GHz			
Az	Elev	Plane	2nd	1st	1st	2nd	2nd	1st	1st	2nd	2nd	1st	1st	2nd
0°	0°	EP	28	17	17	28	27	17	17	28	28	18	17	28
0°	0°	HP	34	27	23	35	35	25	22	35	35	21	28	37
0°	35°	EP	28	20	16	28	28	17	16	27	28	19	16	29
0°	35°	HP	36	21	27	38	37	24	29	37	38	22	29	38
0°	70°	EP	24	16	16	26	28	17	16	28	25	17	16	30
0°	70°	HP	34	23	28	37	32	24	28	36	34	26	29	36
45°	0°	EP	26	16	17	26	25	17	17	25	27	18	18	28
45°	0°	HP	34	28	24	34	34	30	24	35	36	29	22	36
45°	35°	EP	29	19	18	26	26	18	17	27	27	19	18	29
45°	35°	HP	36	27	24	35	34	23	27	36	36	28	23	35
45°	70°	EP	28	17	16	27	27	20	16	26	29	20	17	29
45°	70°	HP	34	24	27	33	35	23	28	35	36	22	27	35
90°	0°	EP	25	17	17	26	25	18	17	26	26	19	17	27
90°	0°	HP	33	26	27	34	34	28	26	33	35	29	27	36
90°	35°	EP	26	18	19	26	24	17	18	26	26	17	20	27
90°	35°	HP	35	26	26	31	35	30	25	34	36	28	25	35
90°	70°	EP	25	19	19	28	26	16	18	27	26	17	19	30
90°	70°	HP	38	29	22	35	39	28	23	35	40	25	25	36

Witnessed: John L Stapleton - RADC Certified: S. W. Kenyon G.E.

PRINTS TO

MADE BY S W Kenyon	APPROVALS	HMES, APD DIV OR DEP.	
ISSUED 22 July 1970		Syracuse LOCATION	CONT ON SHEET 2 SH NO 1

CODE IDENT NO

FF-000-WA (10-60) PRINTED IN U.S.A.

GENERAL ELECTRIC

REV NO.	TITLE	CONT ON SHEET SH NO. 2
CONT ON SHEET SH NO. 2	Acceptance Test Report FIRST MADE FOR NARHORN Model Antenna	

REVISIONS

Gain Measurements

Antenna Position		Polarization	Frequency		
Az	Elev	Plane	31 GHz	33.5 GHz	36 GHz
0°	0°	HP	40.6 dB	41.75 dB	42.3 dB

3 dB Beamwidth Measurements

in Degrees

Az	Elev	Plane	31 GHz	33.5 GHz	36 GHz
0°	0°	EP	1.65	1.50	1.45
0°	0°	HP	1.95	1.85	1.75
90°	0°	EP	1.65	1.5	1.45
90°	0°	HP	1.95	1.85	1.75
0°	70°	EP	1.65	1.52	1.45
0°	70°	HP	1.95	1.85	1.75
90°	70°	EP	1.64	1.50	1.45
90°	70°	HP	1.95	1.85	1.75

The preceding data was taken in accordance with the Acceptance Test Plan.

Witnessed: John L Stapleton - RADC Certified: S.W. Kenyon G.E.

PRINTS TO

MADE BY S.W. Kenyon	APPROVALS	HMES, APD DIV OR DEPT.	
ISSUED 22 July 1970		Syracuse LOCATION	CONT ON SHEET SH NO 2

CODE IDENT NO

FF-000-WA (10-60) PRINTED IN U.S.A.

ADDENDUM No. 1

to

ACCEPTANCE TEST PLAN

NARHORN

RF DESIGN

Submitted to

Rome Air Development Center
as part of
Contract F30602-70-C-0073
GE Requisition EH-61777
Project No. 4506

Prepared by

Heavy Military Electronic Systems
General Electric Company
Syracuse, New York

This addendum to the Acceptance Test Plan, NARHORN RF Design, is submitted as a result of the discussion Wednesday, August 12 between representatives of RADC and General Electric. This addendum includes the following:

1. The mount and the antenna positioning for pattern testing is described.
2. The meanings of the angles referenced on the data sheets are explained.
3. A figure which will make clear the gain measuring technique is included.
4. A statement that there were no sidelobes observed exceeding the specification level will be made.

The RF design acceptance tests are intended only to demonstrate compliance with the parts of the antenna specification which cannot be effectively demonstrated on the final antenna. Considerable other data about the antenna will appear in the interim technical report and in the final report which will include typical patterns, a complete discussion of the design approach, and patterns taken in the cross-polarized sense.

The test range, with the antenna in position, is shown in the photograph. In the foreground is the test pedestal. In the background is the source antenna mounted on the building roof with the source transmitter located in the trailer. The range has been checked and no reflections from the ground or the fences were located. There are reflections from a stairway railing and a stack out of sight to the right of the picture, and well behind the antenna position. Their levels are sufficiently low and their position far from the beam direction during test that their effect can be neglected except in the 360-degree tests where they are specifically identified.

The antenna test mount is a commercial, remotely controlled, elevation-over-azimuth unit. A polarization axis has been added in the form of a steel shaft through pillow blocks on the pedestal table. This bar is concentric with the antenna radiation axis. Rotation about this axis permits any desired pattern to be taken by azimuth

rotation of the pedestal. The polarization of the model antenna changes as it is adjusted to different "azimuth" and "elevation" positions. During tests the antenna will be rotated about the polarization axis until the desired pattern direction with respect to the aperture polarization is in the azimuth direction. The source polarization is set to vertical for H-plane, or horizontal for E-plane, principal plane patterns. Other pattern cuts can be made by suitably positioning the antenna on the polarization axis and properly changing the source polarization.

In the photograph, the model antenna is shown with azimuth set at 90° and elevation at 90°. The model is positioned at boresight, and will be rotated in azimuth for an E-plane pattern.

The antenna position descriptions are based upon rotation of the azimuth and elevation joints. The elevation joint positions correspond exactly to those which the antenna will take for the corresponding beam azimuthal positions, relative to the building nominal north. That is, the 0°, 0° position of the antenna corresponds to the beam aimed parallel to the roof beams, in the northerly direction and at zero degrees elevation angle. The 90°, 0° position will produce an east directed beam aimed at the horizon.

The model antenna assembly will be positioned to the angles given. It will be rotated about the beam axis, on the "polarization" axis, to place the on-boresight polarization either vertical for H-plane patterns, or horizontal for E-plane patterns.

GENERAL ELECTRIC

REV NO.	TITLE	SK-62667-799-4 CONT ON SHEET SH NO 1
SK-62667-799-4 CONT ON SHEET SH NO 1	Gain Measuring Technique FIRST MADE FOR NARHORN	REVISIONS

a. First Test Configuration

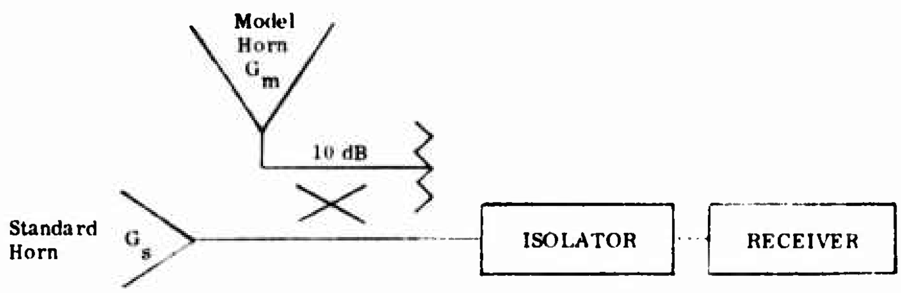

SYMBOLS:

G_m	Model Horn Gain
G_s	Standard Horn Gain
C_d	Coupler Diagonal Coupling (10 dB nom)
C_s	Coupler Straight Coupling (0.5 dB nom)
ΔG_a	Difference in peak gain, first configuration
ΔG_b	Difference in peak gain, second configuration

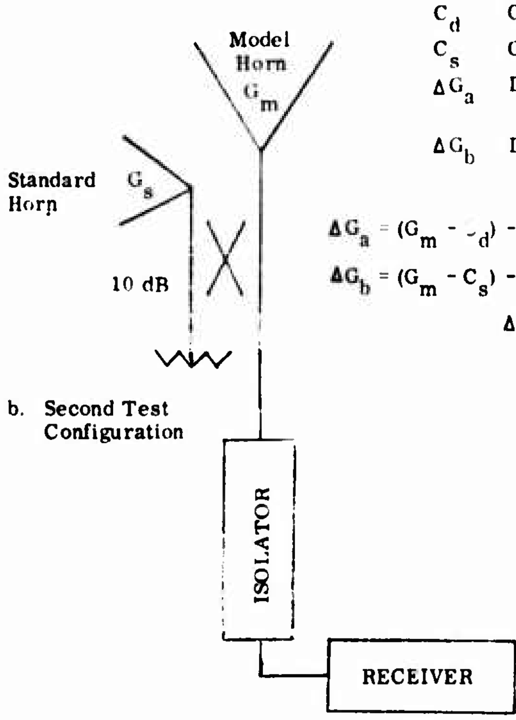

b. Second Test Configuration

$$\Delta G_a = (G_m - C_d) - (G_s - C_s) = G_m - C_d - G_s + C_s$$

$$\Delta G_b = (G_m - C_s) - (G_s - C_d) = G_m - C_d - G_s + C_s$$

$$\Delta G_a + \Delta G_b = 2G_m - 2G_s$$

$$G_m = G_s + \frac{\Delta G_a + \Delta G_b}{2}$$

PRINTS TO

MADE BY *R Blumgenwath* ISSUED *17 AUG 1970*	APPROVALS	HMES DIV OR DEPT Syracuse LOCATION	SK 62667-799-4 CONT ON SHEET SH NO 1

FF-803-WA (10-68)
PRINTED IN U.S.A.

CODE IDENT NO

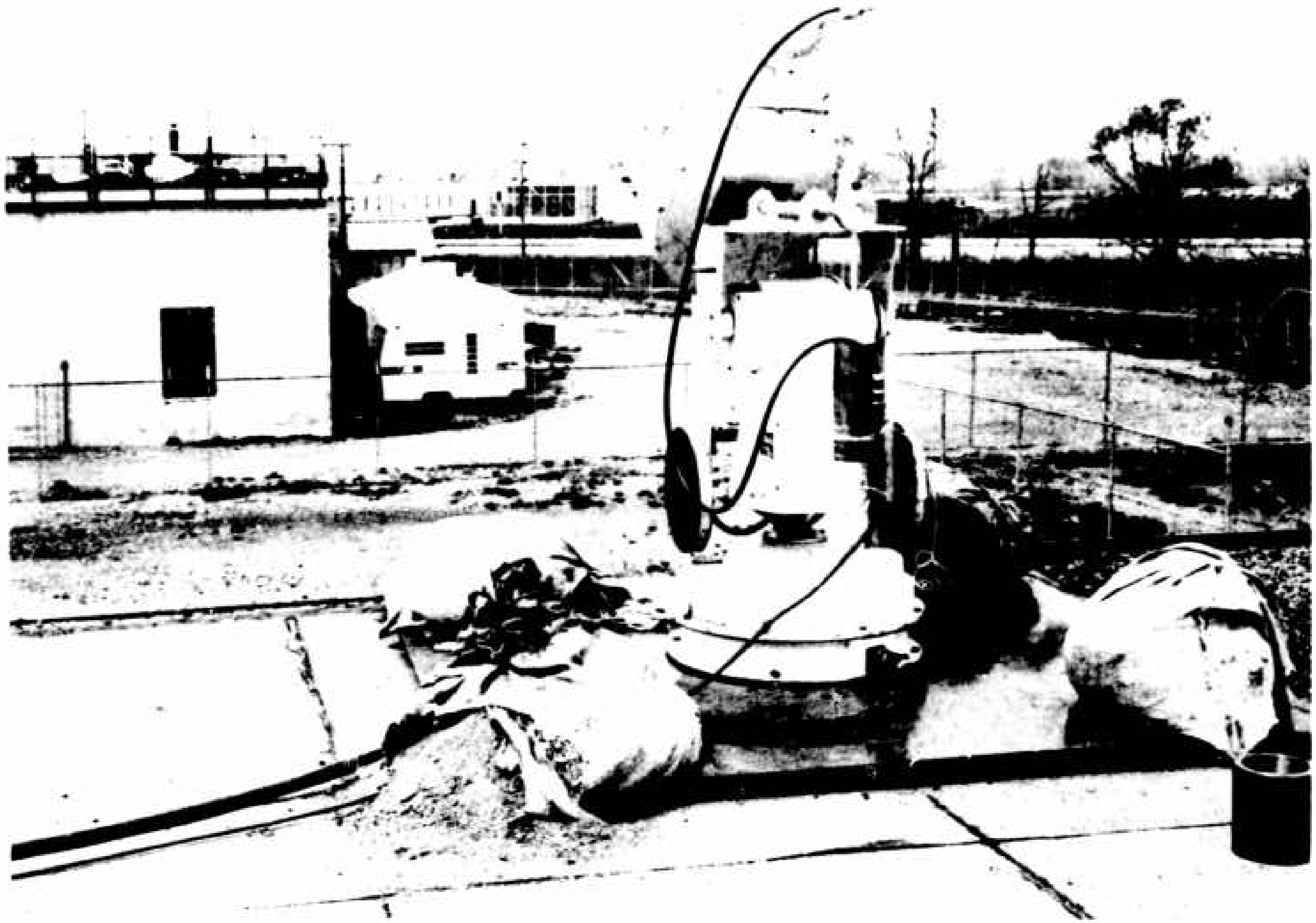

Figure 38. Test Range with Antenna in Position

APPENDIX II

STRUCTURAL SPECIFICATION

The following pages are a reproduction of the specification for the antenna structure. This specification is the requirement placed upon Fleet Manufacturing, Ltd., Fort Erie, Ontario, who will be fabricating the antenna structure.

GENERAL ELECTRIC

SK 62677-801-5-50

CONT. ON SHEET 1 SH. NO.

COVER SHEET

TITLE

WORK-SPECIFICATION FOR FOLDED CONE ANTENNA (NAROWS)

SPECIFICATION REVISION STATUS

REVISIONS A.N. / DATE	[illegible]	[illegible]	[illegible]	[illegible]	[illegible]	15 [illegible] 70	3 Sept 70	[illegible] 70	8 Oct 70	[illegible] 70	2 Nov 70	3 [illegible] 70	12 [illegible] 70	22 Dec 70								
SYMBOL	A	B	C	D	E	F	G	H	J	K	L	M	N	P	R	S	T	U	V	W	Y	Z
SHEET NO.							SHEET REVISION STATUS															
1		X																				
2		X																				
3		X				X		X														
4		X																				
5		X	X																			
6		X	X																			
7		X																				
8		X																				
9		X																				
10		X																				
11		X																				
12		X																				
13				X																		
14												X	X									
15	X				X							X										
16					X	X	X	X	X	X	X			X								
17					X																	

• ADDED SHEET
•• DELETED SHEET

NOTE: THIS COVER SHEET IS FOR G.E. AND ITS VENDORS USE. IT MAY BE SUPPLIED TO THE GOVERNMENT AGENCY WHERE DATA IS REQUIRED.

PRINTS TO

MADE BY [illegible signature]

ISSUED May 21, 1974

HMED
SYRACUSE

SK 62677-801-5-50

CONT. ON SHEET 1 SH. NO.

CODE IDENT. NO.
03538

HMED-0007

TITLE

Folded Cone Antenna

20 May 1970

FIRST MADE FOR

REVISIONS

Revision B May 2 1970

SECTION 1. GENERAL INSTRUCTIONS

1.1 The subcontractor shall furnish parts as itemized in Section 2 of this specification when such requirements for parts are released.

1.2 APPLICABLE DOCUMENTS

Documents listed below form a requirement of the Work Specification. In case of conflict between this and any of the documents listed below or any Military Specifications referenced, this purchase specification shall govern.

1.2.1 GENERAL ELECTRIC COMPANY FURNISHED DOCUMENTS

PQR-980 Procurement Quality Control Requirements
SK-62677-801-5-50 Work Specification Folded Cone Antenna, see Section 4.

1.3 CHANGES TO WORK - SPECIFICATION

1.3.1 Change Procedure - Changes to any of the requirements of this work-specification and/or contract terms and conditions will be made by formal change order amendment to the order by Subcontract Purchasing. Any price and/or delivery revision resulting from authorized changes shall be submitted to the Buyer within fifteen (15) days after receipt for evaluation and/or negotiation.

SECTION 2. DEFINITION OF MATERIALS AND SERVICES BY PART NUMBERS

2.1 Folded Cone Antenna in accordance with Section 4 of this specification.

2.2 Manuals in accordance with Section 5 of this specification.

PRINTS TO

MADE BY Maurice C Swann

ISSUED May 21, 1970

APPROVALS

HMES DIV OR DEPT

Syracuse, N. Y. LOCATION

SK 62677-801-5-50
CONT ON SHEET 2 SH NO 1

FF-803-WA (H-67) PRINTED IN U S A

CODE IDENT NO

2.3 Technical documentation (reproducible manufacturing drawings (sepias). In accordance with Section 8 of this specification.

2.4 Test Data - per Section 10 of this specification.

2.5 Spare Parts - to be negotiated at later date, if required.

2.6 Spare parts documentation to negotiated at later date, if required.

2.7 Reports in accordance with Section 9 of this specification.

2.8 Tooling in accordance with Section 6 of this specification.

2.9 Acceptance - per Section 10.

SECTION 3. GENERAL REQUIREMENTS

This specification governs the engineering design and performance of the equipment and tooling to be manufactured for the Heavy Military Electronic Systems, General Electric Company, Syracuse, New York, and shall enable the subcontractor to perform the following tasks:

3.1 Design of folded cone antenna.

3.2 Fabrication of folded cone antenna.

3.3 Installation and consultation at site of erection of folded cone antenna.

3.4 Test of the folded cone antenna described herein together with its control and drive system, data pickoff assemblies and supporting structure.

REVISIONS

SECTION 4. FOLDED CONE ANTENNA

4.1 GENERAL DESCRIPTION

The antenna described in Figure 1 will consist of a right circular cone with an effective length of about twenty-one feet, an included angle of twenty-five degrees and folded at a point on the centerline approximately six feet from the plane of the base.

The cone portion of the structure from the apex to a plane approximately eight feet (8) from the apex, measured along the centerline, will be omitted.

The energy fed into the apex will be reflected ninety degrees by a flat reflector at the fold and ninety degrees by a parabolic reflector at the base.

The interior and reflective surfaces will be aluminum. An extension of the cone will be part of the parabolic reflector assembly.

A cylindrical shield will extend from the upper end of the parabolic reflector about six inches in the direction of the beam.

One man crank to stow position must be provided in both elevation and azimuth.

4.2 CONSTRUCTION DETAILS

4.2.1 HORIZONTAL JOINT (AZIMUTH)

At this location, the antenna will match with a horn described by drawing STI 1146 B and located as shown on drawing SK 58019-778-1RevB with an included flange detail.

The choke area relation and configuration will be generally as shown in Figure 2 with a one-quarter inch clearance requirement and a base ring, R.F. absorbing material and weather shield.

PRINTS TO

4.2.2 VERTICAL JOINT (ELEVATION)

This joint will be generally located at the junction of the base of the parabolic mirror.

A choke area will be generally as shown in Figure 3 with a one-quarter inch clearance.

4.3 PARABOLIC REFLECTOR

The overall size of the parabolic reflector will be such that a twelve foot diameter antenna aperture will be realized.

The parabolic reflector must rotate about the horizontal centerline (axis) of the cone with a servo-control with a variable rate up to 0.6 RPM.

The bearing and support arrangement must insure that a one-quarter inch gap plus or minus one-eighth inches, will be maintained between the fixed and the rotating portions of the antenna.

The parabolic reflector will rotate from zero elevation angle (horizon) to plus seventy degrees, as well as between minus seventy to ninety degrees below horizon for weather protection and storage.

4.4 AZIMUTH ROTATION

The antenna cone assembly together with the parabolic reflector will rotate in a horizontal track through a four hundred and fifty degree arc at any rate up to 3 RPM.

Control and power cables will be allowed to wrap around the structure.

4.5 SERVO DRIVE INTERFACE

Antenna rotation in azimuth will be produced by DC power servo-motor(s) driven from a motor-generator set. The number and type of motors and any gear ratio will be specified by GE based on antenna characteristics to be supplied by the vendor.

Rotation of the antenna in elevation will be produced by a DC power servo-motor driven from a power amplifier. The type of motor and any gear ratio will be specified by GE based on antenna characteristics to be supplied by the vendor.

Antenna characteristics to be supplied for selection of the power elements and gear ratios include inertia; wind/snow/ice loadings; friction; and, unbalance; in both the azimuth and elevation axes.

The data pick-off assembly for azimuth will position a 13-bit binary encoder operating at .64 speed. The assembly should be so mounted and driven as to produce stable position signals with an accuracy from antenna azimuth position to encoder shaft position of ± 0.05 degrees. A multi-turn, helical potentiometer operating at 5.6 speed (tentative) and a pair of limit switches will be used to supply signals for position limiting in the servo azimuth drive system.

The data pick-off assembly for elevation will position a 13-bit binary encoder operating at 64 speed. The assembly should be so mounted and driven as to produce stable position signals with an accuracy from antenna elevation position to encoder shaft position of ± 0.05 degrees. A multi-turn, helical potentiometer operating at 36 speed (tentative) and a pair of limit switches will be used to supply signals for position limiting in the servo elevation drive system.

Final configuration of the azimuth and elevation power drive systems and data pick-off assemblies (including methods of mechanically connecting rotating components) must be approved by GE.

REV NO. SK 62677-801-5-50 CONT ON SHEET 7 SH NO. 6

TITLE Folded Cone Antenna

FIRST MADE FOR

REVISIONS

Revision C May 27, 1970

4.5 (contd)

Wiring from weatherproof junction box(es) to the azimuth and elevation components will be performed by the antenna vendor. Proposed method and wire sizes must be approved by GE.

The required drive motors, encoders, and potentiometers will be supplied by GE.

4.6 ENVIRONMENT

4.6.1 OPERATION

The antenna must operate without degradation of performance under the following conditions:

1. Temperature minus 35°F to plus 110°F.
2. Wind
   a. Steady up to 15 knots.
   b. Gusts up to 40 knots.

4.6.2 STOW POSITION

The antenna must survive:

1. Wind
   a. Steady - 50 knots.
   b. Gusts - 80 knots.
2. Snow load - 40 lbs. per sq. foot on all horizontal surfaces.
3. Ice load - 1 inch on all surfaces.

4.6.3 NORMAL CLIMATIC CONDITIONS

Provisions shall be made to prevent damage to the structure and/or interference to operation as a result of normal climatic conditions.

PRINTS TO

MADE BY	APPROVALS		
Maurice C. Sutherland		HMES DIV OR DEPT.	SK 62677-801-5-50
ISSUED May 21, 1970		Syracuse, N.Y. LOCATION	CONT ON SHEET 7 SH NO. 6

FF-880-WA (H-67) PRINTED IN U S A

CODE IDENT NO

4.7 **TOLERANCES**

Allowable deviation from the theoretical shape is plus or minus one-quarter inch from the cone surfaces and plus or minus one-tenth inch of the reflective surfaces.

The angular locations of the centerlines in both the azimuth and elevation planes should be within plus or minus five minutes.

SECTION 5. MANUALS

The Contractor shall furnish a quantity of eight (8) equipment handbooks concurrent with the delivery of the equipment and five (5) preliminary copies thirty (30) days prior to equipment delivery. The handbooks shall be prepared in accordance with the following general guidelines.

5.1 Cover Page shall be printed on durable cover stock and shall contain the title with correct nomenclature, security information, contract number, design activities designation, and date of publication.

5.2 Title Page shall contain the same information as appears on the cover page.

5.3 Table of Contents shall be a complete index to all important subdivisions comprising the text of the manual, with page number on which they appear.

5.4 List of Illustrations shall list in numerical sequence all illustrations by figure number and caption, with the page number on which they appear.

5.5 Description of Equipment should include data such as part number, model, size, weight, capability limitations, cubage, power characteristics, tolerance/accuracies, external view, functional description, method of operation, etc.

REVISIONS

Revision B May 21, 1970

5.6 Normal Operating Instructions shall include instructions sufficient to adjust, stop/start, and operate the equipment properly. Special start-up precautions, as well as other items requiring action before the equipment is put into service, should be noted.

5.7 Preventive Maintenance should cover all cleaning, inspection, and lubrication necessary to properly maintain the equipment. Inspection instructions should describe allowable wear, backlash, discoloration, etc. All lubrication instructions shall be supported by lubrication diagrams and/or figures with lubrication points indexed and recommended types of lubricants identified.

5.3 Scale and Corrosion Control information covering the preventive and removal of scale and corrosion shall be provided but will not duplicate information contained in TO 1-1-2.

SECTION 6. TOOLING

A master gage (egg crate) type inspection fixture shall be a required tool. This fixture shall be capable of accepting the reflector in its normal operating position.

SECTION 7. QUALITY ASSURANCE

7.1 This section contains the quality requirements to which the subcontractor must comply.

7.2 The subcontractor must comply with the requirements of PQR-980.

7.3 General Electric HMES Quality Control will monitor the subcontractor to assure compliance with 7.2 above.

PRINTS TO

REVISIONS

SECTION 8. TECHNICAL DOCUMENTATION

Two complete ... of reproducible manufacturing drawings (sepias) will be furnished with the equipment on or before the delivery date. The drawings and related documents (parts lists, instruction books, specifications, etc.) will be tabulated in a data list in alpha/numerical sequence. All parts, assemblies, subassemblies, and bulk materials necessary to assemble or fabricate items delineated on assembly drawings will be tabulated in a parts list. The drawings need not reveal patented design features made specifically for this contract. All parts peculiar to the contract shall be completely dimensioned. Drawings shall be supplied showing method of assembly of these parts to each other, and to the equipment as a whole.

SECTION 9. REPORTS

9.1 REPORTS

Progress reports relative to the equipment being furnished according to this Work Specification will be forwarded to HMES, General Electric Company not later than the 15th day of each calendar month. The progress reports will be submitted in triplicate to the Subcontract Buyer, Farrell Road, HMES, General Electric Company, Syracuse, New York 13201. The Progress Reports will include information on the following:

9.1.1 Design of each major component of equipment.

9.1.2 Tool Design.

9.1.3 Tool fabrication.

9.1.4 Fabrication of each major component of equipment.

9.1.5 Estimates of technical completion.

PRINTS TO

REVISIONS

9.2 MONTHLY STATUS

The Contractor shall supply monthly status reports. The reports shall be prepared as follows:

9.2.1 Description of approach and progress during the reporting period, supported by reasons for any change in approach reported previously.

9.2.2 Description of any major items of experimental or special equipment purchased or constructed during the reporting period.

9.2.3 Notification of any changes in key personnel associated with the contract during the reporting period.

9.2.4 Summary of substantive information derived from noteworthy trips, meetings, and special conferences held in connection with the contract during the reporting period.

9.2.5 Summary of any problems or areas of concern on which assistance or guidance is required.

9.2.6 Estimate of percent of technical completion.

9.2.7 A minimum of three design review meetings will be scheduled during the contractual period for the purpose of discussing all aspects of the contract.

SECTION 10. ACCEPTANCE TESTS

10.1 THE FOLDED CONE ANTENNA

It shall be subjected to any test which General Electric has considered necessary to determine compliance with the requirements of this specification. All members and parts shall be given a mechanical inspection to determine the quality of material and workmanship and compliance with the requirements of the specification. Particular attention shall be given to the following points:

PRINTS TO

Revision 6 May 21, 1970

10.1.1 Completeness

10.1.2 Nameplates, identification markings and labels.

10.1.3 Finishes

10.1.4 Welded Joints

10.1.5 The fit of components in their respective positions.

10.1.6 Check of the mounting means.

10.1.7 Check of lubrication and rust prevention.

10.1.8 Loose fastening and securing devices and parts.

10.1.9 Accessibility of components, and parts for servicing.

10.1.10 Over-all dimensional check.

10.1.11 Other visible defects.

10.2 FINAL ACCEPTANCE

The General Electric Company will officially accept the antenna and related equipment after it has been installed in its permanent location and has demonstrated that it meets the requirements of this specification.

SECTION 11. PREPARATION FOR DELIVERY

11.1 Preparation for Delivery - The reflector shall be prepared for shipment in accordance with good commercial practice described in General Electric document 7030414, part 7. Shipping instructions and schedules will be given in the Purchase Order or Amendment thereto.

11.2 The subcontractor will be responsible for safe transportation of the folded cone antennas from place of manufacture to site of erection and consultation and support effort during erection cycle.

SECTION 12. GENERAL ELECTRIC FURNISHED DATA

SECTION 13 APPENDIX

DELETE: 4.1 One man crank to stow position must be provided in both elevation and azimuth.

ADD: 4.1 Provision shall be made for one man band crank movement of the antenna system in the event of power failure or motor malfunction. There shall be provided a "stow lock" position in which the antenna can be left when not in operation and during adverse weather conditions. The operation and position should be protected against the possible application of power by interlocks. Overtravel stops should be provided in elevation and azimuth if possible.

ADD: 4.6.4 INSTALLATION REQUIREMENTS.

The structure will be mounted on a roof framework as described on Drawing SK 58019-778-1. It is, permissable to drill through the roof beams. The total weight shall not exceed 13,000 pounds.

REV NO.	TITLE
SK 62677-801-5-50 CONT ON SHEET 14 SH NO. 13	FOLDED CONE ANTENNA
	FIRST MADE FOR

REVISIONS

DELETE SECTION 6 TOOLING

A master gauge....a required tool. This fixture....normal operating position.

ADD SECTION 6 TOOLING

Any tooling required for the manufacture of this antenna shall be the property of General Electric and/or the customer will be given disposition at a later date.

DELETE:	9.1.5	Estimates of technical completion.
DELETE:	9.2.7	A minimum....the contract.
ADD:	9.3	A minimum....the contract.
DELETE:	10.1	It shall be subjected...of this specification.
ADD:	10.1	The antenna shall be subjected to those tests necessary to determine compliance with the requirements of this specification.

PRINTS TO

MADE BY	APPROVALS	HMES	DIV OR DEPT	SK 62677-801-5-50
Maurice C Juerson				
ISSUED June 1, 1970		Syracuse, N.Y.	LOCATION	CONT ON SHEET SH NO 13

FP-803-W (12-68) PRINTED IN U.S.A.

CODE IDENT NO

GENERAL ELECTRIC

SK 62677-801-5-50

CONT ON SHEET 15 SH NO. 14

REV NO.

SK62677-801-5-50

CONT ON SHEET 15 SH NO. 14

TITLE

FOLDED CONE ANTENNA

FIRST MADE FOR NAROWS

REVISIONS

REV M- CHGD DELIN OF APERT TO AGREE WITH REV M ON SH 15 3 DEC 70

REV N- 88.221 WAS 87.24 9 DEC 70

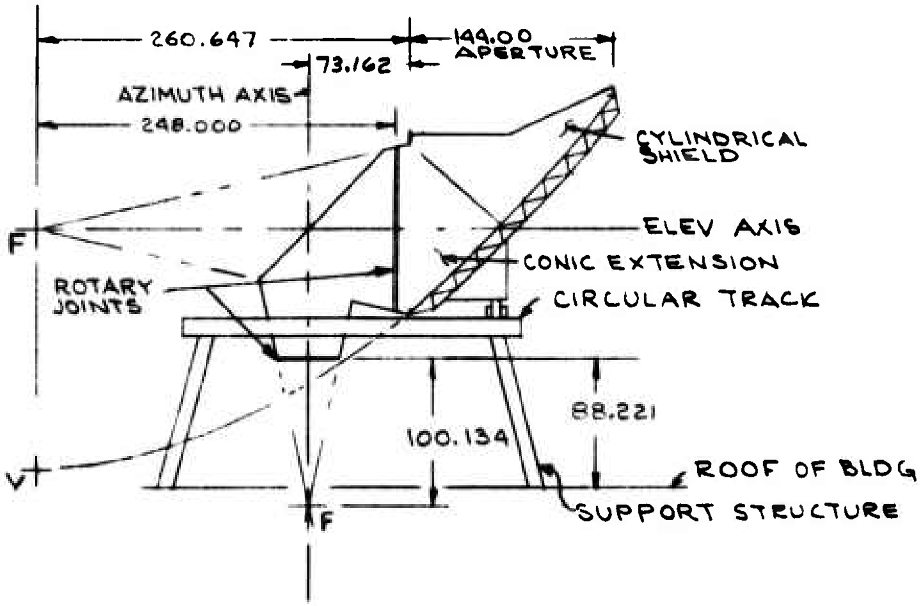

FIG. 1

DIM. IN INCHES

PRINTS TO

MADE BY 15 MAY 70

APPROVALS

HMES DIV OR DEPT.

Syracuse, N.Y. LOCATION

SK62677-801-5-50

CONT ON SHEET 15 SH NO. 14

CODE IDENT NO

PRINTED IN U.S.A.

GENERAL ELECTRIC

REV NO.	TITLE
SK 62677-801-5-50 CONT ON SHEET 16 SH NO. 15	FOLDED CONE ANTENNA FIRST MADE FOR NAROWS

SK 62677-801-5-50
CONT ON SHEET 16 SH NO 15

REVISIONS

REV M - 61.785 WAS 66.785
92.710 WAS 94.710 SLOPE OF ANGLE WAS FROM 260.647 TO 94.710

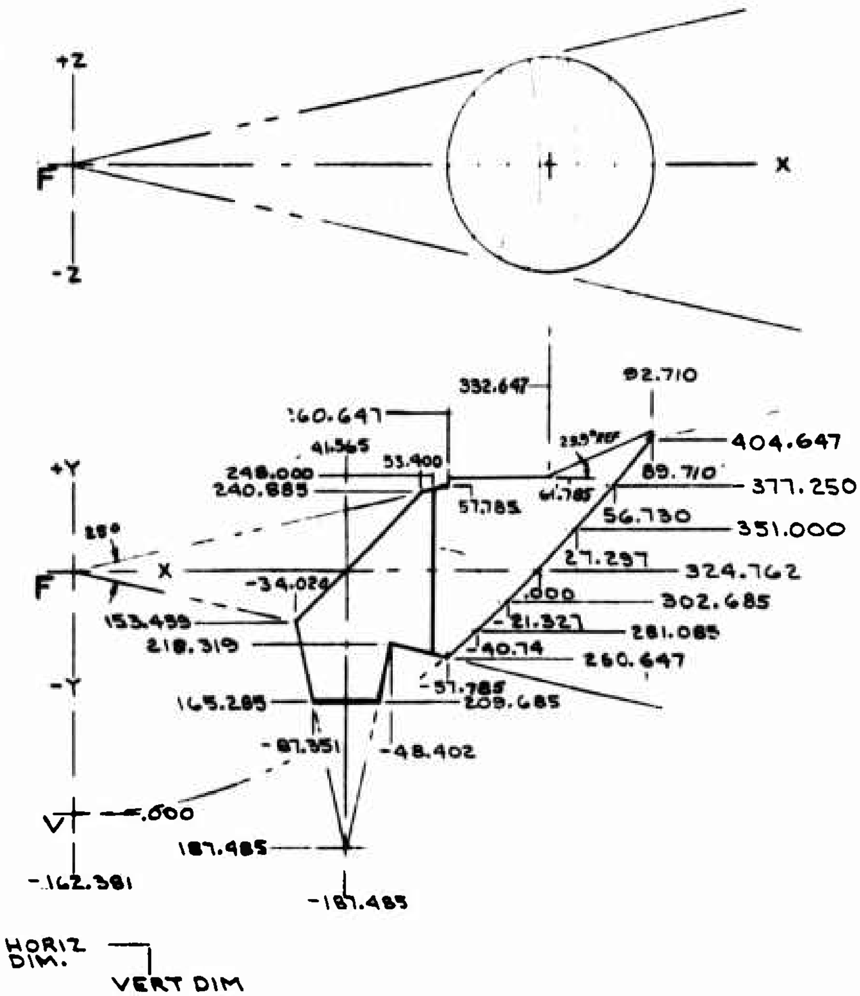

FIG. 1A

DIM. IN INCHES

MADE BY	APPROVALS		
15 May '72		HMES Syracuse, N.Y.	SK62677-801-5-50 CONT ON SHEET 16 SH NO. 15

PRINTS TO

CODE IDENT NO

PRINTED IN U.S.A.

GENERAL ELECTRIC

SK 62677-801-5-50	CONT ON SHEET 17 SH NO. 16

REV NO.	TITLE
SK62677-801-5-50	FOLDED CONE ANTENNA
CONT ON SHEET 17 SH NO. 16	FIRST MADE FOR NAROWS

REVISIONS

REV D 101.628 WAS 101.585 22 DEC 70

REV F CHGD TO AGREE WITH STI DWG 114G 15 ... 70

REV G ADDED 5.00 DIM 8 SEPT 70

REV H CHGD DELIN TO AGREE WITH STI 1146B

REV J - AIR GAP DIM .50 WAS .25 ADDED .50 BY RF ABSORBER

REV K ADD .090 THK SHIELD RING 19 OCT 70

REV L ADDED DIM FROM APEX 24 NOV 70

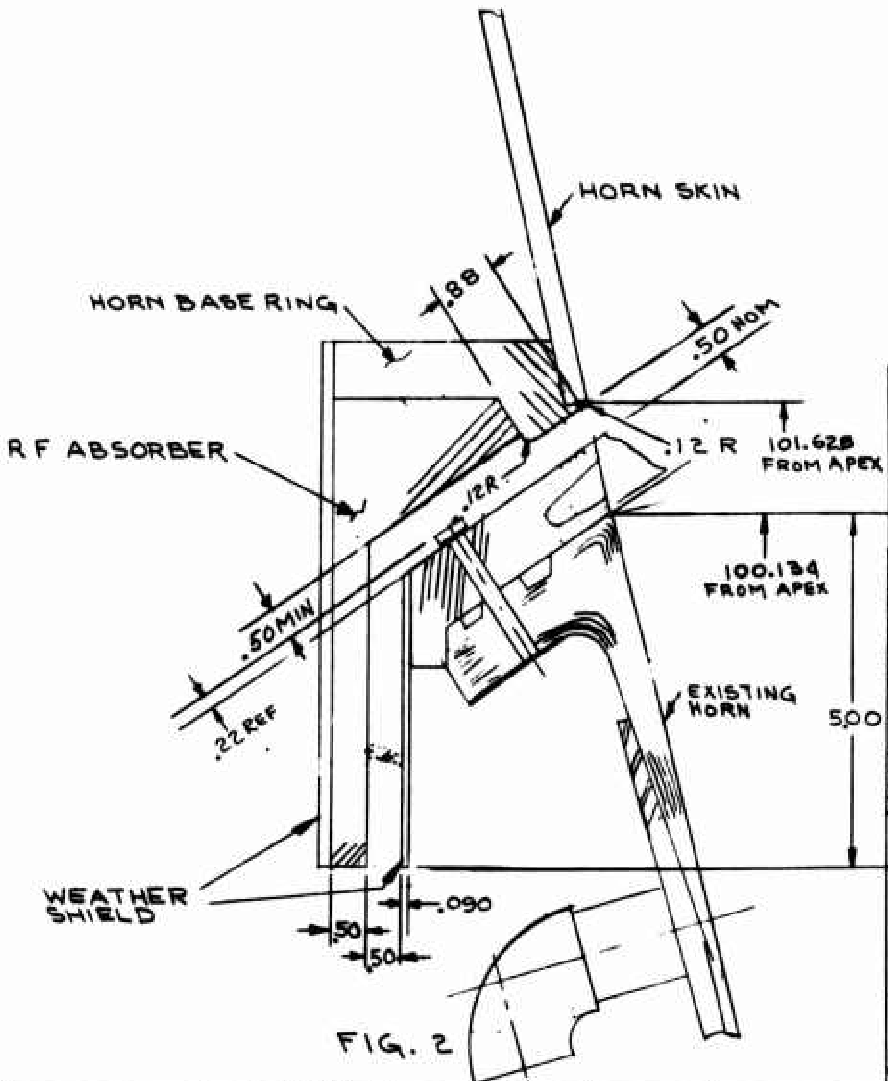

FIG. 2

PRINTS TO

MADE BY	APPROVALS		
15 MAY 70		HMES DIV OR DEPT.	SK62677-801-5-50
ISSUED		Syracuse, N.Y. LOCATION	CONT ON SHEET 17 SH NO 16

CODE IDENT NO

FF-... PRINTED IN U.S.A.

GENERAL ELECTRIC

SK 62677-801-5-50

CONT ON SHEET SH NO. 17

REV NO.

SK62677-801-5-50

CONT ON SHEET SH NO. 17

TITLE FOLDED CONE ANTENNA

FIRST MADE FOR NAROWS

REVISIONS

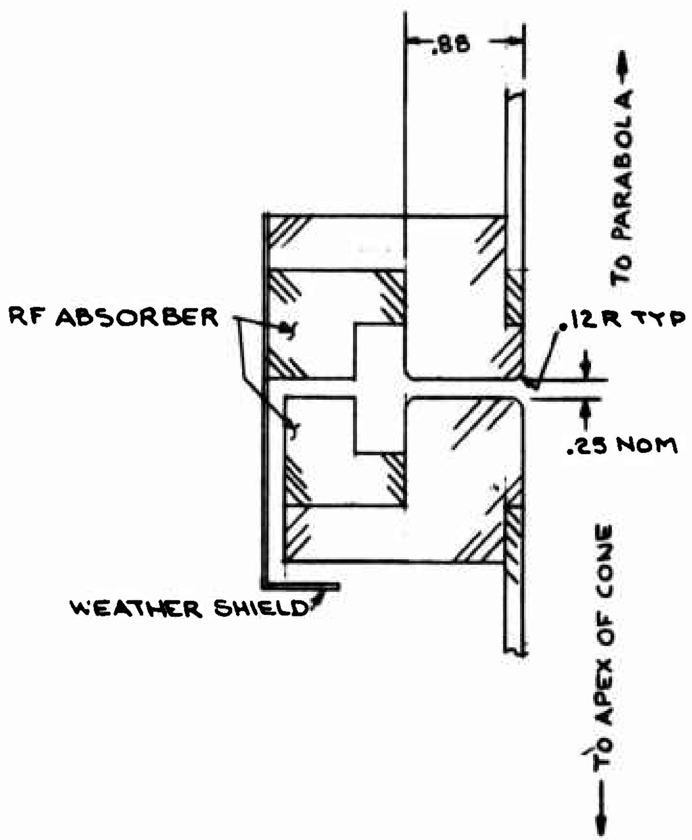

ELEVATION JOINT

FIG. 3

PRINTS TO

MADE BY 15 MAY 70

APPROVALS

HMES Syracuse, N.Y.

DIV OR DEPT. LOCATION

SK62677-801-5-50

CONT ON SHEET SH NO. 17

CODE IDENT NO.

PRINTED IN U.S.A.

APPENDIX III

THE EFFECTS OF TRANSITION GENERATED MODES ON THE ANTENNA

1. SOURCES OF PATTERN DISTORTION AND LOSS OF GAIN

The Nanosecond Pulse Antenna (NPA) differs from previously constructed conical folded horn paraboloids chiefly in the throat region. Instead of a purely conical horn fed from circular waveguide in which only the TE^{o}_{11} and TM^{o}_{01} modes can propagate (Ref. 8), the NPA is fed from oversized rectangular waveguide in which several higher order modes can propagate. In addition, the first 78 inches of the NPA is actually the NAROWS horn, which is a flared transition from the rectangular throat to the 25° conical horn (see Figure 6.1 in Ref. 10). Thus, the effect of the higher order modes generated at the NAROWS horn throat must be considered, as well as the rectangular-to-round horn transition.

Other effects to be considered are those of the rotating joints in the NPA, the plane mirror, the radome at the mouth of the NAROWS horn, and the asymmetric paraboloid illumination (see Ref. 7, particularly Figures 1 and 4, and Appendices I and II).

The loss of gain occurs in two ways. First, there is power diverted from the principal radiating mode which is not radiated in the direction of the beam peak. Either it is radiated in other directions or it is absorbed as heat. Second, some of the power lost from the principal radiating mode may be radiated in the direction of the beam peak. If it is approximately 180° out of phase with the principal radiating mode pattern, the effect will be to reduce the beam peak field and further decrease the gain.

The radiation patterns of higher order modes will affect the overall radiation pattern. The half power beamwidth and the sidelobes may be affected. A critical direction is that of the relatively large first E-plane sidelobe of the principal radiating mode. This is only about 16 dB down, with 15 dB acceptable.

2. THE TRANSITION AND CONICAL HORN

a. Modes and Reflections

The first effect in the transition is that of the rectangular throat flare, which causes the dominant $TE^{\square}_{10}$ mode to scatter to some extent into higher order modes which then propagate through the NPA. The principal higher order modes are the $LSE^{\square}_{12}$ and the TE_{30}. The throat amplitude coupling coefficient for the LSE_{12} mode, C^{12}_{10}, is -12.4 dB. This value is obtained from Eq. 10 in Reference 11, with the numerator of the right-hand side changed to $b_1(b_2 - b_1)$. The coefficient for the TE_{30} mode, C^{30}_{10} is -18.1 dB. This value is obtained from Eq. 9 in Reference 11, with the numerator of the right-hand side changed to $0.375a_1(a_1 - a_2)$.

These two modes are largely converted to the corresponding circular modes in the NAROWS horn. The $LSE^{\square}_{12}$ converts to the TM^{o}_{11} and the $TE^{\square}_{30}$ to the TE^{o}_{12}.

The dominant $TE^{\square}_{10}$ mode is affected by the NAROWS horn. The geometry is so complicated that there appears to be only one reasonably simple approach to calculating the effect of the horn on the $TE^{\square}_{10}$ mode, and that is by the use of geometric optics. The first step is to consider a square throat of the same area in place of the 8-in. x 5.36-in. rectangular throat. The square of the same area has a side of 6.55 in. Then, Figure 39 shows a view looking into the NAROWS horn from the mouth. The geometric optics ray from a given point A in the square throat would go to the corresponding point B in a square mouth, except that the circular cone intervenes. Thus, the ray from A is reflected from the cone and reaches point B' in the mouth. B' is at the same polar angle as B (this is the result of using a square throat) and the distances from the circle to B and B' are almost equal.

The polarization of the reflected electric field is changed. The component of the incident electric field in the plane formed by the normal at the point of incidence and the incident ray does not undergo a phase change at reflection, whereas the component normal to that plane does undergo a 180° phase change.

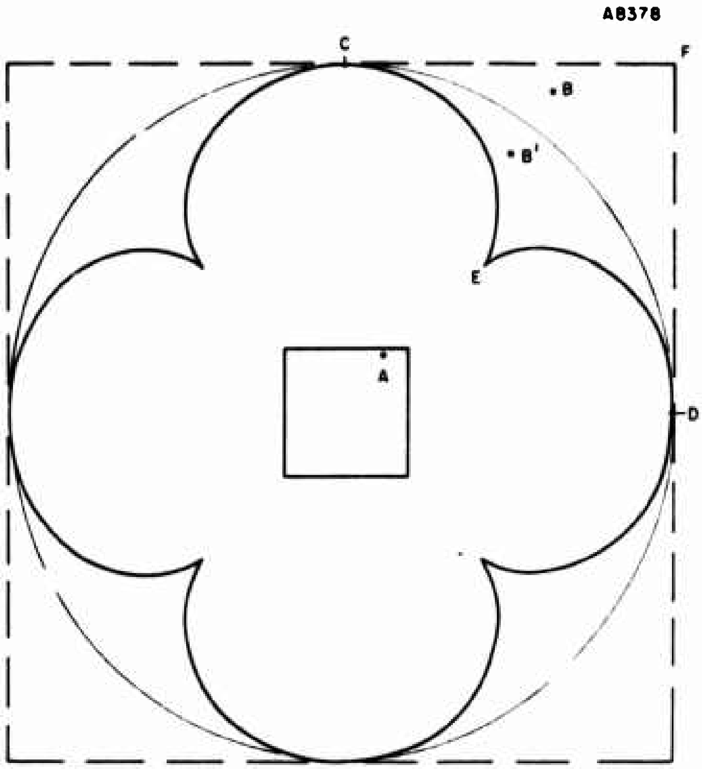

Figure 39. NAROWS Horn Geometric Optics Model

Thus, some of the power in the dominant $TE_{10}^{\square}$ mode is reflected off the conical walls of the transition and appears in the area of Figure 39 bounded by the circular arc CD and the curves CE and ED. This reflection will be termed the <u>first</u> reflection. Geometric optics appears to be a reasonable approach because the dimensions of the conical portion of the NAROWS horn are reasonably large in terms of wavelength, particularly near the mouth.

There is a second reflection of power. This occurs past the NAROWS horn, in the NPA purely conical horn itself, and is caused by the difference in the location of the apices of the cone and the square pyramid. The square pyramid is formed by the assumed square throat and square mouth of the NAROWS horn; its apex is 7.1 in. closer to the horn throat than the 25° cone apex. After the first reflection, the $TE_{10}^{\square}$ mode in the horn that has not been reflected may be described as a circular $TE_{10}^{\square}$ mode. It is what is left of a $TE_{10}^{\square}$ mode in square waveguide after being passed

through an inscribed circle. This circular $TE_{10}^{\square}$ mode passes into the pure cone. It has spherical phase fronts centered at the pyramid apex, not at the cone apex, and thus, its edge rays are reflected off the pure cone. At the mouth of the 21-foot, 25° cone, there are thus two bands of reflection, as shown in Figure 40, which is a quadrant of the cone mouth. The region between the circular arc CE and the curves CD and DE is that of the first reflection. The region between the circular arcs AB and CE is that of the second reflection. The arrows show the polarization of the reflected rays. Of course, in the regions of the reflected rays, there are also rays that have come from the throat with no reflection. These rays form the principal radiating mode of the horn. This mode is a circular $TE_{10}^{\square}$ mode cut off by a circle of somewhat smaller diameter than the inscribed circle.

The first and second reflections are tapered in magnitude as well as varying in polarization. The magnitude decreases from a maximum along AC in Figure 40 in a very crudely linear fashion, with angle to nearly zero at EB. The magnitude variation is, of course, a result of the cosinusoidal variation of the $TE_{10}^{\square}$ mode in the H-plane.

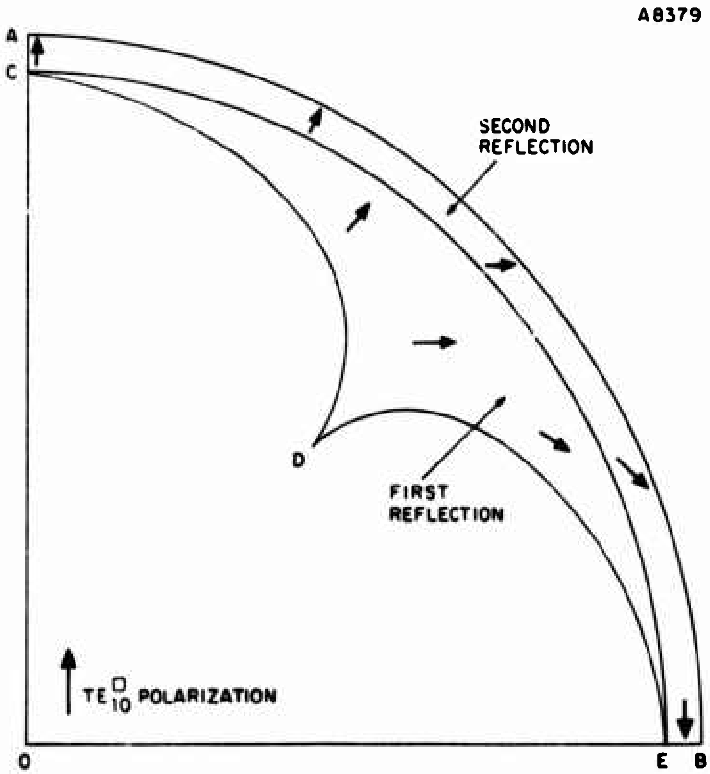

Figure 40. Aperture Reflection Zones and Polarization

Several calculations are necessary at this point. First, the percent of power in the first and second reflections is needed.

The first reflection power can be calculated in the following manner.

The total power of a $TE_{10}^{\square}$ mode in square waveguide is proportional to the integral of the square of the electric field magnitude

$$TP = Qx_o \int_o^{x_o} E^2 \, dx$$

$$E = \cos \frac{\pi x}{2x_o}$$

Q is a constant of proportionality.

x_o is half the square dimension.

$$TP = \frac{Qx_o^2}{2}$$

From Figure 39, the total power not reflected is

$$TPNR = Q \int_o^{x_o} E^2 \, \Delta y \, dx$$

$$\Delta y = \sqrt{x_o^2 - x^2}$$

Let

$$z = \frac{x}{x_o}$$

$$TPNR = Qx_o^2 \int_o^1 \cos^2 \frac{\pi z}{2} \sqrt{1 - z^2} \, dz$$

Evaluating the integral by Simpson's Rule,

$$\text{TPNR} = Qx_o^2 \, (0.4638)$$

Thus, the total power not reflected is 93 percent of the total power, or 7 percent of the power is reflected. Note that this is the first reflection.

For the second reflection, the total power is that in the circular TE_{10}^0 mode

$$\text{TP} = Q' \int_0^1 \cos^2 \frac{\pi x}{2} \sqrt{1 - x^2} \, dx$$

Q' is another constant of proportionality.

The total power not reflected is contained in a smaller circle:

$$\text{TPNR} = Q' \int_0^{x_o} \cos^2 \frac{\pi x}{2} \sqrt{x_o^2 - x^2} \, dx$$

Here x_o is slightly less than 1.

Let $z = \frac{x}{x_o}$

$$\text{TPNR} = x_o^2 \, Q' \int_0^1 \cos^2 \frac{\pi x_o z}{2} \sqrt{1 - z^2} \, dz$$

$$\cos^2 u = \frac{1}{2} + \frac{1}{2} \cos 2u$$

Thus,

$$\text{TP} = Q' \int_0^1 \left(\frac{1}{2} + \frac{1}{2} \cos \pi x \right) \sqrt{1 - x^2} \, dx$$

$$\text{TPNR} = Q' x_o^2 \int_0^1 \left(\frac{1}{2} + \frac{1}{2} \cos \pi x_o z\right) \sqrt{1 - z^2}\, dz$$

But

$$\int_0^1 \sqrt{1 - x^2}\, dx = \frac{\pi}{4}$$

From Reference 12, pg. 360, Eq. 9.1.20:

$$\frac{1}{2} J_1(\pi) = \int_0^1 \sqrt{1 - x^2} \cos \pi x\, dx$$

$$\frac{1}{2x_o} J_1(\pi x_o) = \int_0^1 \sqrt{1 - z^2} \cos \pi x_o z\, dz$$

Thus,

$$\text{TP} = Q' \left[\frac{\pi}{8} + \frac{1}{4} J_1(\pi)\right]$$

$$\text{TPNR} = Q' x_o^2 \left[\frac{\pi}{8} + \frac{1}{4x_o} J_1(\pi x_o)\right]$$

$x_o = 0.955$

TP = 0.4638Q' (a good check on the use of Simpson's Rule above)

TPNR = 0.4390Q'

Thus, 1 - (4390/4638), or 5.4 percent, is the amount of the second reflected power.

b. The Principal Radiating Mode Pattern

Thus, there are now available approximations for the amount of power in the TM_{11}^o mode, the TE_{12}^o mode, the first reflection, and the second reflection. The principal radiating mode at the mouth of the 21-ft, 25° cone is a modified circular $TE_{10}^{\square}$ mode,

with $E = \cos \frac{\pi x}{2}$, $0 \leq |x| \leq 0.955$. The pattern of the modified circular $TE_{10}^{\square}$ mode would be little different from that of the unmodified circular $TE_{10}^{\square}$ mode; $E = \cos \frac{\pi x}{2}$, but $0 \leq |x| \leq 1$. The E-plane and H-plane patterns of the unmodified circular $TE_{10}^{\square}$ mode were calculated.

The H-plane pattern of the unmodified circular $TE_{10}^{\square}$ mode is (Ref. 13, Chap. 6):

$$g(u) = \int_0^1 \cos \frac{\pi x}{2} \sqrt{1 - x^2} \cos ux \, dx$$

$u = \frac{\pi D}{\lambda} \sin \theta$, D is the diameter of the circle.

$$g(u) = \frac{1}{2} \int_0^1 \sqrt{1 - x^2} \cos \left(u - \frac{\pi}{2}\right) x \, dx$$

$$+ \frac{1}{2} \int_0^1 \sqrt{1 - x^2} \cos \left(u + \frac{\pi}{2}\right) x \, dx$$

From Reference 12, pg. 360, Eq. 9.1.20:

$$g(u) = \frac{\pi}{4} \frac{J_1\left(u - \frac{\pi}{2}\right)}{u - \frac{\pi}{2}} + \frac{\pi}{4} \frac{J_1\left(u + \frac{\pi}{2}\right)}{u + \frac{\pi}{2}}$$

But

$$\Lambda_1(u) = 2 \frac{J_1(u)}{u}$$

(See Ref. 14, pg. 128 and pg. 181.)

$$g(u) = \frac{\pi}{8} \left[\Lambda_1 \left(u - \frac{\pi}{2}\right) + \Lambda_1 \left(u + \frac{\pi}{2}\right)\right]$$

The E-plane pattern is more difficult to obtain accurately.

$$g(u) = \int_0^1 \sin\left(\frac{\pi}{2}\sqrt{1 - y^2}\right) \cos uy \, dy$$

Numerical integration could have been used here, but a sufficiently accurate approximation is to use $(1 - y^2)^{1/4}$ in place of $\sin\left(\frac{\pi}{2}\sqrt{1 - y^2}\right)$. g(u) can then be integrated directly by the use of Reference 12, pg. 360, Eq. 9.1.20.

$$g(u) = \frac{J_{3/4}(u)}{u^{3/4}}$$

(Some multiplicative constants have been omitted.)

$J_{3/4}(u)$ can be obtained by interpolation in Reference 14, pp. 171-172.

The normalized E-plane and H-plane patterns are plotted in Figure 41. This may be compared with Figure 5 of Reference 15, which gives the patterns of the TE_{11}^{o} mode. The patterns are quite similar; the first E-plane sidelobe of the circular $TE_{10}^{\square}$ mode is slightly larger, being 0.15 in voltage as against 0.13.

The actual patterns of the principal radiating mode will have filled nulls and in general be slightly different from Figure 41. The differences will largely be due to such effects as the asymmetric paraboloid illumination and the small phase error in the mouth of the 21-foot conical horn caused by the difference in the location of the pyramid and cone apices.

c. Other Patterns

There are four additional patterns to be considered. These are the ones caused by the TM_{11}^{o} mode, the TE_{12}^{o} mode, the first reflection and the second reflection. Of these the most important is that of the TM_{11}^{o} mode, which will be considered in some detail.

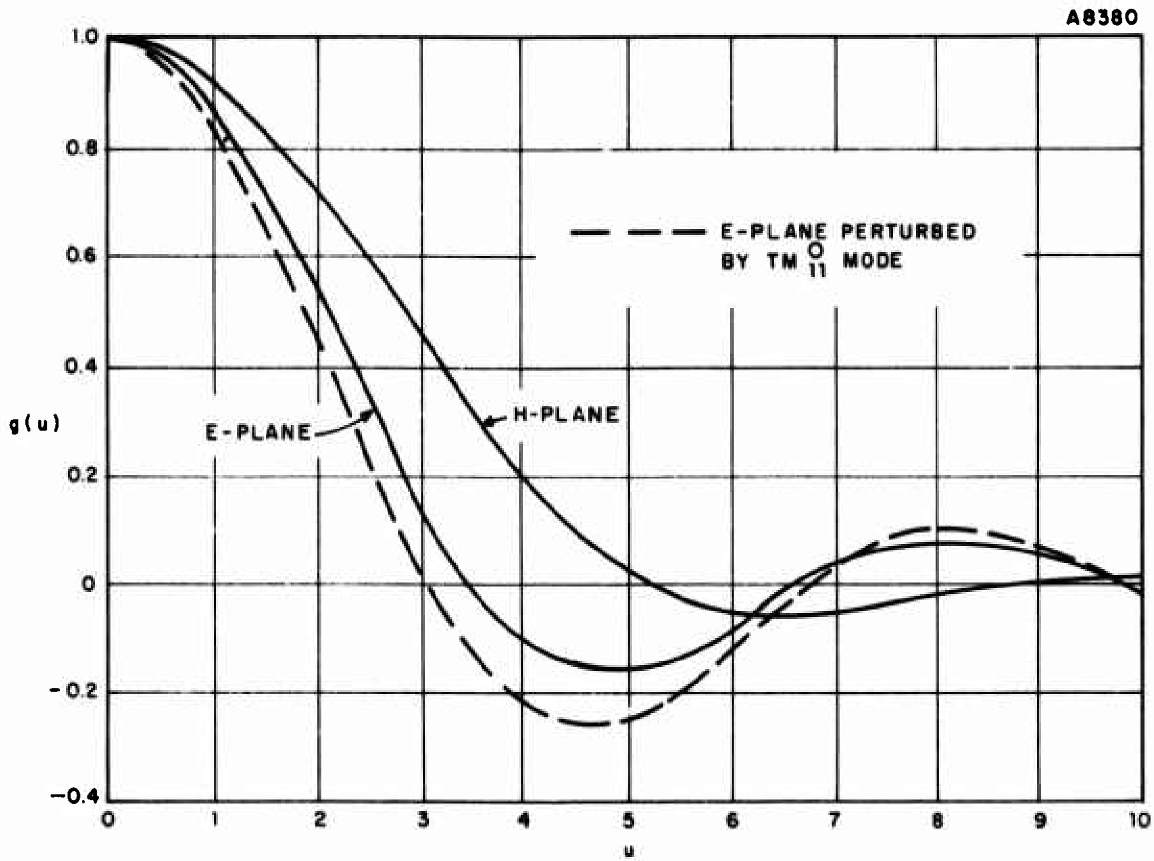

Figure 41. Estimated Patterns

The TM^{O}_{11} mode is formed from the $LSE^{\square}_{12}$ mode generated at the horn throat. Probably 80 percent to 90 percent of the LSE_{12} power goes into the TM^{O}_{11} mode. Patterns of the TM^{O}_{11} mode are shown in Reference 16, pg. 260. The equations for the patterns of the TM^{O}_{11} mode radiating from circular guide are given in Reference 13, pg. 338. In the E-plane the pattern is

$$g(u) = \frac{uJ_1(u)}{u^2 - (3.83)^2}$$

This is a bifurcated pattern, with a null at u = 0 and a peak at about u = 4. The pattern is down about 2 dB from the peak at u = 5*, which is the location of the first E-plane sidelobe peak of the principal radiating mode. The H-plane pattern of the TM^{O}_{11} mode radiating from circular waveguide is zero.

* Note that the definition of u in Reference 16 differs from the present definition by a factor of π.

From Reference 16, the peak gain of the TM^{o}_{11} mode is perhaps 5 dB less than that of the TE^{o}_{11} mode. The gain of the TE^{o}_{11} mode is 82 percent, or 0.85 dB, of the gain of a uniform circular aperture. The gain of the circular $TE^{\square}_{10}$ mode is 88 percent, or -0.55 dB, of that of a uniform circular aperture. Thus, the gain of the TM^{o}_{11} mode in the direction u = 5 may be taken as approximately -7 dB below the peak gain of the circular $TE^{\square}_{10}$ mode. Since the coupling coefficient for the $LSE^{\square}_{12}$ mode at the horn throat is -12.4 dB, and perhaps 1 dB is lost when the $LSE^{\square}_{12}$ mode is converted into the TM^{o}_{11} mode, the TM^{o}_{11} pattern in the direction u = 5 is approximately -20 dB compared to the circular $TE^{\square}_{10}$ mode peak. In other words, it is only 4-dB less than the first E-plane sidelobe of the principal radiating mode, which is -16 dB.

The next question to be answered is that of the relative phase between the TM^{o}_{11} pattern and the first E-plane sidelobe of the principal radiating mode. If the two contributions add, a sidelobe of roughly 12 dB could result.

There are three contributions to the relative phase. There is a quadrature effect at the horn throat, a phase difference as the modes traverse the 21-ft horn, and a 180° phase difference because the E-plane sidelobe is reversed in phase from the peak of the principal radiating mode, which is in phase with the bifurcated main lobes of the TM^{o}_{11} pattern.

The phase difference in traversing the horn length must be calculated. Physically, the horn looks like a rectangular quasi-pyramid near the throat (it is <u>not</u> a true pyramid because the flat sides of the horn, if extended, would not meet in a common point). Further along, the horn looks more and more like a cone. The procedure adopted was the following: the factor $\sqrt{1 - (\lambda/\lambda_c)^2} = \lambda/\lambda_g$ was calculated for four modes as a function of distance along the horn. These modes were the TE^{o}_{11} and TM^{o}_{11} modes in the 25° cone and the $TE^{\square}_{10}$ and $LSE^{\square}_{12}$ modes in the quasi-pyramid. The local cross-sectional dimensions were used to determine λ_c, the cutoff wavelength. Table I shows the result for ℓ = 0 to 78.44 in., the length of the NAROWS horn. (ℓ = 0 is at the throat.) Note that the values of λ/λ_g for the $TE^{\square}_{10}$ and TE^{o}_{11}

modes are very close. The values for the LSE$_{12}^{\square}$ and TM$_{11}^{\square}$ modes differ significantly only in the first twenty inches. Since in the first twenty inches the horn looks more like a quasi-pyramid than a cone, the decision was made to use the values for the TE$_{10}^{\square}$ and LSE$_{12}^{\square}$ modes to calculate the phase difference in the NAROWS horn.

TABLE I

CALCULATION OF $\sqrt{1 - (\lambda/\lambda_c)^2} = \lambda/\lambda_g$

ℓ	TE_{11}^{o}	TE_{10}^{o}	TM_{11}^{o}	$LSE_{12}^{\square}$
0	0.977	0.976	0.900	0.723
5		0.9855		0.877
10	0.989	0.990	0.952	0.931
20	0.994	0.995	0.973	0.968
30	0.996	0.997	0.982	0.982
40	0.997	0.998	0.987	0.988
50	0.998	0.9985	0.991	0.991
60	0.998	0.999	0.993	0.994
70	0.999	0.999	0.994	0.995
78.44	0.999	0.999	0.995	0.996

The phase length of a mode with varying guide wavelength is

$$\Phi = 2\pi \int_{L_1}^{L_2} \frac{d\ell}{\lambda_g} = 2\pi \int_{L_1}^{L_2} \frac{d\ell}{\lambda} \sqrt{1 - (\lambda/\lambda_c)^2}$$

λ_g and λ_c are functions of ℓ, the length. Thus, the phase difference between two modes is

$$\Delta\Phi = \frac{2\pi}{\lambda} \int_{L_1}^{L_2} \left(\sqrt{1 - (\lambda/\lambda_{c1})^2} - \sqrt{1 - (\lambda/\lambda_{c2})^2} \right) d\ell$$

Over the length of the NAROWS horn $\Delta\Phi$ was calculated to be 2π (0.655), or 236° at center frequency. Over the length of the purely conical horn past the NAROWS horn $\Delta\Phi$ was calculated to be 2π (0.061), or 22°. In the pure cone the TE_{11}^{o} and TM_{11}^{o} mode values were used.

The total phase difference of 258° is the phase length of the dominant mode minus the phase length of the higher-order mode. The dominant mode is further above cutoff, has a shorter wavelength and thus more wavelengths in a given length.

If the convention is used that the phase of a point further down the horn toward the mouth is delayed as compared to the phase at a given point, then the higher-order mode is less delayed -- or is advanced -- with respect to the dominant mode in traversing the horn. If this same convention is used, then the $LSE_{12}^{\square}$ mode generated at the throat is delayed 90° with respect to the $TE_{10}^{\square}$ mode.

The net phase of the TM_{11}^{o} mode radiation pattern in the direction of the principal radiating mode first E-plane sidelobe is then -90° + 258° - 180° = -12° at the band center. This means that the effect of the TM_{11}^{o} pattern is to increase the first E-plane sidelobe considerably. At the frequency band edges, the only number to change is the 258°, which will decrease to 239° at the upper frequency limit and increase to 281° at the lower frequency limit. Thus, the TM_{11}^{o} effect will be approximately in phase over the frequency band.

The 258° figure is, of course, only an approximation, but it should be accurate within about 10 percent. This indicates that the TM_{11}^{o} effect will definitely increase the first E-plane sidelobe.

Since the TM^{o}_{11} effect is largely to add to the first E-plane sidelobe, it will tend to subtract from the main beam. The effect on the 3-dB beamwidth will, however, be small; possibly reduced by a few percent. The TM^{o}_{11} pattern has a sidelobe in the vicinity of the second E-plane sidelobe of the principal radiating mode; and tend to add here also. The result would be a sidelobe of roughly 20 dB. The effects of the TM^{o}_{11} mode on the E-plane pattern are shown in Figure 41 where the TM^{o}_{11} mode effect is considered to be in phase with the first E-plane sidelobe. Note again that the patterns of Figure 41 are idealized since various-relatively small effects are neglected. Among these are the illumination asymmetry caused by the offset paraboloid, the slight phase error of the principal radiating mode, and the patterns of the first and second reflections.

The $TE^{\square}_{30}$ mode generated at the horn throat will have some effect on the overall radiation pattern, though the effect is not nearly as drastic as that of the $LSE^{\square}_{12}$ mode. The $TE^{\square}_{30}$ mode is largely converted to the TE^{o}_{12} mode in the horn. The H-plane pattern of the TE^{o}_{12} mode is shown on Figure 42; the normalized E-plane pattern is the same as for the TE^{o}_{11} mode (See Ref. 13, pg. 337). The H-plane pattern has a gain on axis 10.5 dB below that of the TE^{o}_{11} mode (See Ref. 16, pp. 257-258). The maximum gain of the TE^{o}_{12} mode in the H-plane is at $u = 4.75$ and it is about 5.5 dB greater than the on-axis gain, or about 5 dB less than the peak gain of the TE^{o}_{11} mode. The $TE^{\square}_{30}$ mode at the throat is down 18.1 dB and there is probably about 1 dB conversion loss when it converts to the TE^{o}_{12} mode. Thus, at $u = 4.75$ in the H-plane, the TE^{o}_{12} mode is about $18 + 1 + 5 = 24$ dB below the TE^{o}_{11} peak. It is thus also about 24 dB below the peak of the principal radiating mode. The principal radiating mode pattern is still in the main beam at $u = 4.75$. At $u = 6.68$ occurs the first H-plane sidelobe peak of the principal radiating mode, which is down roughly 26 dB. At the same value of u the TE^{o}_{12} mode is about 5 dB below its peak, so it is 24 + 5 dB below the principal radiating mode peak, and will probably affect the size of the first H-plane sidelobe. At the worst, the first H-plane sidelobe should still be down more than 20 dB.

On-axis, the TE^{o}_{12} mode is about 30 dB below the principal radiating mode, or about 3 percent in voltage. This could result in a gain decrease.

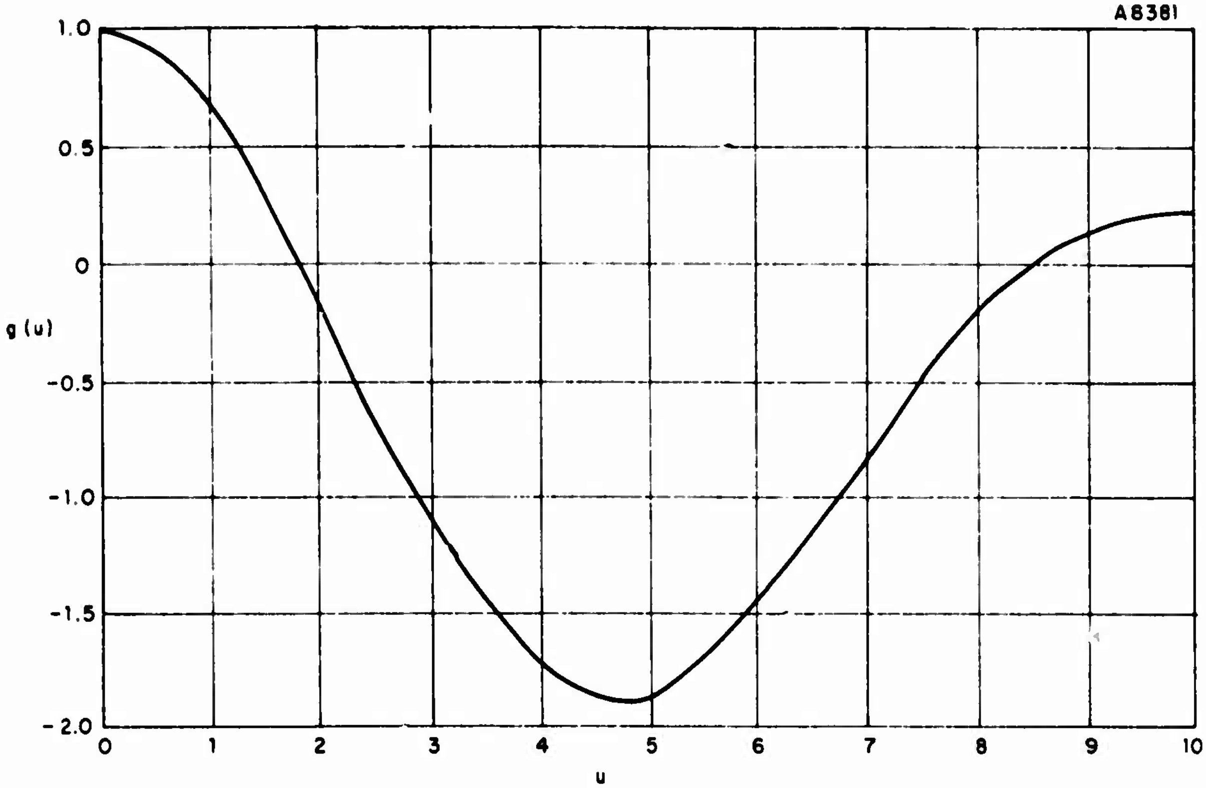

Figure 42. H-Plane Pattern, TE_{12}^{o} Mode

The first and second reflections must be considered. A reasonably complete calculation of their patterns would be very complicated, but some rather simple approximations can be made. If the polarization is considered, it may be seen that the horizontally polarized components cancel out on the principal planes, at least if the asymmetry introduced by the offset paraboloid is neglected. The vertically polarized components of the two reflections each give a field on-axis about 2 percent of the principal radiating mode. They have an effect of roughly the same size in the E-plane sidelobe region and somewhat less in the H-plane sidelobe region. Thus, the effect on the gain and pattern will be rather small, if each reflection is considered by itself.

With numbers now available for the effects of the TM_{11}^{o} and TE_{12}^{o} modes, plus the first and second reflections, the resultant effects on the gain and patterns may be estimated. The loss of gain because of power in the modes generated at the throat is about 7 percent or 0.3 dB. There is about 12 percent loss of power in the

two reflections, or 0.55 dB. The total is 0.85 dB. In addition, the patterns of these modes and reflections may subtract from the principal radiating mode on-axis, and thus, reduce the gain. The total possible subtraction is about 7 percent in voltage, or about 0.6 dB.

The patterns will therefore be affected by the two modes and the two reflections. The major effect will be at the first E-plane sidelobe, where it appears that the acceptable level of 15 dB will not be achieved. This sidelobe might be as large as 12 or even 11 dB.

Only the principal plane patterns have been discussed so far, and only the principal polarization has been considered. There will be cross-polarized sidelobes off the principal planes and, to a certain extent, on the horizontal principal plane because of the asymmetry caused by the paraboloid. It does not appear that any of the cross-polarized sidelobes will be large enough to be important.

3. ROTATING JOINTS, PLANE MIRROR AND RADOME

The effects of the rotating joints, the plane mirror and the radome at the mouth of the NAROWS horn are relatively small. These all subtract from the power of the dominant mode, and thus cause a loss of gain. There are also effects on the pattern, but these are probably small and will be neglected.

The analysis in the proposal (Ref. 17, pp. 26) gives a maximum loss of power of about 0.2 dB in the joints by a simplified computation. This power will largely be absorbed in the joints by absorbing material.

The insertion loss of the radome will also be about 0.2 dB. This is largely reflection in various modes. The lower order modes will go back into the waveguide system and may eventually come back again and go out the horn. The higher order modes will be reflected in the horn. The net result will be very complicated but the effects are so small that it seems reasonable to consider only the 0.2 dB loss.

The loss in the plane mirror can be estimated from (Ref. 8, Table I). The gain difference between the straight horn and the triple-folded horn is about one dB. With one fold in the NPA, the loss of gain would then be about 0.3 dB. Thus, the total loss of gain in the joints, radome and mirror is about 0.7 dB.

4. OVERALL PERFORMANCE

The half-power point of the principal radiating mode (the circular $TE_{10}^{\square}$) occurs at about u = 1.50 in the E-plane and u = 2.08 in the H-plane. As indicated previously, there are various effects that will perturb the main beam, as well as the pattern in general. Some of these will increase the beamwidth and some will decrease it. Overall, it appears that the use of u = 1.50 and 2.08 is reasonable for obtaining the pattern beamwidths of the NPA.

$$u = \frac{\pi D}{\lambda} \sin \theta$$

$$D = 144 \text{ in.}, \quad \lambda = 3.523 \text{ in. (at center frequency)}$$

$$\sin \theta = \frac{(3.523)(1.5)}{\pi (144)} = 0.0117 \text{ (E-plane)}$$

The full half-power width in the E-plane is thus 0.0234 radian, or 1.34°. The full half-power width in the H-plane is then $\frac{(1.34 \times 2.08)}{1.50} = 1.86°$.

The gain of a uniform, circular aperture is

$$G_o = \frac{4\pi A}{\lambda^2} = \frac{\pi^2 D^2}{\lambda^2}$$

For a 12-foot diameter aperture,

$$G_o = 16500 = 42.4 \text{ dB}$$

The circular $TE_{10}^{\square}$ mode has 88 percent the gain of the uniform circular mode, or -0.55 dB.

The losses of power caused by the TM_{11}^{o} and TE_{12}^{o} modes and the two reflections are estimated at 0.85 dB. The losses of power in joints, mirror and radome is estimated at 0.7 dB. The total loss of power is then 1.55 dB. In addition, there is a possible loss of gain of 0.6 dB caused by the TE_{12}^{o} mode and the reflections subtracting from the peak of the beam. Further, the illumination asymmetry caused by the offset paraboloid will result in an additional gain loss of perhaps 0.1 dB.

The net gain is then 42.2 - 0.55 - 1.55 - 0.6 - 0.1 = 39.4 dB. The efficiency is 52 percent, which is close to the values given for the triple-folded horn in Ref. 8, Table I, for the lower frequency. This seems reasonable, because the triple-folded horn has perhaps 0.7 dB more loss because of the two extra folds, but it does not have the higher order modes generated at the throat.

It seems fairly certain that the first E-plane sidelobe will be higher than 15 dB because of the TM_{11}^{o} mode effect, which apparently is more or less in-phase with the first E-plane sidelobe of the principal radiating mode. This sidelobe could be as large as 11 or 12 dB at some point in the frequency band. A somewhat similar effect will probably take place at the first H-plane sidelobe cause of the TE_{12}^{o} mode, but the resultant sidelobe will be considerably smaller, being in the order of 20 dB.

Overall, then, the gain of the NPA is quite acceptable, but the first E-plane sidelobe appears to be too high by several dB. The beamwidth in the E-plane is below the specified lower limit, but this does not appear to be a serious deficiency.

APPENDIX IV

STRUCTURAL LOAD ANALYSIS OF THE ANTENNA

The structural load analysis was made using conventional approaches. The complete analysis is a large volume of worksheets. Review of the approach noting the important assumptions and coefficients follows. (Samples of the computations have been supplied separately to RADC.)

These are the basic sequence of calculation events:

1. The coordinates for the reflector parabola were set.

2. The area and the center of gravity for the various projected areas of the antenna, in several positions, were developed.

3. The wind loading was calculated:

   a. Stagnation pressures at velocities of 15, 40, and 80 knots and 15°C air temperature were computed.

   b. The following drag coefficients were obtained from component references:

• Cylinders and cones with sharp ribs	1.00
• Open cup	1.50
• Structural members	2.00
• Tubing and flat plates	1.20

   c. Wind loading pressures on various parts of antenna and structure using above data were computed in pounds per square foot.

4. The antenna was broken up into elements of exposed area from different directions and for different antenna aperture positions.

   a. The cross sectional area for each of the geometric components for each of the different directions was developed.

   b. The effective lever arms for each of these areas with respect to the azimuth axis, elevation axis, and horizontal overturning axis was calculated.

   c. Wind loads and moments resulting from these loads about the various axes and for the various conditions were computed.

5. A weight breakdown was made and the centers of gravity with respect to the various axes of rotation and overturning were derived.

6. The azimuth-wheel loading was computed for the various conditions.

7. The base foot-loadings (eight of them) were computed for the various conditions.

8. The moments and forces at the vertical rotary joint were derived for the various wind loads and directions.

9. The force necessary to rotate the antenna in azimuth and elevation at the various wind conditions was calculated.

   a. The tangential force at a 10 ft radius including rolling friction at 40 knots is 1450 lbs, and at 80 knots it is 5648 lbs.

   b. The force required to rotate the antenna in elevation at 40 knots is 400 lbs at a 5 ft radius.

10. The flat reflector deflection of hat section center at 40 knots was calculated as 0.054 in. The deflection of the skin between the hat sections is 0.0026 in. The total worst deflection is, therefore, 0.057 in.

11. The significant data on the parabolic reflector assembly has been found to be

    a. The reflector skin stress at 80 knots is 5421 psi. The deflection at 40 knots is 0.047 in.

    b. The maximum deflection of the skin stiffening rib at 40 knots is 0.011 in.

    c. The cross members located behind the ribs will have a maximum stress at 80 knots of 12,209 psi and a maximum deflection of 0.038 in. The deflection will probably be much less because the calculation does not take into account the effect of the surface curvature.

    d. The three trusses behind the above members have maximum buckling stresses which are considerably less than the allowable stress for the corresponding l/r ratio. The deflection is also well within the specification limit.

12. The elevation geared quadrants are clamped and doweled together to provide smooth transition. The quadrants which do not experience gear motion have clearance at the ends to allow for the difference in expansion between the steel gear quadrant and the backup aluminum ring. The gear tooth stress was checked for the forces from the 80-knot wind and found to be 25,000 psi. This is well within the allowable 30,000 psi for a 245 Brinnell hardness steel.

13. The superstructure truss loads and deflections were considered and found to be nominal as designed.

14. The stiffener rings and shells of the conical and cylindrical sections were checked for thickness, spacing of the hat section stiffeners, stress and deflection, for the 80-knot wind condition. The mounting ring at the elevation drive gear, the steel part, and the aluminum part, were checked for stress and deflection.

15. The mass moment of inertia around the azimuth and the elevation axis was calculated.

The azimuth rotating assembly has three wheels. Two sheels are power driven and the third is an idler. The track loads at the wheels are as follows, where both wind direction and antenna position change the results.

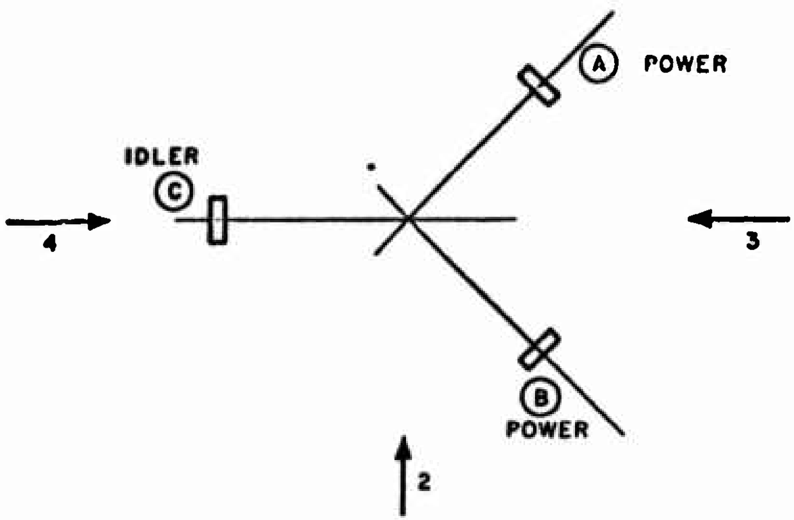

Case 2 - Wind against aperture facing horizontal

Case 3 - Wind against reflector, aperture up

Case 4 - Wind against parabolic reflector, aperture down

TRACK LOAD AT WHEEL (lbs)

		A	B	C
1.	No Wind (Total 8600 lbs)	3992.5	3992.5	615
2.	80 knots, survival Case 2, wind direction 2	7025	960	615
3.	80 knots, survival Case 4, wind direction 3	2380	2380	3840
4.	80 knots, survival Case 3, wind direction 4	5605	5605	-2610
5.	40 knots gust Case 3, wind direction 4	4395.5	4395.5	-191

There are eight mounting pads which bolt to the support beams provided on the roof. The mounting pads are identified counterclockwise in the plan view, with A and B on the east side. For an 80-knot wind from each of three directions, the computed loads are as follows, for the antenna stowed in the position which produces the worst load distributions.

ANTENNA MOUNTING PAD LOADING (lbs)

Case 1 - Wind from south to north

Case 2 - Wind from 30° west of south

Case 3 - Wind from 45° west of south

LOAD ON PADS OF EACH OF 8 SUPPORTING PADS (lbs)

Case	A	B	C	D	E	F	G	H
1	0	4287	1920	1920	4287	0	-1083	-1083
2	948	0	3787	3787	0	645	482	602
3	687	0	7198	0	507	620	0	864

LIST OF REFERENCES

1. Quine, J.P., Younger, C., and Maurer, J.W., "Ultra-High Power Transmission Line Techniques," RADC-TR-65-164, Final Report Contract AF30(602)-2990, September 1965.

2. Quine, J.P. and Younger, C., "Gaseous Discharge Switch in Oversized Waveguide," RADC-TR-65-521, Final Report Contract AF30(602)-3544, February 1966.

3. Quine, J.P. and Younger, C., "High Power Microwave Components in Oversized Waveguide," RADC-TR-67-117, Final Report Contract AF30(602)-3682, May 1967.

4. Tomiyasu, K. et al, "Super Power CW Transmission Line Techniques," RADC-TR-67-609, Final Report Contract AF30(602)-3810, December 1967.

5. Quine, J.P. and Younger, C., "Low-Dispersion High-Power Waveguide Systems," RADC-TR-68-154, Final Report Contract F30602-67-C-0136, June 1968.

6. Dolling, J.C., Blackmore, R.W., Kinderman, W.J., and Woodard, K.B., "The Mechanical Design of the Horn Reflector Antenna and Radome," Bell System Technical Journal, Vol. 42, July 1963, pp. 1137-1186.

7. Hines, J.N., Li, Tingye, and Turrin, R.H., "The Electrical Characteristics of the Conical Horn-Reflector Antenna," Bell System Technical Journal, Vol. 42, July 1963, pp. 1187-1211.

8. Giger, A.J. and Turrin, R.H., "The Triply-Folded Horn Reflector: A Compact Ground Station Antenna Design for Satellite Communications," Bell System Technical Journal, Vol. 44, September 1965, pp. 1229-1253.

9. Hoerner, S.F., Fluid-Dynamic Drag, Dr.-Ing. S.F. Hoerner, Midland Park, New Jersey, 1958.

10. Younger, C. et al, "Nanosecond Radar-Oversize Waveguide System (NAROWS)," RADC-TR-69-253, Contract F30602-69-C-0066, Rome Air Development Center, September 1969.

11. Quine, J. P., "Oversize Tubular Metallic Waveguides," in Microwave Power Engineering, (E.C. Okress, ed.) New York: Academic Press, 1968, Vol. 1, pg. 191.

12. Abramowitz, M. and Stegun, I.A., Handbook of Mathematical Functions, National Bureau of Standards, Third Printing, March 1965.

13. Silver, S., Microwave Antenna Theory and Design, M.I.T. Radiation Laboratory Series, Vol. 12, New York: McGraw-Hill, 1949.

14. Jahnke, E. and Emde, F., Tables of Functions, New York: Dover Publications, 1943.

15. Horton, C.W., "On the Theory of the Radiation Patterns of Electromagnetic Horns of Moderate Flare Angles," Proc. I.R.E., Vol. 37, pp. 744-749, July 1949.

16. Kitsuregawa, T. et al, "The Radiation Characteristics of the Conical Horn-Reflector Antenna Excited in Higher Modes," 1966 I.E.E.E. Conv. Record, Pt. 5, pp. 252-260.

[redacted]